Phosphonium salt catalysts for reductive and non-reductive CO_2 fixation

Dissertation

in kumulativer Form

zur Erlangung des akademischen Grades

Doctor rerum naturalium (Dr. rer. nat.)

der Mathematisch-Naturwissenschaftlichen Fakultät

der Universität Rostock

vorgelegt von

Changyue Ren

Geboren am 14.09.1986 in P. R. China

Rostock, den 25.03.2024

https://doi.org/10.18453/rosdok_id00004759

Gutachter:

Prof. Dr. Thomas Werner, Universität Rostock, Leibniz-Institut für Katalyse e.V.

Prof. Dr. Jan Paradies, Universität Paderborn, Fakultät für Naturwissenschaften

Jahr der Einreichung: 2024

Jahr der Verteidigung: 2024

Die vorliegende Arbeit entstand in der Zeit von März 2020 bis März 2024 am Leibniz-Institut für Katalyse e.V. an der Universität Rostock unter der Betreuung von Prof. Dr. Thomas Werner.

Erklärung

Hiermit versichere ich an Eides statt, dass ich die vorliegende Arbeit selbständig angefertigt und ohne fremde Hilfe verfasst habe. Dazu habe ich keine außer den von mir angegebenen Hilfsmitteln und Quellen verwendet. Die aus den benutzten Werken inhaltlich und wörtlich entnommenen Stellen sind als solche kenntlich gemacht.

Changyue Ren

Rostock, den 25.03.2024

Acknowledgement

At the very beginning, I would like to express my deepest appreciation to my supervisor Prof. Dr. Thomas Werner, who offered the great opportunity for my PhD studies in our group in LIKAT. I would like to thank all my dear group partners. Many thanks go to Dr. Christoph Wulf, Dr. Lars Longwitz, Dr. Vivian Stefanow, Dr. Xin Liu, Dr. Yuya Hu, Dr. Everaldo Krake, Sascha Bierbach and Viktorija Medvaric for sharing a comfortable and pleasant working atmosphere, offering me generous help in the lab and the friendship. Especially, I would like to thank for Dr. Hanna Sebode, Constanza Terazzi, Jan Tönjes, Lukas Kell, always showing me the great insights in scientific research, thanks to their outstanding cooperation and numerous scientific discussions, as well as a lot of generous help in the lab work and the daily life. My sincere thanks also go to my cooperation partners: thanks to Dr. Sebastian Wohlrab, Dr. Marcus Klahn, Dr. Anke Spannenberg, Alexander Wotzka for the scientific support. Also, I would like to thank analysis team of LIKAT.

I greatly appreciate and wish to thank for all colleagues and friends in LIKAT: Dr. Bei Zhou, Dr. Chenyang Wang, Dr. Jie Gao, Dr. Junhao Huang, Dr. Qiyang Zhang, Dr. Ruiyang Qu, Dr. Shuoping Ding, Dr. Tao Zhang, Dr. Yue Hu, Dr. Zhuang Ma, Rui Ma, Jiali Liu, Qi Dong, Yanan Han. Many thanks go to my dear friends Yanzhuo Yin and Qin Tu.

I really appreciate my family' love and support throughout my life. And here I wish they are always fine. Last but not the least, I would like to thank my husband Dr. Xinmin Li, who always understand, believe in me, offers companionships and supports whenever I need.

Abstract

The use of carbon dioxide (CO_2) as a building block in organic synthesis is a topic of high interest. In this context, the focus of this work was on the development of catalytic systems to efficiently convert CO_2 to valuable products. Herein, a series of phosphonium salts were designed and used as catalysts for CO_2 fixation and conversion to different valuable products via reductive and non-reductive reactions.

In this work, two bifunctional phosphonium salts bearing perfluorinated side chains were prepared. The activity of those phosphonium salts for the cycloaddition of CO_2 and epoxides was evaluated. The isolation and recyclability of the two phosphonium salts bearing perfluorinated chains was tested and the deactivation of catalysts was studied in detail.

Subsequently, phosphonium salt-catalyzed selectively reductive C–N bond forming reaction between amines and CO_2 as C1-source in the presence of hydrosilanes were developed. In these reactions, CO_2 and amines were converted to formamides and methylamines at different temperatures. Initially, an air-stable internal phosphonium salt was developed for both transformations. The formylation reaction and methylation reaction could be performed under mild conditions. The protocol was applied to pharmaceutical compounds. The upscale reactions were performed under mild conditions. Additionally, a phosphonium methylcarbonate salt was proven to be an efficient catalyst for these reactions. The reactions were tuned by using different hydrosilanes: methylation products were obtained with polymethylhydrosiloxane (PMHS), which is an industrial waste product. Formylated products were obtained with trimethoxysilane, including benzoheterocycles which were obtained from diamines and CO_2 in one step. The mechanistic studies illustrated the pathways for the two catalytic systems. A novel catalytic cycle was proposed in the presence of phosphonium methylcarbonate salt, illustrating the interaction between the catalyst and reducing agent.

Kurzfassung

Die Verwendung von Kohlendioxid (CO_2) als Baustein in der organischen Synthese ist ein wichtiges aktuelles Thema. In diesem Zusammenhang lag der Schwerpunkt dieser Arbeit auf der Entwicklung katalytischer Systeme zur effizienten Umwandlung von CO_2 in wertvolle Produkte. Dabei wurde eine Reihe von Phosphoniumsalzen entwickelt und als Katalysatoren für die CO_2-Fixierung und Umwandlung in verschiedene wertvolle Produkte über reduktive und nicht-reduktive Reaktionen verwendet.

In dieser Arbeit wurden zwei bifunktionelle Phosphoniumsalze mit perfluorierten Seitenketten hergestellt. Die Aktivität dieser Phosphoniumsalze für die Cycloaddition von CO_2 und Epoxiden wurde untersucht. Die Isolierung und Wiederverwendbarkeit der beiden Phosphoniumsalze mit perfluorierten Ketten wurde erprobt und die Desaktivierung der Katalysatoren im Detail analysiert.

Anschließend wurde eine Phosphoniumsalz-katalysierte selektiv reduktive C–N bindungsbildende Reaktion zwischen Aminen und CO_2 als C1-Quelle in Gegenwart von Hydrosilanen entwickelt. Bei diesen Reaktionen wurden CO_2 und Amine bei verschiedenen Temperaturen in Formamid und Methylamin umgewandelt. Für beide Transformationen wurde zunächst ein luftstabiles internes Phosphoniumsalz entwickelt. Die Formylierungs- und Methylierungsreaktionen konnten unter milden Bedingungen durchgeführt werden. Das Protokoll wurde auf pharmazeutische Verbindungen angewendet. Die hochskalierten Reaktionen wurden unter milden Bedingungen durchgeführt. Darüber hinaus erwies sich ein Phosphoniummethylcarbonatsalz als leistungsfähiger Katalysator für diese Reaktionen. Sie konnten durch den Einsatz verschiedener Hydrosilane gesteuert werden: Mit Polymethylhydrosiloxan (PMHS), einem industriellen Abfallprodukt, wurden Methylierungsprodukte erhalten. Mit Trimethoxysilan wurden formylierte Produkte synthetisiert, darunter Benzoheterocyclen, die in einem Schritt aus Diaminen und CO_2 erhalten wurden. Mechanistische Untersuchungen erlaubten Einblick in die zwei katalytischen Systeme. Infolgedessen wurde ein neuartiger Katalysezyklus in Gegenwart von Phosphoniummethylcarbonatsalz vorgeschlagen, der die Wechselwirkung zwischen Katalysator und Reduktionsmittel veranschaulicht.

List of abbreviations

atm	Atmosphere
CCS	Carbon capture and storage
CCU	Carbon capture and utilization
cat.	Catalyst
DBU	1,8-Diaza¬bicyclo[5.4.0] undec-7-ene
DMA	Dimethylacetamide
DMC	Dimethylcarbonate
DMF	N,N-Dimethylformamide
DMSO	Dimethyl sulfoxide
DFT	Density functional theory
Et	Ethyl
equiv	Equivalent
g	Gram
Gt/yr	Gigatonnes/year
ΔGf°	Standard Gibbs free energy of formation
h	Hour
^{i}Pr	Iso-Propyl
IPCC	Intergovernmental Panel on Climate Change
IL	Ionic liquid
Me	Methyl
MPa	Megapascal
Mt	Megaton
MT *p.a*.	metric tons per annum
^{n}Bu	*n*-Butyl
NIPU	Nonisocyanate polyurethane
NMR	Nuclear magnetic resonance
NHC	*N*-heterocyclic carbene
PMHS	Polymethylhydrosiloxane
p	Pressure
Ph	Phenyl
ppm	parts per million
Rf_8	1,1,1,2,2,3,3,4,4,5,5,6,6,7,7,8,8-heptadecafluorononyl
r.t.	Room temperature
t	Time
TBAF	Tetra-*n*-butylammonium fluoride
TBD	1,5,7-Triazabicyclo(4.4.0) dec-5-en
T	Temperature
^{t}Bu	tert-Butyl
TBA	Tetra-*n*-butylammonium cation
THF	Tetrahydrofuran
9-BBN	9-Borabicyclo[3.3.1]no

Contents

1 Introduction 1
1.1 Carbon dioxide as a C1 building block in organic synthesis 1
1.2 Coupling of CO_2 and epoxides to cyclic carbonates 3
1.3 *N*-Formylation of amines with CO_2 6
1.4 *N*-Methylation of amines with CO_2 12
1.5 Tunable *N*-methylation reaction and *N*-formylation reaction 15
2 Objectives of this work 17
3 Results and Discussion 18
3.1 Phosphonium salt catalyzed CO_2 coupling reaction with epoxides 18
3.2 Phosphonium salt catalyzed *N*-methylation and *N*-formylation of amines with CO_2 22
3.3 Tunable reduction of CO_2-organocayalyzed selective formylation and methylation of amines. 29
4 Summary 35
5 References 37
6 Appendix 44
6.1 Catalytic, Kinetic, and Mechanistic Insights into the Fixation of CO_2 with Epoxides Catalyzed by Phenol-Functionalized Phosphonium Salts I
6.2 Synthesis of Bifunctional Phosphonium Salts Bearing Perfluorinated Side Chains and Their Application in the Synthesis of Cyclic Carbonates from Epoxides and CO_2 II
6.3 Phosphonium Salt-Catalyzed *N*-methylation and *N*- formylation of Amines with CO_2 III
6.4 Tuneable reduction of CO_2 – organocatalyzed selective formylation and methylation of amines IV

1 Introduction

1.1 Carbon dioxide as a C1 building block in organic synthesis

The prospect of a worsening climate situation due to global warming has caused widespread public concern. The carbon dioxide emissions was regarded as the primary driver of climate change. The current global average concentration of CO_2 has reached 423 ppm by 2023, which was around 280 ppm at the start of the industrial revolution.[1] The reason for this sharp rise is the growing reliance on the combustion of fossil fuels (coal, petroleum, and natural gas) which accounts for 80% of anthropogenic greenhouse gas emissions, with the rest arising from the change of land use (primarily deforestation) and chemical processing.[2] The urgent need to develop strategies to reduce the concentration of CO_2 and other greenhouse gases in the global atmosphere has prompted national and international governments and industries to take action and establish a number of high-profile collaborative programs, including the Intergovernmental Panel on Climate Change (IPCC), the United Nations Framework Commission on Climate Change, and the Global Climate Change Initiative.[3] A series of assessment reports, special reports, and technical papers have been produced by IPCC, focusing on two technologies as mitigation pathways: carbon capture and storage (CCS) and carbon capture and utilization (CCU). CCS process involves separating CO_2 from industrial and energy-related sources, transporting to a CO_2 storage site where it is sequestered from the atmosphere for long periods of time. Before 2022 CCS remains central to climate mitigation strategies. In 2022 the IPCC Assessment Report mentioned for the first time CCU as a solution to reduce net CO_2 emissions, as well as a necessary technology to weaning off fossil carbon by using CO_2 as an alternative feedstock for the production of renewable chemicals and fuels.[4] From the perspective of CCU technology, CO_2 is not considered a waste, but as an accessible, inexpensive, and renewable carbon source that can be used for the chemical synthesis or biosynthesis of commercially important chemicals and fuels.[4b, 5] The CO_2 capture and the conversion into value added products are of great economic, social and ecological significance.[6] It was estimated that the demand for CO_2 will increase from 0.6 to 6.1 gigatons in 2050, thus using CO_2 as feedstock in organic synthesis is a visionary technologies for the future.[7] However, CO_2 is the most oxidized form of carbon, and well-known to be both thermodynamically stable and kinetically inert ($\Delta Gf° = -396$ kJ/mol), as a result, the activation and utilization of CO_2 is still problematic.[8] Related research had been widely reported in the past decades and a number of value-added products were prepared from CO_2. The reductive reactions of CO_2 include hydrogenation to formic acid;[9] carboxylation to carboxylic acids;[10] reduction to fuels such as CO,[11] methanol,[12] methane,[6] and reduction to fine chemicals such as *N*-formamides;[13] *N*-methylamines[14] and benzoheterocycles,[15] among others.[16] The non-reductive reactions include coupling to form cyclic carbonates [17] and oxazolidinones,[18] synthesis of urea

derivatives,[19] and polymerization to non-isocyanate polyurethanes[20] and polycarbonates[21] with epoxides (Figure 1).

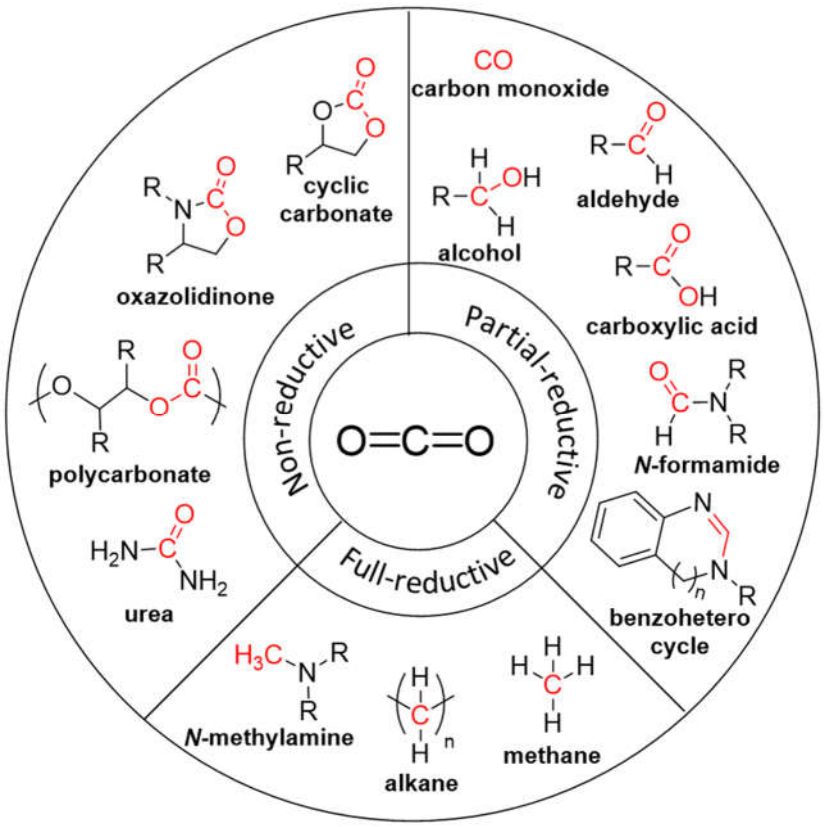

Figure 1. Selected products obtained through non-reductive and reductive transformation of CO_2.

Utilizing CO_2 as a raw material is not a new topic from an industrial point of view. More than 110 MT *p.a*. CO_2 are used in the industrial synthesis of value-added chemicals, mainly on the production of urea,[22] carbonates,[23] methane,[6] and salicylic acid.[24] The reaction between CO_2 and ammonia to produce urea was first industrialized in 1921 and is used to prepare around 150 million tons of urea annually, being the largest consumer of exhaust CO_2 emission. The synthesis of salicylic acid from phenol and carbon dioxide under basic conditions, known as Kolbe-Schmitt reaction, is the first step in the industrial synthesis of aspirin (Scheme 1). It is an even older process than the production of urea dating back to 1890.[25] Besides, the industrial production of polycarbonates (>10 Mt/yr), cyclic carbonates (0.8 Mt/yr), methanol (100 Mt/yr) from CO_2 have been achieved.[26]

From the energetic point of view, lower energy is required if CO_2 is incorporated as the entire moiety into a compound (carbonation or carboxylation reactions), while if oxidation state of the carbon atom is reduced by two units or more, the processes will be endergonic (reduction reactions).[4a] Normally catalysts are employed in all the reductive reactions and most of non-reductive reactions. The concept of catalysis was invented by Elizabeth Fulhame, her theoretical work on catalysis was regarded as "a major step in the history of chemistry". Since then, five Nobel Prizes that have been awarded for work in the field of catalysis within

the last two decades, demonstrating the great interest in catalysis research. Whereas transition metals sometimes attract most of the attention in the study of catalysis, small organic molecules without metals can also exhibit catalytic properties. The Nobel Prize in Chemistry 2021 was awarded jointly to Benjamin List and David W.C. MacMillan for the development of asymmetric organocatalysis. Nowadays organocatalysts become an indispensable component in the green chemistry toolbox.

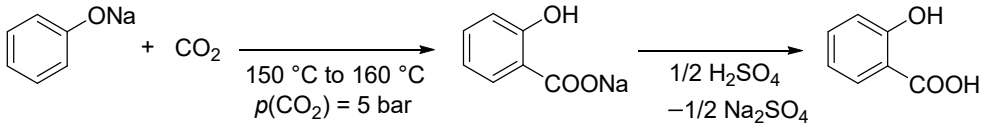

Scheme 1. Kolbe–Schmitt carboxylation of phenol to salicylic acid with CO_2.

1.2 Coupling of CO_2 and epoxides to cyclic carbonates

The coupling of CO_2 with epoxides to form cyclic carbonates (Scheme 2) is known since 1943 and commercialized since 1958, but the synthesis of cyclic carbonate is still a topic of enormous current activity. Cyclic carbonates find applications amongst others as electrolytes in Li-ion batteries,[27] intermediates for fine chemicals and raw materials for the synthesis of polycarbonates.[28] They also provide a green alternative to produce non-isocyanate polyurethanes (NIPU) in which the use of harmful isocyanates is avoided.[21, 29]

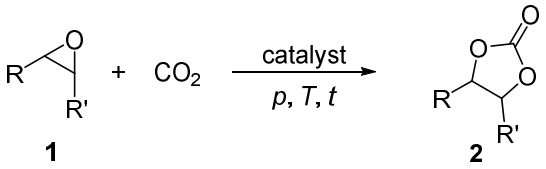

Scheme 2. Synthesis of cyclic carbonates from CO_2 and epoxides.

Cyclic carbonates can be produced via different routes. As early as 1883, Nemirowsky reported the synthesis of ethylene carbonate from highly toxic phosgene and ethylene glycol.[30] Other C1 building blocks such as dimethyl carbonate,[31] urea,[32] CO,[33] and CO_2[34] have also been converted with diols to yield cyclic carbonates. Among all the chemical routes, the currently most attractive one, especially with respect to sustainability, is the atom-economic addition of CO_2 to epoxides.[5d, 5f, 35] The addition of CO_2 to epoxides to produce cyclic carbonates complies with several of the 12 Green Chemistry Principles such as waste prevention, atom economy, safer solvents and auxiliaries, use of renewable feedstocks, etc., which makes it a promising reaction. Numerous catalytic systems have been published in this field, which were generally categorized into two approaches to achieve the transformation: the CO_2 activation mode and the epoxide activation mode. In CO_2 activation mode, normally the catalysts are carbenes,[36] and strong organic bases,[37] which activate CO_2 by forming a adduct being a nucleophile to open the ring of the epoxide and followed by ring-closure to form the cyclic carbonate (Scheme 4A). The employed catalysts are normally halogen-free, but the reaction conditions are relatively harsh. Epoxide activation is by far the

most reported strategy due to the mild reaction conditions adopted and broad substrates scope.

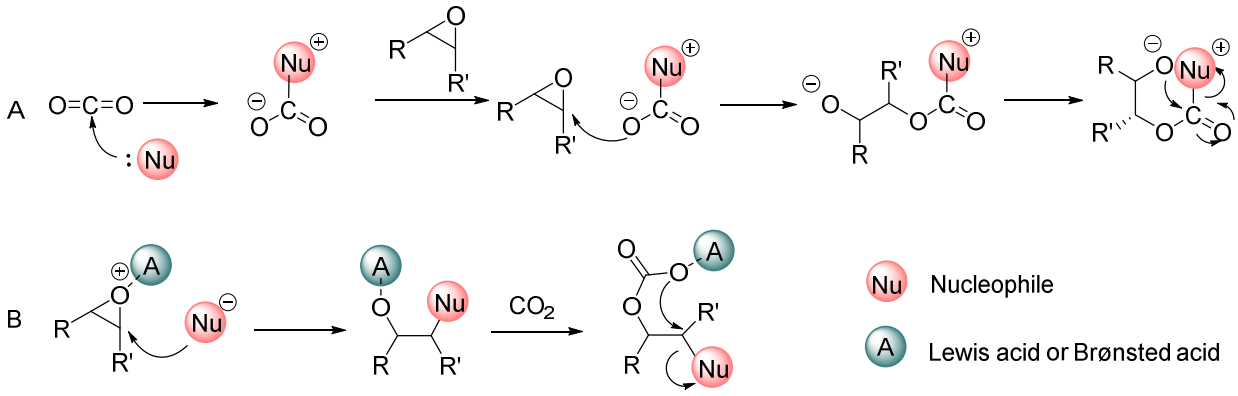

Scheme 4. Two modes of mechanism for the synthesis of cyclic carbonates.

The catalysts employed in the mode are normally Lewis or Brønsted acids (Scheme 4B).[17a, 17b, 38] The Lewis or Brønsted acid catalyst firstly coordinates to the epoxide, activating the epoxide towards ring-opening by a nucleophile. The nucleophile, acting as a leaving group, is almost always a halide and may be part of the Lewis or Brønsted acid catalyst or added separately. The resulting alcohol or alkoxide intermediate then reacts with CO_2 to form a carbonate intermediate that forms the cyclic carbonate and regenerates the catalyst. The most readily recognized difference between the epoxide activation and CO_2 activation mechanisms is in the stereochemistry of the cyclic carbonate product.[39] In epoxide activation mode the stereochemistry can be retained. In contrast, the inversion of the epoxide stereochemistry is observed in the ring-closure step in CO_2 activation mode. Comparing with heterogeneous catalysts, homogeneous ones are easier to design and study mechanistically, thus the development of new homogeneous catalysts for cyclic carbonate synthesis remains an important and widely studied area, such catalysts are discussed in more detail below.

The reported catalysts are categorized into two types: The bi-component catalysts and the one component catalysts. The bi-component catalysts normally compose of Lewis or Brønsted acid and additional halogen salts (Scheme 5). The Lewis or Brønsted acid is used for the activation of epoxides while additional halogen salts are used for the ring-opening of epoxides. Han group reported the cellulose and KI as bi-component catalysts for the transformation from epoxides and CO_2 to cyclic carbonates, illustrating that the hydroxyl groups on the vicinal carbons of cellulose play a key role for the high efficiency of the catalyst.[40] Werner group reported amino alcohols **4** and KI catalytic system in which amino alcohols are known to complex alkali metal halides might increase the solubility of the salt thus acting as a phase transfer catalyst. In addition, the hydroxyl function of the amino alcohol activates the substrate by hydrogen bonding.[41] Shirakawa group reported that the

transformation was achieved via the use of KI–tetraethylene glycol **5** as readily available catalyst, allowing the reaction to be performed at mild conditions.[42]

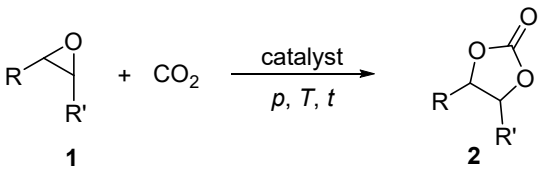

1 2

2011 Han et al.

Cellulose KI

3

reaction condition: 110 °C, 2 MPa, 1 h, catalyst: 66 wt%

2014 Werner et al.

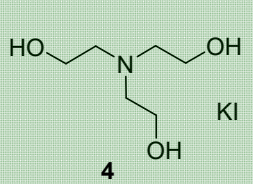

4

reaction condition: 90 °C, 1 MPa, 2 h, catalyst: 2 mol%

2018 Shirakawa et al.

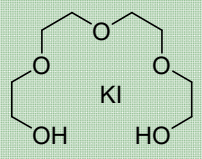

5

reaction condition: 40 °C, 1 atm, 24 h, catalyst: 10 mol%

2022 Werner et al.

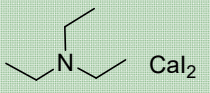

6

reaction condition: 23 °C, 1 bar, 24 h, catalyst: 5 mol%

Scheme 5. Selected bi-component catalysts of transformation from epoxides and CO_2 to cyclic carbonates.

Most recently, Werner group reported the efficient and economical catalytic system of triethylamine **6** in the combination with CaI_2. The amine and CaI_2 formed the complex, activated the epoxides and converted various substrates including challenging internal epoxides.[43]

The one-component catalysts are mostly ammonium or phosphonium zwitterion salts with or without halide anions (Scheme 6). The halogen-free catalysts go through CO_2 activation mode while halogen-containing catalysts can react by activating the epoxide under relatively mild conditions. The one-component organocatalysts **7** bearing an ammonium betaine framework have been developed by Sakai group for the activation of CO_2 and epoxides to

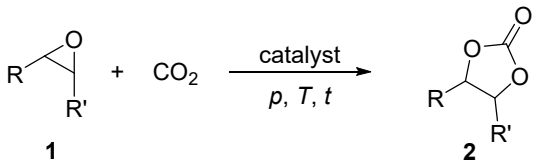

1 2

2010 Sakai et al.

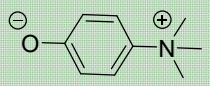

7

reaction condition: 90–120 °C, 1 MPa, 24 h, catalyst: 3 mol%

2015 Lu et al.

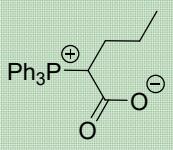

8

reaction condition: 25 °C,1 atm, 6 h, catalyst: 5 mol%

2017 Werner et al.

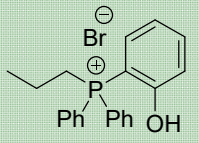

9

reaction condition: 80 °C, 2.5 MPa, 24 h, catalyst: 5 mol%

2022 Wu et al.

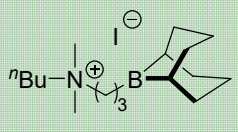

10

reaction condition: 120 °C, 20 bar, 6–24 h, catalyst: 0.02–0.20 mol%

Scheme 6. Selected one-component catalysts of transformation from epoxides to cyclic carbonates.

produce cyclic carbonates.[44] The transformation can be achieved under 1 MPa and 90–120 °C in the absence of halide anions, the adduct of catalyst **7** and CO_2 activates the epoxide via mechanism A (Scheme 4) to give the product. Lu et al. isolated the adduct of phosphorus ylide and CO_2 and used as the halogen-free catalyst **8** for the transformation, allowing the reaction to be performed at extremely mild conditions of 25 °C and 1 atm.[45] The group of Werner reported the phosphonium salts bifunctional catalyst **9** for the conversion of fatty acid esters and CO_2 to the respective cyclic carbonates. The catalytic system was then used to produce eight carbonated fatty acid methyl esters and even four carbonated vegetable oils in excellent isolated yields.[46] Most recently Wu and co-workers developed an ammonium salt organocatalyst **10** converting epoxides to cyclic carbonates in the presence of only 0.02–0.20 mol%.[35d] Although the homogenous catalysts exhibited high activity towards the reaction, the separation and recycling of homogenous catalysts is generally challenging. In some cases, it is possible to separate the catalyst from the cyclic carbonate by distillation.[35d, 47] However, for higher boiling cyclic carbonates the thermal stress might lead to decomposition of the catalyst.

1.3 *N*-Formylation of amines with CO_2

N-formamide derivatives are attractive chemicals with extensive applications in pharmaceutical industry, biosciences, agrochemicals, etc.[48] In chemical industry, they are important intermediates for transforming into other valuable materials such as isocyanides,[49] benzoheterocycles, valuable reagents in Vilsmeier reaction[50] and allylation reaction.[51] In nature, formamide, formed by HCN and H_2O is regarded as a key prebiotic precursor and the origin of life.[52] Formamide derivatives, such as *N*-methylformamide and *N*,*N*-dimethylformamide (DMF) are most commonly used solvents.

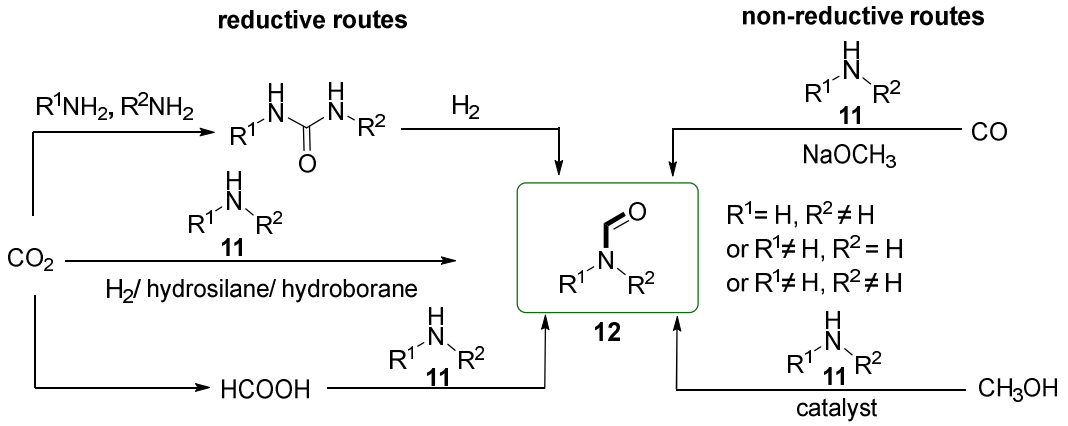

Figure 2. The synthesis routes of formamides.

Industrially, formamides are produced by amines with toxic and flammable CO in methanol in the presence of catalyst $NaOCH_3$ (Figure 2).[53] The transformation can also be achieved by cross-coupling reaction between amines and methanol.[54] Urea,

the major product of CO_2 in the CCU chemical process paths, can be converted to formamides through hydrogenation reduction reaction.[55] Also, formamides can be obtained by the reaction between amines and formate, which is industrially produced from CO_2.[56] Compared with the methods with dangerous reagents or indirect synthesis from CO_2, direct reductive functionalization of CO_2 with amines and reductants to produce formamides is a promising methodology to prepare *N*-formamides. H_2, hydrosilanes and hydroboranes are the most dominant reductants. Using hydrosilanes or hydroboranes as reductants for the transformation is appealing in the synthesis of fine chemicals, especially considering the safety and high expense of high-pressure techniques required by employing H_2, although the disposal of accompanying by-products and possible isolation process of hydrosilanes or hydroboranes are also problematic. Employing PMHS as reducing agent is one of the solutions in terms of the workup and expense because PMHS is an abundant, low cost, nontoxic, and highly moisture stable chemical waste from silicone industry.[25] It is cheaper and more easily removed compared to phenylsilanes that were widely used in the fixation of CO_2 into amines in previous reports.

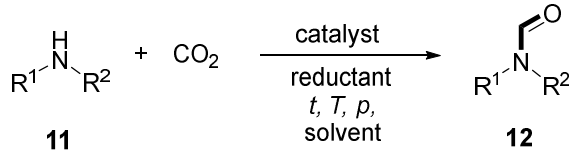

11 **12**

Scheme 7. *N*-formylation of amines with CO_2 and reductant.

Chemists have developed many efficient methods and catalysts for the conversion of CO_2 into formamides (Scheme 8 and Table 1). The organocatalysts for the *N*-formylation reaction can be generally categorized into several groups. The first category is organic strong bases. The reported catalysts for the conversion including TBD (**13**) [57] and DBU (**14**) [58] (Entries 1 and 2). In 2012, Cantat group reported the first strong base catalyst that using TBD as catalyst for the *N*-formylation reaction of CO_2 and amines at 100 °C and solvent-free condition (Entry 1). In the reported mechanisms, CO_2 was activated by TBD by forming adducts in the form TBD–CO_2, which have been hypothesized to allow CO_2 reduction by the hydrosilanes to silylformate intermediate. A second example is the use of DBU as catalyst which allows the employment of PMHS as reducing agent (Entry 2). The second category of organocatalysts is *N*-heterocyclic carbenes (NHCs). They were also reported to form the stable adducts with CO_2, facilitating their reduction. In 2012, the group of Cantat reported IPr NHC **15** catalyst which is more efficient than TBD, allowing the reaction to be performed at room temperature and showed tolerance to more substances, including imines, hydrazines and hydrazones (Entry 3).[59] Dyson and co-workers developed a thiazolium carbene **16** catalyst for the *N*-formylation of primary amines under mild condition using PMHS as reducing agent (Entry 4).[60] Their mechanistic studies illustrated that NHCs acted as

Lewis bases in the same way as organic bases: NHCs bound CO_2 and then the NHC–CO_2 adducts nucleophilically activated of the hydride of reducing agents to form the intermediate silylformate, which gave the formylated products through the nucleophilic attack by amines.

Besides the above-mentioned two types of catalysts, NHC-silyliumylidene cation complex **17**,[61] 1,3,2-diazaphospholene **18**,[62] $B(C_6F_5)_3$ **19** [63] are all reported active for the transformation via CO_2 activation. NHC-silyliumylidene cation complex **17** prepared by So's group recently, was proved to follow the CO_2 activation mode. The DFT calculation support that the Si lone pair electrons of the complex catalyst interacted with CO_2 to form a new adduct complex and the Si−H bond of $PhSiH_3$ inserts into the C−O bond subsequently to form the same intermediate (Entry 5). 1,3,2-diazaphospholene **18** and $B(C_6F_5)_3$ **19** followed the different reaction pathway or CO_2 reduction mechanism from other metal-free catalysts for

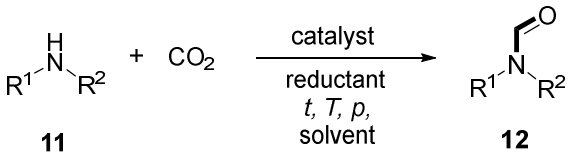

CO_2 activation:

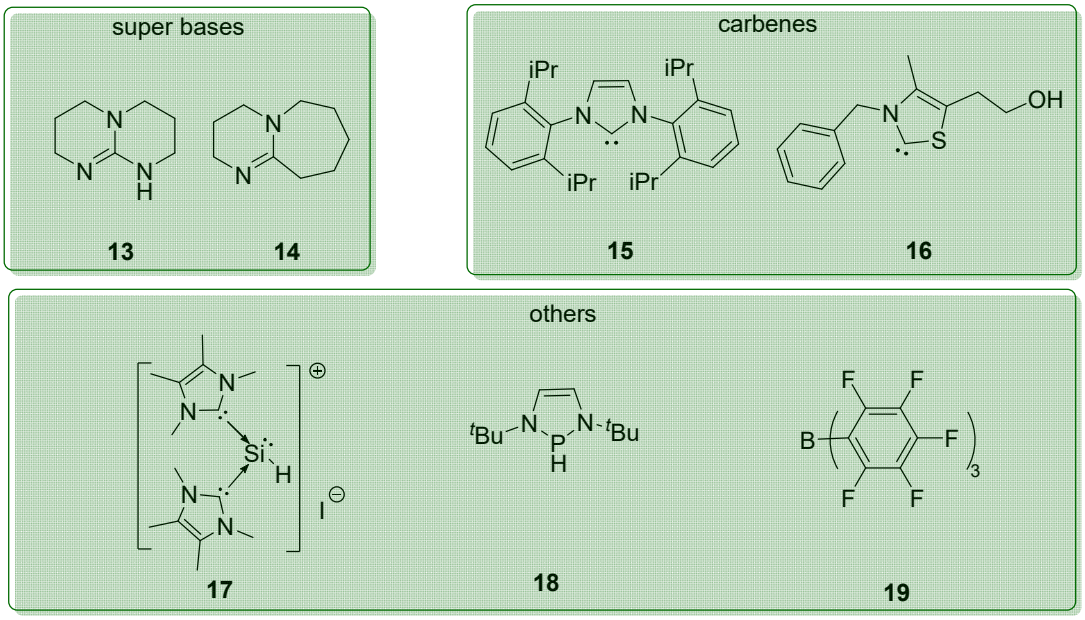

Reducing agents activation:

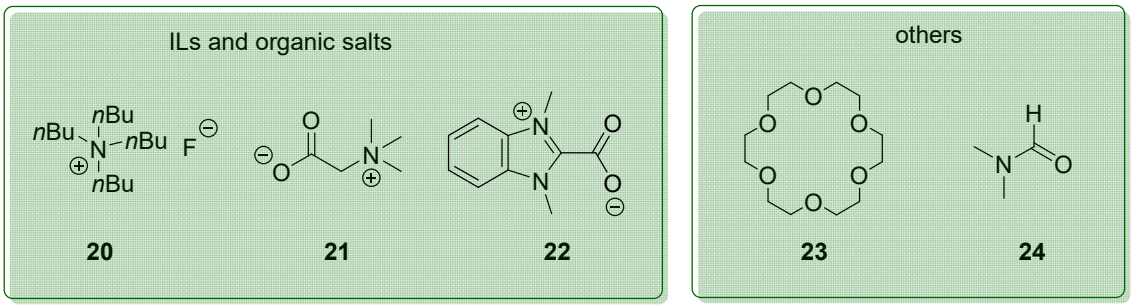

Scheme 8. Representative organocatalysts for *N*-formylation reaction.

N-formylation (Entries 6, 7). In the mechanistic study of 1,3,2-diazaphospholene **18**, CO_2 was proposed to directly insert into the strongly polarized $P^{\delta+}$–$H^{\delta-}$ bond of 1,3,2-diazaphospholene 18, followed by the transfer of formate to a hydrosilane reducing agent, which generated the silylformate intermediate and regenerated the 1,3,2-diazaphospholene. The $B(C_6F_5)_3$ **19** catalyst was proposed to promote carbamate salt formation from CO_2 and amines through binding boron center to the oxygen atom of carbamate and followed by the direct reduction of the carbamate by the hydroborane reducing agent. The third group of organocatalysts includes ionic liquids (ILs) and other organic salts which are the most reported in the past ten years. Almost all the reported ILs and organic salts are reducing agent activation mode. In 2016, Dyson reported the transformation catalyzed by TBAF **20** at room temperature and 0.1 MPa (Entry 8).

Table 1. Representative organocatalysts and reaction conditions for *N*-formylation reaction.

Entry	cat. (mol%)	*T*/ °C	*t*/ h	*p*(CO_2)/ bar	Reductant (equiv.)	Subtract	Yield%	Ref.
1	**13** (5)	100	24	1	$PhSiH_3$ (1)	*N*-Methylaniline	40	[57]
2	**14** (10)	30	72	1	PMHS (8)	*N*-Methylaniline	84	[58]
3	**15** (5)	r.t.	24	1	$PhSiH_3$ (3)	*N*-Methylaniline	99	[59]
4	**16** (7.5)	50	24	1	PMHS (200 μL)	Ethylphenylalaninate	90	[60]
5	**17** (5)	40	3	1	$PhSiH_3$ (2)	*N*-Methylaniline	85	[61]
6	**18** (5)	r.t.	4	1	Ph_2SiH_2 (3)	*N*-Methylaniline	95	[62]
7	**19** (0.08)	80	4	10	$Me_2NH\cdot BH_3$ (2)	*N*-Methylaniline	87	[63]
8	**20** (5)	30	4	1	$(EtO)_3SiH$ (4)	*N*-Methylaniline	87	[64]
9	**21** (10)	50	18	10	Ph_2SiH_2 (2)	*N*-Methylaniline	92	[65]
10	**22** (5)	r.t.	12	1	$PhSiH_3$ (2)	*N*-Methylaniline	85	[66]
11	**23** (20)	90	6	20	$PhSiH_3$ (2)	Aniline	99	[15b]
12	**24** (−)	50	24	10	BH_3NH_3 (3)	*N*-Methylaniline	91	[67]

The fluorine anions activated the silica center of hydrosilane to liberate hydride instead of initially activating CO_2.[68] The same activation mode was also observed in betaine **21** and derivatives (Entry 9).[65, 69] The mechanistic study showed the catalyst acted as nucleophile directly to activate the hydrosilane, followed by the CO_2 insertion to form the same

intermediate silylformate. The adduct of *N*-heterocyclic carbene and CO_2 **22** was isolated by Yang's group and used as the catalyst in the transformation under mild conditions (25 °C, 1 atm CO_2) with hydrosilane as a hydrogen source (Entry 10).[66] Apart from the above mentioned category, other examples such as crown ether and polar aprotic solvents are reported to be able to enhance the reaction or be used independently to achieve the transformation, so in some cases *N*-formylation reaction can be performed "catalyst free" in these solvents.[67, 70] In 2023, Xu group reported that 18-Crown-6 **23** activated the hydrosilane by forming a semi-enclosed adduct, in which three of the oxygen atoms are bonded to the silica center (Entry 11).[15b] DMF **24** was reported to form the intermediate with BH_3NH_3 to lower the transition state and enabled to attack CO_2 easily, to some extent, DMF played the role of the catalyst (Entry 12).

In all cases, at first CO_2 is reduced by the respective reducing agents, such as hydrosilane or hydroborane, to silylformate or borylformate intermediates. Second, the amine nucleophilically attacks the carbon of carbonyl group to give the product. Nevertheless, the formation of the intermediate follows different pathways and can be summarized as the CO_2 activation mode A and reducing agent activation mode B (Scheme 9). The CO_2 activation normally requires a nucleophile bearing unpaired electrons to form an adduct with CO_2 which facilitates the reduction by the reducing agent. The reducing agent is normally activated by anions, mostly oxygen-containing anions, and then liberates a hydride, transferring to the inserted CO_2 to form the intermediate.

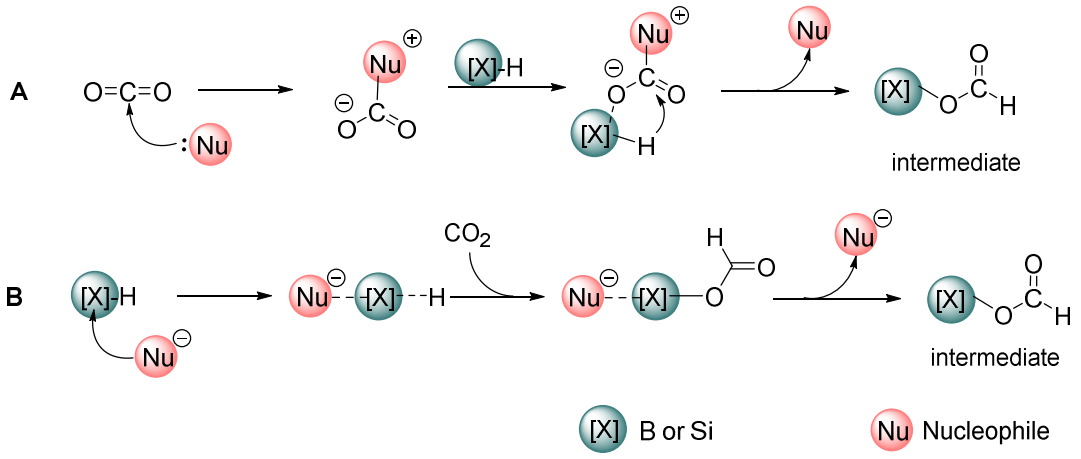

Scheme 9. The two plausible reduction modes. A: CO_2 activation mode. B: Reducing agent activation mode.

Benzoheterocycles are ubiquitous motifs in natural products and biologically active molecules, for which they have gained considerable attention.[71] Especially benzimidazoles, find wide application in antimicrobial compounds, anthelmintic and antipsychotic drugs, antiulcer and anticancer agents, such as Liarozole, Lansoprazole, Flubendazole and Bendamustine hydrochloride. The synthesis of benzimidazoles or other benzoheterocycles by cyclization of *o*-phenylenediamines with CO_2 and reducing agents has been revealed using

similar catalysts employed for *N*-formylation reaction, such as NHC, zwitterion salts, or $B(C_6F_5)_3$. However, Some *N*-formylation catalysts, such as DBU **13** and TBD **14**, were reported to be efficient for the *N*-formylation reaction but no reports showed their activities for the cyclization reaction. The synthesis of benzoheterocycles from CO_2 and diamines in the presence of organic reducing agents goes through a two-step reaction. For instance, the formation of the benzimidazoles: initially, the monoformylation of *o*-phenylene diamines **25a** leads to the formylated product **26a** and followed by the subsequent cyclization reaction to give the benzimidazoles product **27a** (Scheme 10). Although the cyclization reaction is based on the *N*-formylation reaction, a part of catalysts active for *N*-formylation reaction are incompatible with cyclization reaction.

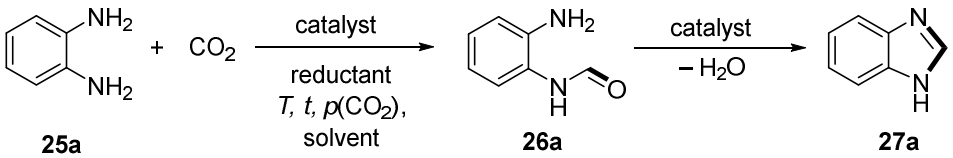

Scheme 10. Two individual steps of benzimidazole synthesis by the tandem *N*-formylation-cyclization reaction.

The *N*-heterocyclic carbene **15** was reported to catalyze the *N*-formylation reaction efficiently in combination with $PhSiH_3$ by Cantat and then was reported to be active for cyclization reaction in the presence of PMHS by the same group (Table 2, entry 1).[72] Although the same catalysts were employed in both *N*-formylation reaction and cyclization reaction, the cyclization reaction normally needed higher temperature or more catalyst loading. For instance, $B(C_6F_5)_3$ **19** is active for both *N*-formylation reaction and cyclization reaction, however, cyclization reaction needed to be performed under harsher conditions (120 °C, 10 mol%) than the *N*-formylation reaction (80 °C, 0.08 mol%) (Entry 2).[73] In 2021, the group of Yang developed the NHC-CO_2 adduct **22** catalyst for the cyclization reaction, allowing the reaction to be performed at room temperature and 1 bar of CO_2 (Entry 3).[66] The group of Dyson revealed that the organic salt [TBA][OAc] had significant activity on first *N*-formylation step but had no effect on the cyclization of *N*-(2-aminophenyl)formamide to benzimidazole.[74] Therefore, different catalytic strategies for the two steps are required for cyclization reaction from *o*-phenylenediamines, such as DMF **24** and DMSO **28** which are solvents highly active for formylation reaction but presented low conversion to benzoheterocycles, thus NaOH and BBr_3 were needed in the second step (Entries 5 and 6).[74-75] In 2023, Gao and co-workers developed a catalytic system with aminoguanidine **29** as catalyst for the transformation, the reaction was performed at 100 °C for 6 hours (Entry 7).[76]

Table 2. Representative organocatalysts and reaction conditions for cyclization reaction.

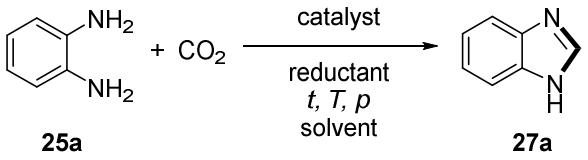

25a **27a**

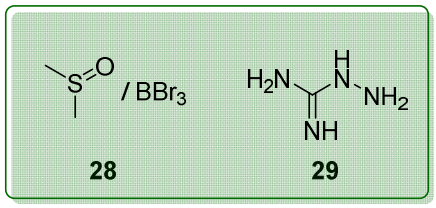

28 **29**

Entry	cat. (mol%)	*T*/ °C	*t*/ (h)	$p(CO_2)$/ bar	Reductant (equiv.)	Yield (%)	Ref.
1	**15** (5)	70	24	2	PMHS (3)	90	[72]
2	**19** (10)	120	24	10	$PhSiH_3$ (4)	83	[73]
3	**22** (5)	25	24	1	$PhSiH_3$ (3)	96	[66]
4	**23** (10)	90	16	20	Et_3SiH (2)	79	[15a]
5	**24** (–)	80	18 (1)	10	BH_3NH_3 (1)	94	[75]
6	**28** (–)	70	6 (2)	1	$PhSiH_3$ (1)	93	[74]
7	**29** (10)	100	6	1	$(EtO)_3SiH$ (5)	97	[76]

1.4 *N*-Methylation reaction of CO_2 and amines

The *N*-methylation reaction is an important reaction in the modulation of biological functions of proteins and late-stage isotope labeling in the pharmaceutical industry.[77] Carbon isotope-labelled methylated drug compounds are commonly used for the measurement of the absorption, distribution, metabolization and excretion.[48b, 78] The *N*-methyl unit is an integral and ubiquitous motif in 17 drug molecules of the top 200 selling medications in 2022, and it plays a vital role in the functionalities of these life science molecules.[79] The *N*-methylation reaction can be achieved by both a non-reductive route and a reductive route (Scheme 11). The methylation agents, such as methyl iodide,[80] diazomethane,[81] dimethyl sulfate,[82] and dimethyl carbonate,[83] are employed in the non-reductive *N*-methylation reaction with amines to give the methylated amines directly, however, most of those reagents are toxic or explosive. Besides, *N*-methylated amines can be obtained from amines via Eschweiler–Clarke reaction by using excess formic acid and formaldehyde.[84] *N*-methylamines or *N*-methylanilines are prepared industrially from amines or anilines with methanol in the presence of an acid catalyst.[23]

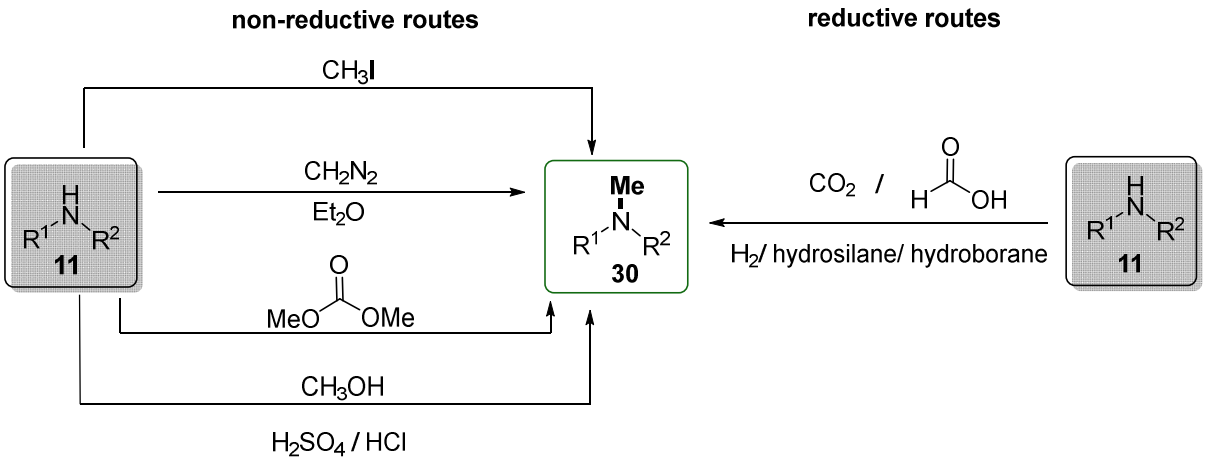

Scheme 11. The synthesis routes to *N*-methylamines.

In the reductive *N*-methylation reaction, the transformation is achieved by employing methylation agents, normally CO_2 or formic acid, in combination with reducing agents, such as H_2, hydrosilanes and hydroboranes.[85] The reductive *N*methylation reaction can avoid the use of toxic methylation agents mentioned above. Recently the use of CO_2 as methylation agent for *N*-methylation reaction has attracted considerable attention and researchers are committed to develop various high-efficienct catalysts. Although the *N*-methylation reaction conditions have not been optimized for all *N*-formylation catalysts, the conversions to methylated products were observed with TBD (**13**),[86] DBU (**14**),[58] carbenes **15**,[13a] $B(C_6F_5)_3$ (**19**),[87] TBAF (**20**),[64] and glycine betaine **21**[65]. The study of the mechanism focused on the transformation with hydrosilanes more than with hydroborane, and the pathways with hydroborane varied, thus only the mechanism in the presence of the hydrosilane is summarized here. Although several speculated pathways of *N*-methylation have been proposed, only two of them are supported by DFT calculations and experiments (Scheme 12). Path I: Majority of metal and metal free catalytic systems are proved via this pathway, such as DBU (**14**), $B(C_6F_5)_3$ (**19**), TBAF (**20**), Cs_2CO_3 , $[Mn_2(CO)_{10}]$. The *N*-formamide **12** is formed and further reduced to *N*-methylamine **30** by the silane. The control experiments were performed with TBAF (**20**), the intermediate silylformate was successfully prepared from CO_2 and trimethoxysilane, *N*-methylformanilide was obtained from silylformate and *N*-methylaniline quantitatively even without catalyst, and then the obtained *N*-methylformanilide was fully converted to *N,N*-dimethylaniline in the presence of catalyst and phenylsilane.[64]

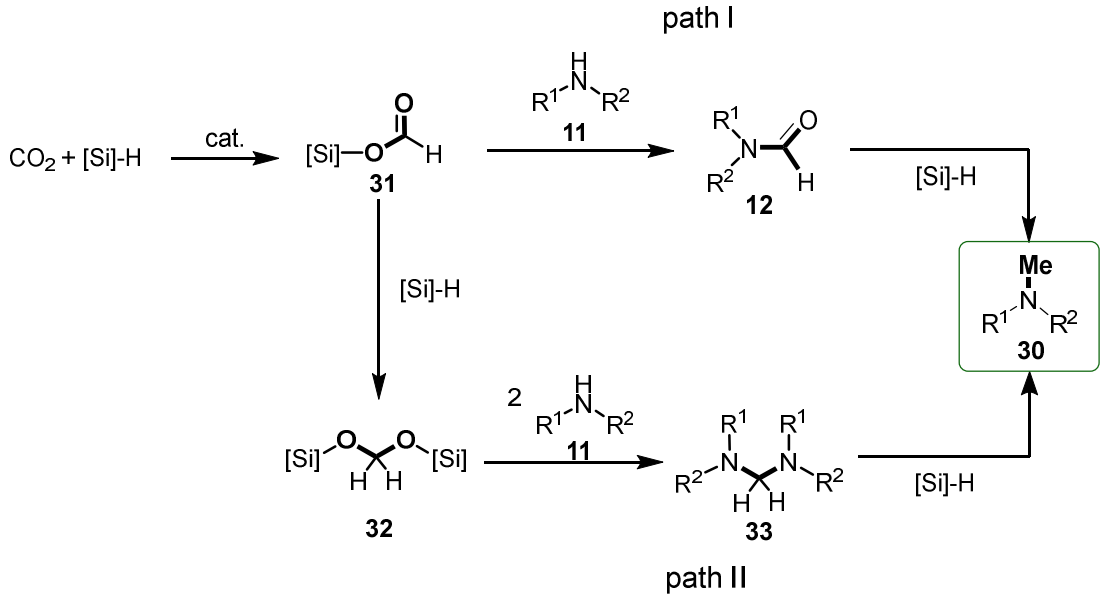

Scheme 12. The pathways from silylformate to *N*-methylamines.

Path II: The silane is reduced to silylacetal **32**, which reacts with the amine to afford the aminal **33**. The sustainable organocatalyst glycine betaine **21** afforded formamides, aminals and methylamines under different conditions. However, formamides cannot afford methylamines or aminals in the presence of catalyst, instead, the silylacetal is observed in the reaction.[65] In addition, aminals were obtained under CO_2 deficiency, which is the evidence of being the intermediate. Besides these two pathways, urea as intermediate was also proposed,[88] but it is never proved in an organocatalytic systems. However, all pathways proceed by a silylformate intermediate which is supported by experimental and computational evidence. The various catalysts will be discussed in more detail below.

The first metal-free catalyst for *N*-methylation reaction was reported by the Cantat group in 2014, using Verkade super base **34** as catalyst which allowed the reaction to be performed at 90 °C for only 1 hour (Entry 7).[14c] In 2021, a mesoionic *N*-heterocyclic olefin **35** was developed as an efficient catalyst for this procedure converting primary and secondary amines to methylated products at 40 °C for 24 hours (Entry 8).[14a] Most recently, Gao successively reported the catalysts 6-amino-2-picoline (**36**) and *N,N'*-diisopropylcarbodiimide (**37**) for *N*-methylation reaction (Entries 9 and 10).[89] The hydroboranes were employed in all the above examples as reducing agent, which revealed that hydroboranes improved the formation of methylated products. Notably, both *N*-methylation and *N,N*-dimethylation of primary amines are selectively achieved using *N,N'*-diisopropylcarbodiimide (**37**) as catalyst. In the presence of hydrosilanes and suitable catalysts, normally both methylated and formylated products were observed by varying reaction conditions.

Table 3. Representative organocatalysts and reaction conditions for *N*-methylation reaction.

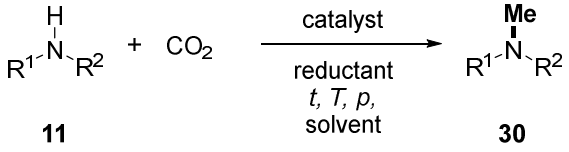

11 30

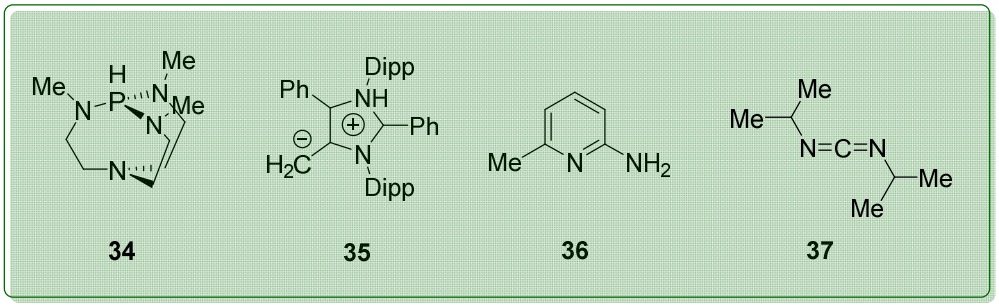

34 35 36 37

Entry	cat. (mol%)	*T*/ °C	*t*/ (h)	*p*(CO_2)/ bar	Reductant (equiv.)	Subtract	yield%	Ref.
1	**14** (1)	100	48	1	PMHS (10)	*N*-Methylaniline	88	[58]
2	**15** (5)	50	24	1	Ph_2SiH_2 (3)	*N*-Methylaniline	91	[13a]
3	**19** (5)	140	24	5	$PhSiH_3$ (2)	*N*-Methylaniline	80	[87]
4	**20** (5)	50	12	1	$PhSiH_3$ (3)	*N*-Methylaniline	90	[64]
5	**21** (5)	70	12	1	Ph_2SiH_2 (4)	*N*-Methylaniline	92	[65]
6	**24** (–)	90	24	1	$PhSiH_3$ (2)	*N*-Methylaniline	80	[90]
7	**34** (1)	90	1	1	9-BBN (4)	*N*-Methylaniline	91	[14c]
8	**35** (5)	40	24	1	9-BBN (4)	*N*-Methylaniline	80	[14a]
9	**36** (10)	95	10	1	BH_3NH_3 (4)	Aniline	86	[89b]
10	**37** (10)	100	10	1	$BH_3 \cdot NMe_3$ (4)	*N*-Methylaniline	65	[89a]

1.5 Tunable *N*-methylation reaction and *N*-formylation reaction

The controllable reaction between *N*-formylation and *N*-methylation catalyzed by organocatalysts or metal catalysts with ligands has been reported to selectively prepare products by changing temperature, pressure, amine, solvent, reductant and/ or the base (Table 4).[91] With TBAF **20**, the methylated product was obtained with the stronger reducing agent phenylsilane while weaker trimethoxysilane only led to formylated product (Table 4, entry 4).[64] This selectivity may be due to the different energy barriers, the energy barriers of 6 e^- *N*-methylation reaction is higher than that of 2 e^- formylation reaction, which requires

a stronger reducing agent. However, catalysts and higher temperature can improve the transformation to methylated products. For instance, amines converted to formylated products under catalyst-free and converted to methylated products in the presence of 6-amino-2-picoline (**36**).[89a] The selectivity in path II may be attributed to the relative rates of CO_2 reduction to silyl formate, silyl formate reduction to silyl acetal and the reaction of the silylformate with the amines, therefore, the procedure is more complicated and difficult to be tuned. More specifically, in the catalytic system proved for path II, almost all of methylation reactions are favored by high temperature, for example in the presence of the

Table 4. Comparison of reaction conditions for *N*-methylation reaction and *N*-formylation reaction.

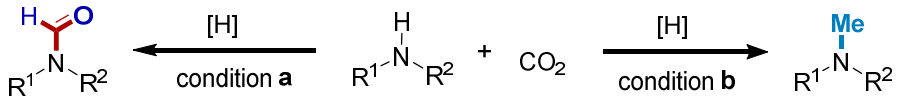

12 **11** **30**

Entry	cat.	Conditions	cat. Loading (mol%)	T/ °C	t/ (h)	p(CO_2)/ bar	Reductant (equiv.)
1	**14**	**a**	10	30	72	1	PMHS (8)
		b	1	100	48	1	PMHS (10)
2	**15**	**a**	5	r.t.	24	1	$PhSiH_3$ (3)
		b	5	50	24	1	Ph_2SiH_2 (3)
3	**19**	**a**	0.08	80	4	10	$Me_2NH \cdot BH_3$ (2)
		b	5	140	24	5	$PhSiH_3$ (2)
4	**20**	**a**	5	30	4	1	$(EtO)_3SiH$ (4)
		b	5	50	12	1	$PhSiH_3$ (3)
5	**21**	**a**	10	50	18	10	Ph_2SiH_2 (2)
		b	5	70	12	1	Ph_2SiH_2 (4)
6	**24**	**a**	–	50	24	10	BH_3NH_3 (3)
		b	–	90	24	1	$PhSiH_3$ (2)

DBU catalyst (**14**), methylated products were obtained at 100 °C which is much higher than the temperature for the formylated reaction (30 °C) (Entry 1).[58] Also, in the CO_2 reduction reaction catalyzed by betaine (**21**), the *N*-methylation was performed at 70 °C under 1 bar, while the temperature of *N*-formylation reaction was 70 °C, however, the pressure of *N*-formylation reaction was increased to 10 bar (Entry 5).[65] In the previous reports, it is interesting to observe that formylation reaction is favored by solvent free conditions. When TBD (**13**) was employed as catalyst for *N*-formylation reaction, higher yields were obtained without solvents for all the substrates.[57] In addition, the solvent has a noticeable influence on the conversion in the *N*-methylation reaction and higher yields are observed for polar solvents.[92]

2 Objectives of this work

The conversion of CO_2 to value-added products is favorable for both greenhouse gas mitigation and carbon resource utilization. However, due to the chemical stability of CO_2, the main challenge of CO_2 utilization is to convert CO_2 efficiently, selectively, and economically to highly valuable products. Phosphonium salts are easily accessible and frequently used intermediates, and long known phase-transfer organocatalysts.

To meet the challenge of CO_2 utilization the first target of this work is developing the phosphonium salts catalyzed protocol for CO_2 non-reductive coupling with epoxides to prepare cyclic carbonates, allowing the reaction to be performed at room temperature. This protocol should be able to be applied for the synthesis of dropropizine via cyclic carbonate.

In the field of homogeneous catalysis, the recycling of catalysts has been the major challenge. Thus, the second target is to attach fluorinated chains to the efficient phosphonium salt catalyst to facilitate the recyclability of homogeneous catalysts from the coupling reaction of epoxides and CO_2.

CO_2 reductive coupling with amines to formamides and methylamines normally need long reaction time, high catalyst loading, high reaction temperature, and/or pressure. The target of CO_2 reduction reaction is design and synthesis of more efficient organocatalysts for the reactions allowing the reaction to be performed at mild condition such as ambient pressure, room temperature as well as low catalyst loading. In addition, it is an important target that exploring more economical catalytic systems employing cost-effective PMHS to replace other expensive hydrosilanes or hydroboranes as reducing agent.

Mechanistic study facilitates to gain deeper insights in the reaction procedure as well as provide information for further catalyst development. Therefore, the mechanism of catalytic cycle and the pathway of *N*-formylation and *N*-methylation reactions with CO_2 need to be revealed, which is the final target.

3 Results and Discussion

3.1 Phosphonium salt catalyzed CO_2 coupling reaction with epoxides.[38d]

Quaternary phosphonium salts have been extensively used in organic synthesis as organocatalysts.[93] Bifunctional phosphonium iodide salts bearing a phenol group are proved to be excellent catalysts in synthesis of cyclic carbonates in previous reports.[94] Based on the previous work in the group, the bifunctional phosphonium salts with a phenolic moiety **38** was prepared and used for the synthesis of antitussive agent dropropizine, which is employed as a racemic mixture in several commercial cough suppressants.[95] In general, it is reported to be synthesized from *N*-phenyl-piperazine and glycerol-1-tosylate.[96] Another reported route for preparing it is direct amination of solketal via ruthenium-catalyzed hydrogen borrowing reaction and subsequent ketal hydrolysis.[97] Herein, the epoxide **1a** was obtained from phenylpiperazine and the respective epichlorohydrin. The subsequent conversion under the standard reaction conditions for terminal epoxides gave the respective carbonate **2a** in 65% after 48 h (Scheme 13). The subsequent cleavage of the carbonate protecting group under basic conditions gave dropropizine **39a** in the total yield of 62%. The formation of carbonate without purification and subsequent cleavage of the carbonate to obtain dropropizine **39a** could lead to in 61% yield.

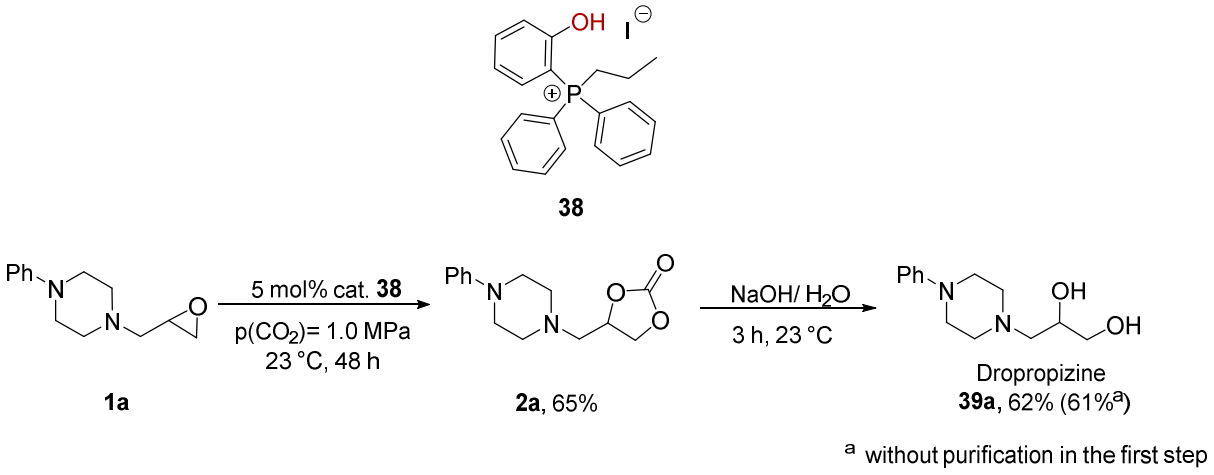

Scheme 13. Synthesis of dropropizine via cyclic carbonate.

Since the high efficiency of catalyst **38** was proved, the fluorinated chains were attached to the organocatalyst **38** to facilitate the separation of the catalyst. The fluorinated bifunctional organocatalyst **40** with the fluorine contents of 38% were prepared by alkylation of the corresponding phosphine. The commercially available phosphine with perfluorinated side chains was alkylated with 2-iodoethanol to give the desired salt **41** with the fluorine contents of 55%. The prepared catalysts were tested in the conversion of CO_2 with butylene oxide (**1b**) at room temperature, under solvent-free conditions (Table 4). At room temperature the catalyst **40** (2 mol%), with a lower fluorine content, led to the desired product **2b** in moderate yields of 55%, respectively (Entry 1). In the presence of catalyst **41,** which has a fluorine content of 55%, only traces of **2b** were obtained (Entry 2). This might be explained

by the observed low solubility of **41** in the epoxide **1b** at room temperature. Excellent yields of up to 98% were achieved by increasing the catalyst loading of **40** to 5 mol% (Entry 3). Notably, at a low CO_2 pressure of 0.1 MPa, **2b** was obtained in 52% at 23 °C in the presence of **39** (Entry 3). In the presence of **41** a yield of 30% was achieved (Entry 4). This is in agreement with previous studies in which catalysts with a phenolic hydroxyl group in the *ortho* position to the phosphonium moiety show higher activity compared to 2-hydroxyethyl-functionalized salts.[94a] Excellent yields of >90 % were achieved with catalysts **40** and **41** when the reaction temperature was increased to 45 °C (Entries 5 and 6). Compared to the solvent-free conditions a similar yield of 99% for **2b** was obtained in the presence of **40** (5 mol%) when perfluorodecalin was used as the solvent (Entry 3).

Table 4. The reaction parameter screening and catalyst screening.

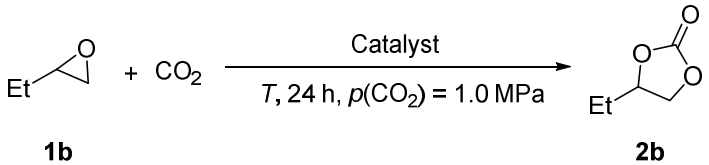

1b **2b**

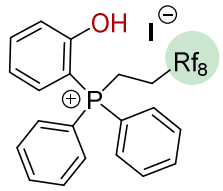

40

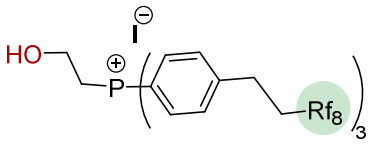

41

Entry	Catalyst	T (°C)	Catalyst loading (mol%)	Yield[a] (%)
1	**40**	23	2	55
2	**41**	23	2	<5
3	**40**	23	5	98, 99[b], 52[c]
4	**41**	23	5	30
5	**40**	45	5	99
6	**41**	45	5	93

Reaction conditions: 1.0 equiv. epoxide **1b** (6.9 mmol), 2–5 mol% catalyst, 23–45 °C, 24 h, $p(CO_2)$ = 1.0 MPa, solvent-free. [a] Yields determined by ^{1}H NMR spectroscopy with mesitylene as internal standard. [b] $p(CO_2)$ = 0.1 MPa. [c] Perfluorodecalin (1 mL) was used as solvent.

We studied the recyclability of catalyst **40** in the conversion of 4-fluorostyrene oxide **2c** at 23 °C. After 30 h reaction time perfluorodecalin and toluene were added to dissolve the product **2c** and 73% of the catalyst was reisolated as a solid by simple filtration (Figure 3A). In the second run, the amount of substrate was adjusted to the amount of catalyst which

was reisolated. Surprisingly the yield of **2c** dropped to 37%. The deactivation of the catalyst and low yield of product is caused by the formation of the halohydrin, which was confirmed by GC-MS. To restore the dehydrohalogenated catalyst, the recycled catalyst was treated with an aqueous solution of hydrogen iodide. Utilizing the regenerated catalyst in the third run afforded a yield of 81% for **2c**.

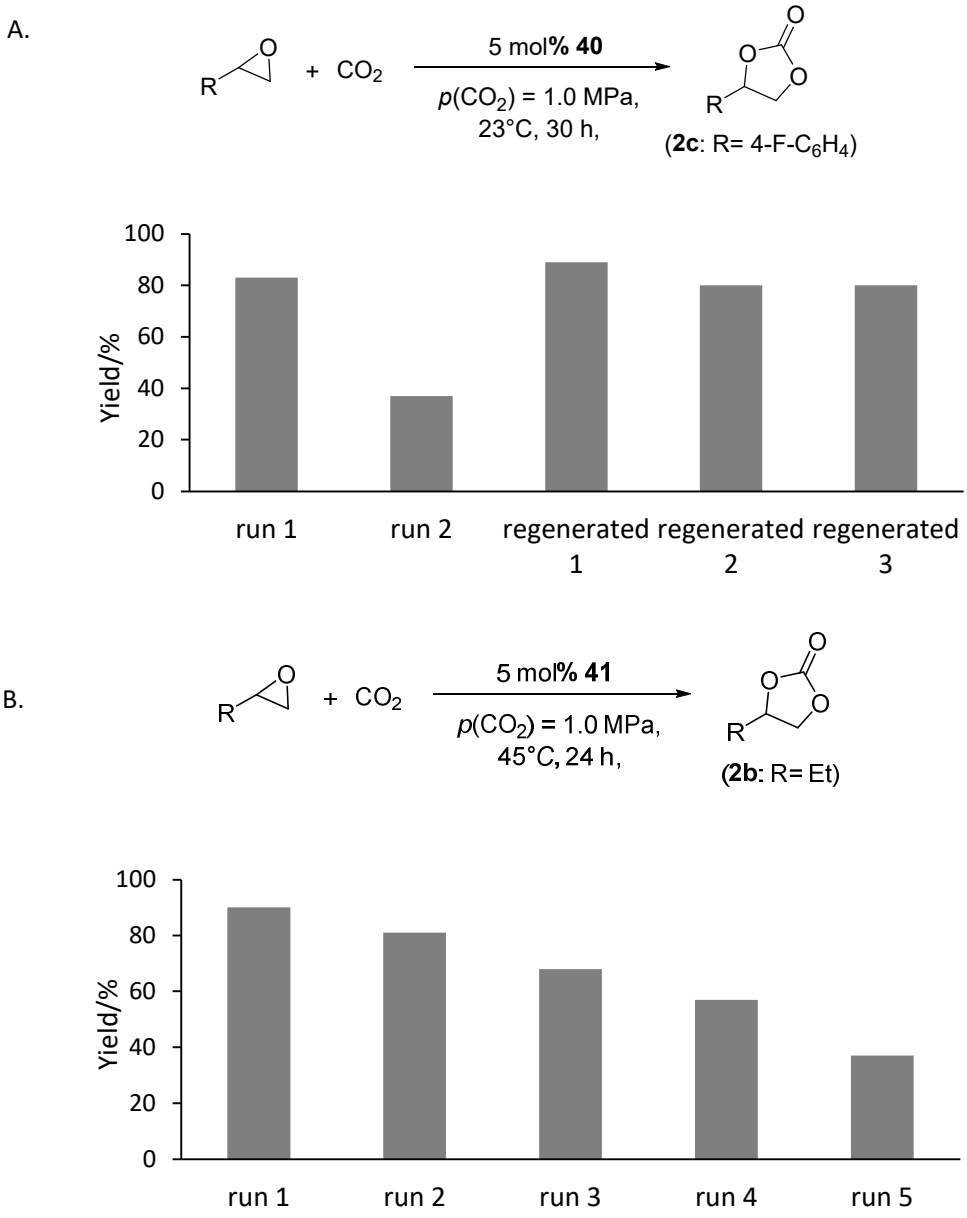

Figure 3. Recycling of catalyst **40** and **41**. Reaction conditions A: **1c** (5.8 mmol), 5.0 mol% **40**, 23 °C, 30 h, 1.0 MPa CO_2, 1.0 mL perfluorodecalin and toluene. Yields were determined by ^{1}H NMR spectroscopy with mesitylene as internal standard. Reaction conditions B: **1b** (0.12 mmol), 5.0 mol% **41**, 45 °C, 24 h, 1.0 MPa CO_2, 0.5 mL perfluorodecalin. Yields of isolated products are given.

Additionally, we tested the recyclability of **41** in the conversion of butylene oxide (**1b**) with CO_2 in perfluorodecalin. As expected from the conditions optimized in Table 4, the desired product was obtained in 90% yield in the presence of 5.0 mol% **41** after 24 h at 45 °C and 1.0 MPa CO_2. At 45 °C the catalyst transferred from perfluorodecalin to the organic phase and

mixed with the reactant, allowing the reaction to proceed. Then cooling the catalyst reaction mixture to 23 °C, the catalyst **41** precipitated from the mixture after the addition of perfluorodecalin. The product was removed by decantation. No signal was observed in the ^{31}P NMR of the product which indicates that the catalyst did not leach into the product phase. Catalyst **41** and perfluorodecalin were directly used for the next run by simply adding new substrate. The isolated yield gradually decreased from 90% in the first run to 37% in the fifth run (Figure 3B). The recycled catalyst in the last run indicated the reason of deactivation was the loss of the alkane chain and oxidation of **41** due to the exposure to air. This was proved by a peak shift in the in ^{31}P NMR from 23.7 ppm for **41** to 27.9 ppm after the fifth run. Based on our results, the reaction mechanism for **40** was proposed to explain the deactivation process. In the initial step, catalyst **40** activates the epoxide via hydrogen bonding (Scheme 14, i). This is followed by the nucleophilic ring-opening of the epoxide by iodide (ii). Subsequent CO_2 insertion affords a linear carbonate intermediate (iii). An intramolecular nucleophilic substitution gives the product **2**, liberating the catalyst **40** (iii). The formation of halohydrins is a frequently observed side reaction in the synthesis of cyclic carbonates catalyzed by onium salts. This might lead to the observed formation of the species **42a**. Thus, **42a** was prepared and comparing with the recycled catalyst. The ^{1}H NMR spectra of the 1:1 mixture is comparable to the one of the recycled catalyst. The elemental analysis of the recycled catalysts for iodide (calcd.: 8.05%, found.: 8.02%) supports this ratio.

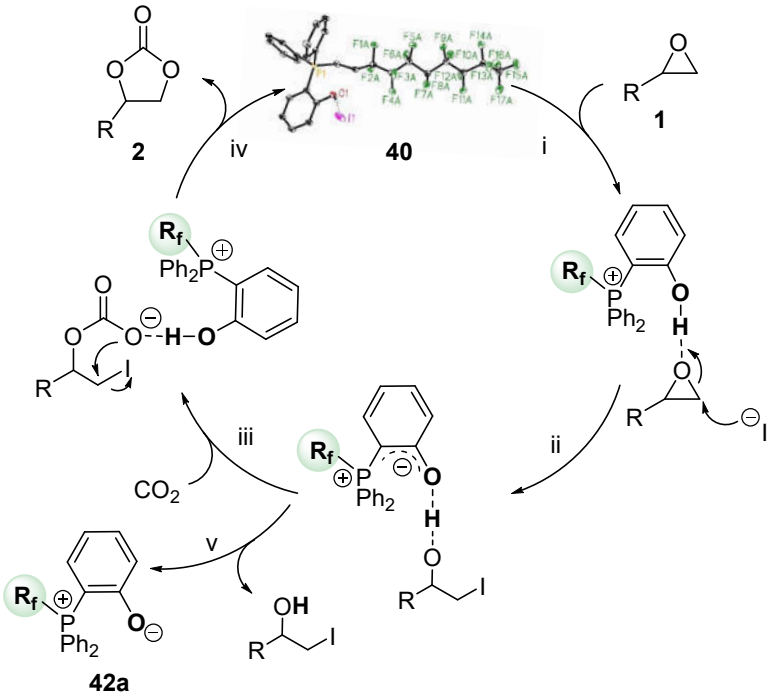

Scheme 14. Putative mechanism for coupling of epoxides **1** with CO_2 catalyzed by bifunctional phosphonium salt **40**.

This formation of the internal phosphonium salt **42a** indicates that it is a stable Lewis base that is probably able to be the catalyst for base catalytic reaction. With this idea in mind, CO_2 reduction reactions were performed, and the results are shown in next chapter.

3.2 Phosphonium salt catalyzed *N*-methylation and *N*-formylation of amines with CO_2

As introduced above, the CO_2 reductive coupling with amine is started from activating reducing agents or CO_2 by nucleophilic catalysts. The obtained internal phosphonium salts bearing phenolate anion can be a nucleophile for this reaction. Therefore, a series of internal salts **42** were synthesized by treating the bifunctional phosphonium salts with NaOH according to literature, leading to air-stable catalysts (Table 5). The investigation was started by optimizing the *N*-methylation of *N*-methylaniline (**11a**) at 1 bar CO_2 in the presence of 2 mol% of catalyst **42** and *n*-hexylsilane as reductant at 45 °C for 6 hours. The reaction in the presence of the obtained phosphonium salt with strong electron-withdrawing perfluoro chain **42a** gave the methylated product **30a** and formylated product **12a** in the yield of 59% and 32% respectively (Entry 1). Catalysts with different alkyl groups attached to the phosphine center **42b**–**42e** were tested in the model reaction, giving the methylated product **30a** in similar yields from 72% to 76% (Entries 2–5). The *n*-propyl-substituted

Table 5. The screening of catalysts **42** for the *N*-methylation reaction.

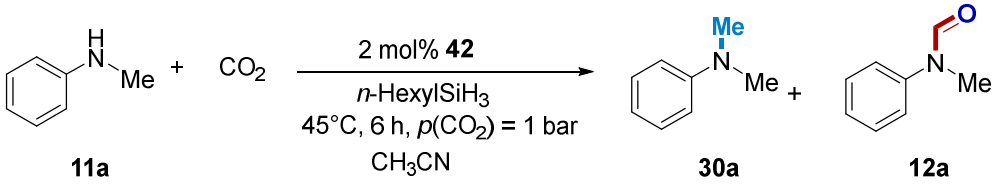

11a **30a** **12a**

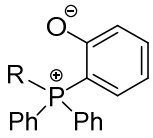

42a, R = $(CH_2)_2(CF_2)_7CF_3$
42b, R = CH_3
42c, R = $(CH_2)_2CH_3$
42d, R = $(CH_2)_5CH_3$
42e, R = $(CH_2)_2OCH_3$
42f, R = $(CH_2)_2OH$

Entry	Catalyst	Yield **30a** (%)	Yield **12a** (%)
1	**42a**	59	32
2	**42b**	74	19
3	**42c**	76	15
4	**42d**	72	21
5	**42e**	72	18
6	**42f**	34	47
7	**40c**	0	0
8	–	0	0

Reaction conditions: *N*-Methylaniline **11a** (0.47 mmol), *n*-$HexSiH_3$ (4 equiv, 1.9 mmol), catalyst **42**: 2 mol% (0.0094 mmol), CO_2 = 1 bar, 45°C, CH_3CN: 4 mL. Yield was determined by ^1H NMR using mesitylene as the internal standard.

catalyst **42c** leads to the highest yield of 76% of dimethylaniline **30a**. The yield of the methylation product decreased a lot when the hydroxyl-substituted catalyst **42f** is used (entry 6), while the formylation reaction was improved, probably because the hydroxyl group reduced the basicity. No conversion was observed in the presence of phosphonium iodide salt **40c** (entry 7). The lower yields of dimethylamine obtained in the reactions with **40c** and **42f** suggest that the phenolic hydroxyl anion probably takes part in a nucleophilic attack on the silicon center to liberate hydride for the reduction reaction. Without catalyst, the transformation cannot be achieved (entry 8). Then different silanes were screened under the temperature of 70 °C (Figure 4). Diphenylsilane was also active for the reaction in slight lower yield, but using triphenylsilane and phenylsilane gave unsatisfactory yields. Moderate yield was obtained with methylphenylsilane, and no conversion was observed with dimethylphenylsilane. Only traces of both products were observed with PMHS, probably because of it is highly stable. The screening revealed that *n*-hexylsilane is the best hydride source for the *N*-methylation reaction. Reducing the reaction time to 4 hours and 2 hours did not lead to any decrease of yield, 90% yield of dimethylamine **30a** can be obtained even within 1 hour.

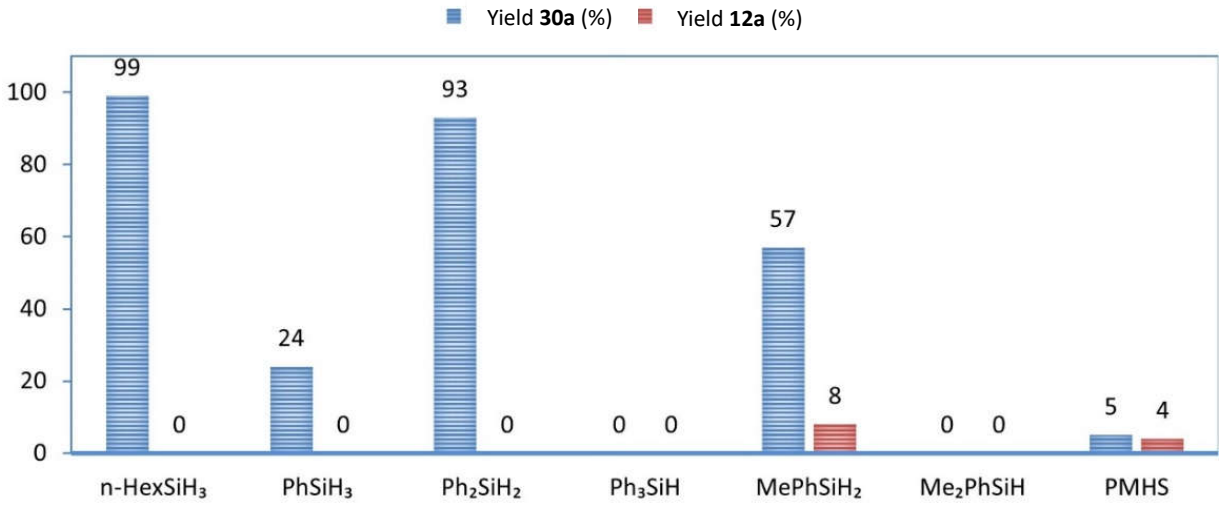

Figure 4. The screening of silane reducing agent for the *N*-methylation reaction with **42c**. Reaction conditions: *N*-methylaniline (**11a**, 0.47 mmol), silane (4 equiv) catalyst **42c** (2 mol%), $p(CO_2)$= 1 bar, 70 °C, CH_3CN (4 mL). Yield was determined by ^1H NMR using mesitylene as the internal standard.

Having the optimal conditions in hand, the scope and limitation of catalyst **42c** in the conversion of secondary amines **11** to methylated products **30** was further evaluated at 70 °C for 4 hours (Scheme 15). 4-Methoxy-methylaniline **11b** gave the corresponding dimethylaniline **30b** in a yield of 75%, however, the less sterically hindered 4-methoxy-substituted aniline **11c** gave the product **30c** in a quantitative yield. The reaction of 4-bromo-dimethylaniline with CO_2 led to the product **30d** in 82% yield. **11e** bearing the strong electron withdrawing acetyl group gave the desired product **30e** in a moderate yield of 43%.

The catalytic protocol was applicable to secondary amines with benzyl group **11f** in excellent isolated yield (90%). Diphenylamine reacted with CO_2 to afford the product **30g** in the isolated yield of 42%, because the resonance between nitrogen and two phenyl groups makes the amine less nucleophilic. The reaction of tetrahydroquinoline proceeded smoothly to afford **30h** in good yield. The heteroarylamine methylpyridin-2-amine (**11i)** gave the corresponding dimethylamine **30i** in moderate yield of 62%. This catalytic protocol was also applied for the aliphatic amine **11j**, affording the methylated product **30j** in moderate yield. 2,2,6,6-Tetramethylpiperidine afforded the corresponding product pempidine **30k** (a ganglion-blocking drug) in the yield of 88%.

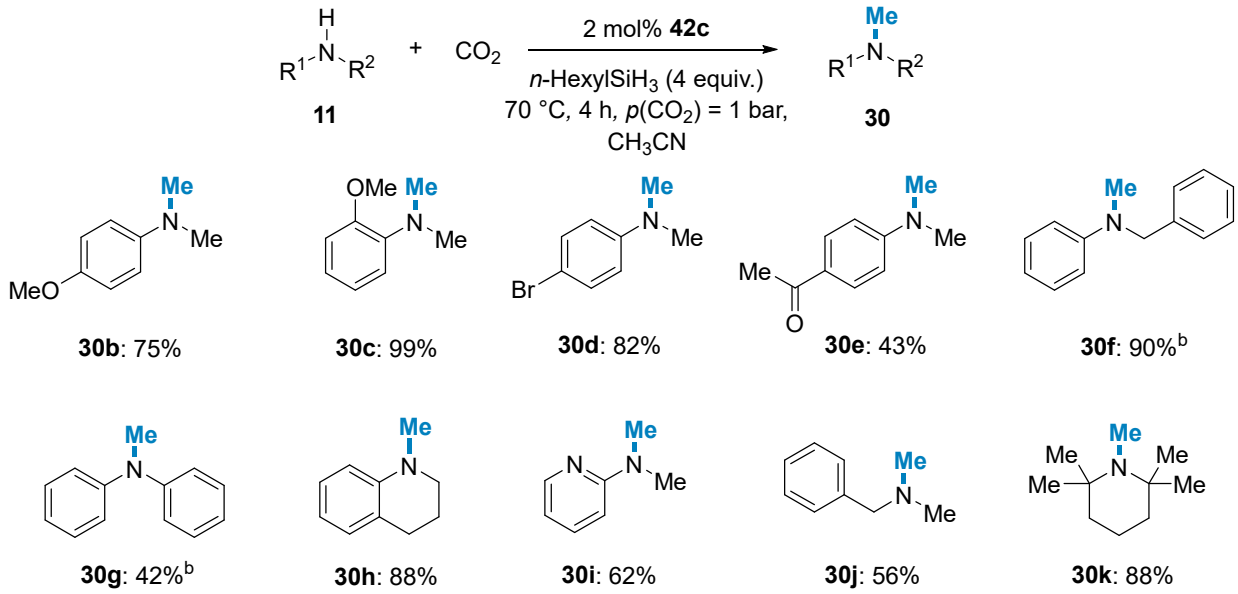

Scheme 15. Selected examples of substrates of *N*-methylation reaction. Yield was determined by ^{1}H NMR, mesitylene as the internal standard. [b] Isolated yields.

In the screening of optimal conditions for the methylation reaction, the formation of the formylated product was found to be more favorable at low temperature, so the formylation reaction was studied at room temperature and 1 bar of CO_2. Higher conversions and yields were obtained in the absence of solvent, thus the reaction conditions screening was performed without solvent (Table 6). Although full conversion and good yield of formylated product was observed with 4 equiv. silane (entry 1), the remaining silane observed in ^{1}H NMR showed that less silane was consumed in the reaction. Therefore, the amount of silane was reduced to 2 and 1 equiv. which boosted the selectivity but simultaneously lowered the conversion (entries 2–3). To counteract this result, the reaction time was extended to 8 hours. The reaction proceeded with full conversion and finally gave the desired product **12a** in 96% (entry 4).

Then the scope and limitation of catalyst **42c** in the conversion of secondary amines **11** to formylated products **12** was studied at room temperature for 8 hours without solvent except in the case of insoluble solid substrates (Scheme 16). Both 4-methoxy and 2-methoxy

methylaniline gave corresponding formylated products **12b** and **12c** in excellent yields. Bromo-substituted methylaniline **11d** was also tolerated, as 62% of **12d** was obtained. Anilines with electron withdrawing groups are a challenge for metal-free catalytic protocols, since much lower yields are reported. **12e** was obtained in an isolated yield of 32% from 4-acetyl-methylaniline **11e**. *N*-butyl aniline converted to desired product **12f** in good yield (81%). *N*-formyl substituted aniline afforded desired product *N,N*-diformylaniline (**12g**) in yield of 88% under methylation conditions. This result indicates that the formylated aniline is not the intermediate for the formation of the methylated aniline. Aliphatic amines **11h** and **11i** gave excellent yield of 96% and 81% respectively.

Table 6. Parameter optimization for the conversion of methylamine with CO_2 to formylated product.

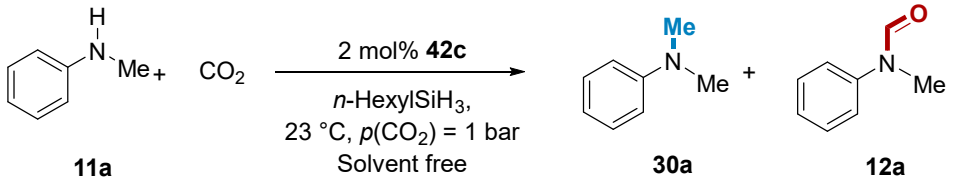

11a **30a** **12a**

Entry	Time	*n*-$HexSiH_3$	Conversion(%)	Yield **30a** (%)	Yield **12a** (%)
1	6	4	100	10	87
2	6	2	90	<5	75
3	6	1	84	0	83
4	8	1	100	4	96
5[a]	8	1	100	27	71

Reaction conditions: aniline **11a** (0.47 mmol), *n*-$HexSiH_3$ (0.47 mmol–1.9 mmol), catalyst **42c**: 2 mol% (0.0094 mmol), CO_2 = 1 bar, 23 °C, 6–8 h. Yield was determined by ^1H NMR using mesitylene as the internal standard. a. Using diphenylsilane.

Adamantanamine **11j** and derivatives are drugs to treat Parkinson's disease and influenza. **11j** converted to the formylated product **12j** under methylation conditions in an isolated yield of 66%. Piperazine derivatives can find wide applications in pharmaceuticals, **11k**, bearing piperazine group, gave an excellent isolated yield of 90%.

The high activity and the controllable property of the catalyst **42c** towards the mono-*N*-methylation and mono-*N*-formylation of secondary amines made us wonder if the catalyst can be used in the hierarchical reduction of primary amines with CO_2. Consequently, two primary amines were evaluated. Although aniline afforded mono-*N*-formylated product, *N,N*-diformylated product and dimethylated product as dominant products in good yields under three different reaction conditions, the conditions are not applicable for *p*-methoxy aniline.

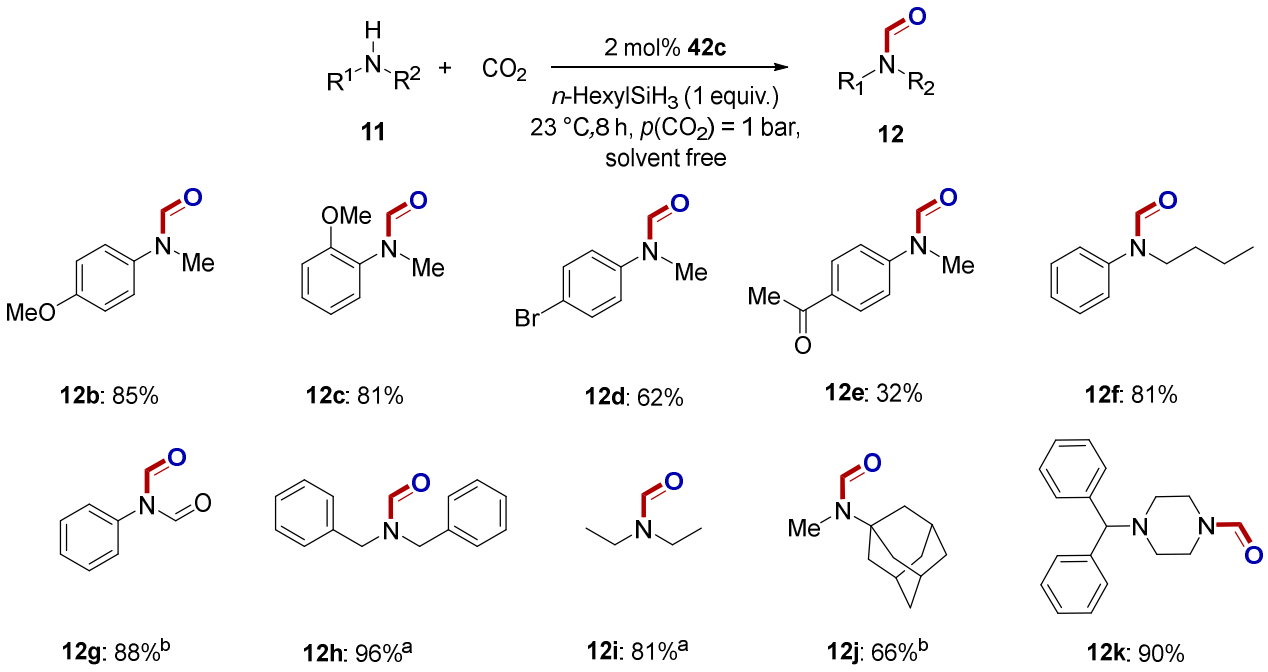

Scheme 16. Selected examples of substrates of *N*-formylation reaction. Isolated yields are given. [a] Yield was determined by ^{1}H NMR, mesitylene as the internal standard. [b] *n*-HexSiH$_3$ (4 equiv.), catalyst **42c**: 2 mol%, CO_2 = 1 bar, 70 °C, CH_3CN: 4 mL.

Furthermore, the current protocol was applied to late-stage functionalization of biological active pharmaceuticals (Scheme 17). Sertraline (**11l**), an antidepressant, converted to the methylated product **30l** in the yield of 76% under improved conditions. At room temperature, Sertraline converted to formylated product **12l** in the isolated yield of 58%.

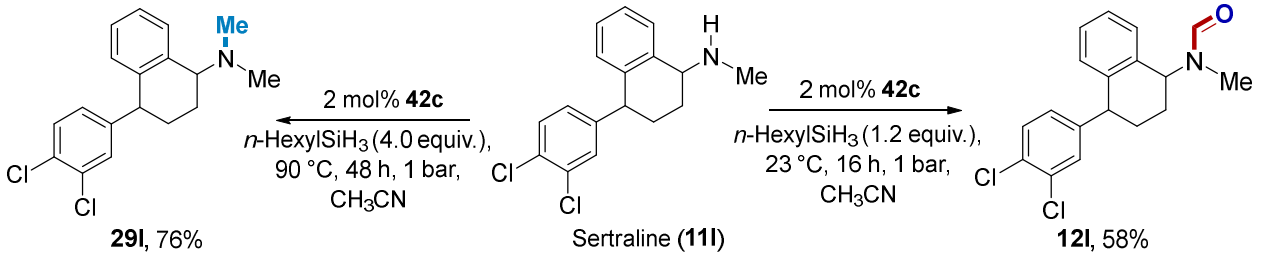

Scheme 17. Methylation and formylation reactions of Sertraline. Isolated yields are given.

To shed some light into the mechanism of this catalytic procedure, the control experiments were investigated and their ^{1}H NMRs were studied. Diphenylsilane was employed for the control experiments since it has a comparable activity to hexylsilane in *N*-methylation and *N*-formylation reaction. In the first step, diphenylsilane and a catalytic loading of **42c** were mixed, resulting in the peak shifts in NMR spectra: The proton signal intensity at 4.93 ppm belonging to Si-H disappeared after the reaction, and a new proton signal at 8.07 ppm appeared which was attributed to silyl formate formed (Figure 5b). Also, a carbon signal at 162 ppm corresponding to C=O in ^{13}C NMR was observed. Subsequently, *N*-methylamine was added to the mixture above immediately and reacted in argon atmosphere under the reaction conditions, yielding 65% *N*-methylformamide.

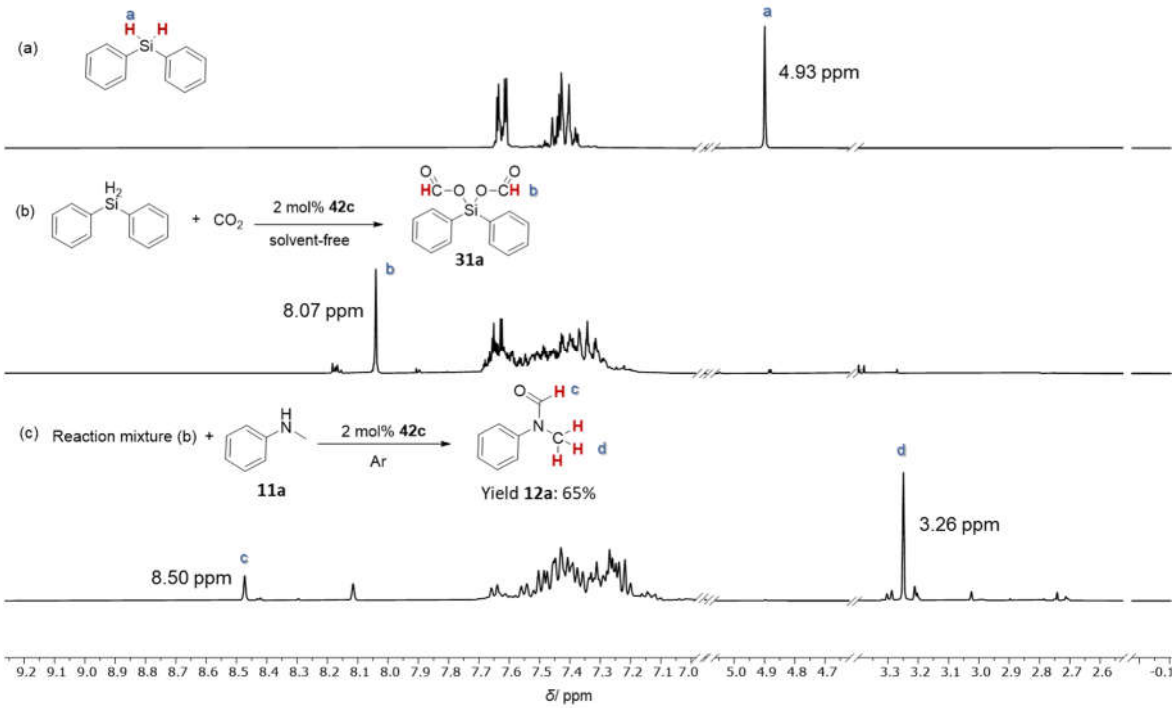

Figure 5. ^{1}H NMR spectra of diphenylsilane and control experiments in CD_3CN. (a) Section of the ^{1}H NMR of diphenylsilane. (b) Section of the ^{1}H NMR of diphenylsilane (2 equiv.) and CO_2 with 2 mol% **42c**, 1 bar, 23 °C, solvent free, 16 h. (c) Section of the ^{1}H NMR of the reaction solution from (b) and *N*-methylamine (1 equiv.) after 16 h at 23°C under Ar in CD_3CN at 23 °C for 16 h with mesitylene as internal standard.

^{1}H NMR shows that the proton signal at 8.07 ppm disappeared and a proton signal at 8.50 ppm attributed to H-C=O of *N*-methylformamide was observed (Figure 5c). Therefore, these results imply that in the presence of catalyst, CO_2 is hydrosilylated by silane resulting in silyl formate, and then the formamide was formed by the formylation of the amine with silyl formate.

A two-step reaction was also performed to observe the intermediate of the methylation reaction. Therefore, diphenylsilane and a catalytic amount of **42c** were mixed at 70°C in Schlenk flask, leading to dimethoxysilane (**43a**), silyl acetal (**32a**) and siloxane (**44a**) as main products (Scheme 18a). In contrast to the reaction at 23°C, the formation of formate **31a** was not observed. Then after the reaction above stopped, *N*-methylamine was immediately added and reacted under argon atmosphere at 70 °C, leading to the aminal (**33a**) in yields of 39% (Scheme 18b). This indicates that **32a** is converted to **33a** which might be subsequently reduced to the product **30a** and *N*-methylamine (**11a**) in next step. To convert of **11a** to **30a** the addition of CO_2 would be required. In next step, fresh CO_2 were added simultaneously in the mixture of step 1, giving the methylated product **30a** in yield of 33%, because CO_2 promoted the cleavage of C–N bond in aminal (**33a**) to give the product *N,N*-dimethylaniline **30a** (Scheme 18c). It was presumed that one in dimethoxysilane (**43a**), silyl acetal (**32a**) and siloxane (**44a**) might be the intermediate in the formation of the methylated product, therefore, the reactions in the presence of (**43a**) and (**44a**) were studied respectively.

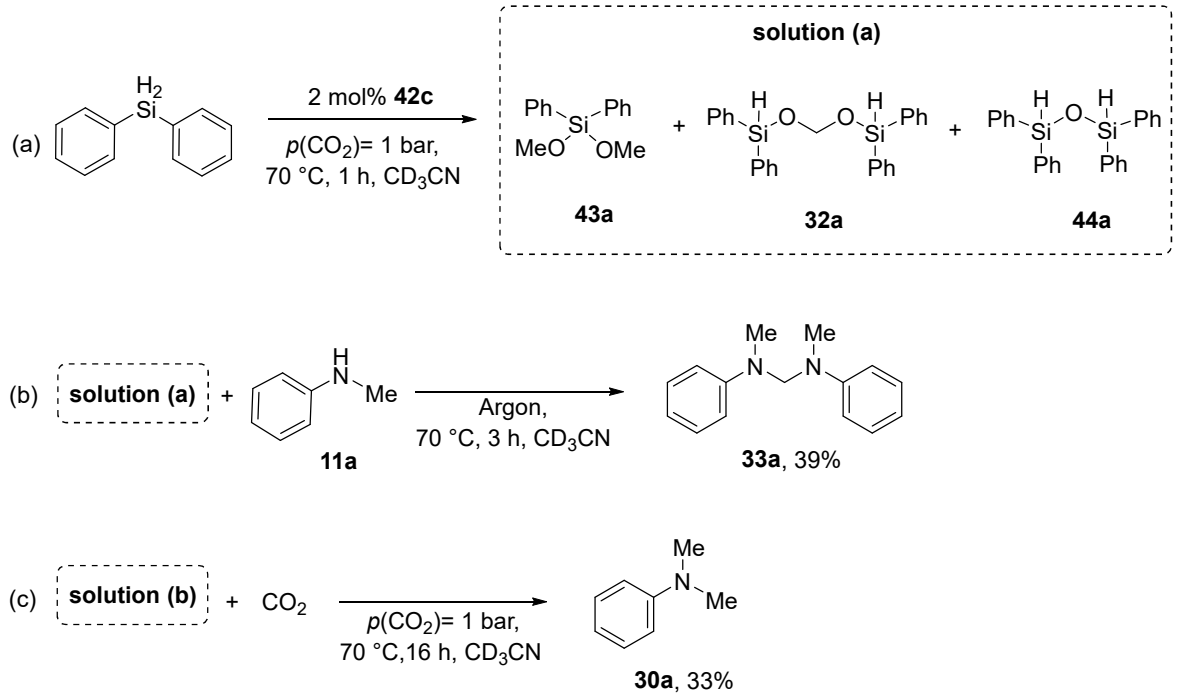

Scheme 18. Control experiments for mechanistic study of *N*-methylation reaction. (a) Reaction of diphenylsilane with CO_2 in the presence of catalyst **42c**. (b) Reaction of **11a** in solution (a) under Argon. (c) Reaction of **11a** in solution (a) in the presence of CO_2.

No conversion was observed in the presence of dimethoxysilane (**43a**) and siloxane (**44a**) under *N*-methylation reaction conditions or under Argon, which excluded the possibility of being intermediates. Based on above results, the scope of intermediate was narrowed down to silyl acetal (**32a**). Finally, a possible pathway was proposed based on the experiments and previous reports (Scheme 19).

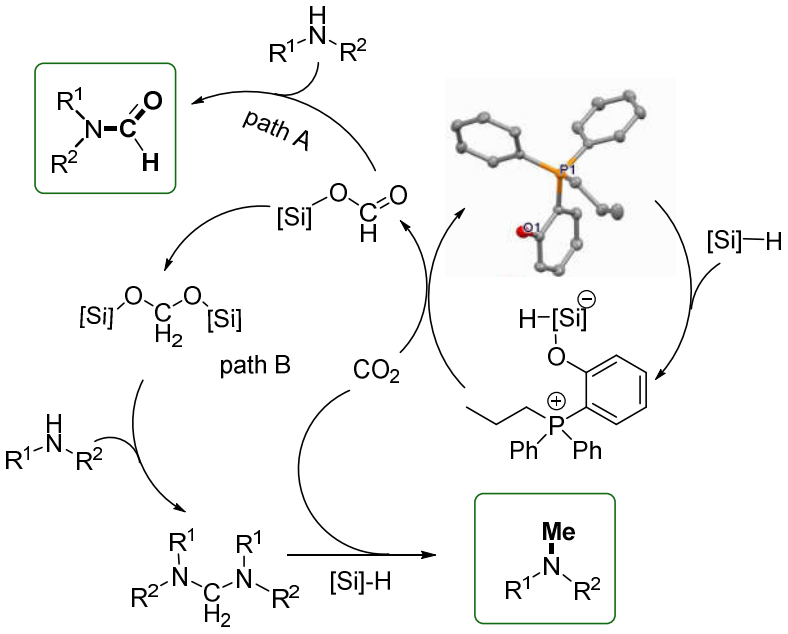

Scheme 19. Proposed reaction pathway of temperature-controlled *N*-methylation and *N*-formylation of amines **11** with CO_2 in the presence of catalyst **42c**.

Initially, at low temperature or in the presence of strong nucleophilic amines the reaction follows path A, in which the catalyst activates silane and allows CO_2 insertion to give silyl formate intermediate. Then, the strong nucleophilic amines attack the carbon atom of the silyl formate, affording the formylated product. Whereas in path B weakly nucleophilic amines are not able to attack the silyl formate intermediate immediately, instead, the silyl formate will be reduced to the acetal intermediate by the silane at higher temperature, which is electrophilic enough to be attacked by weak amines, forming the aminal intermediate. Aminals are further reduced to methylated product by the silane in the presence of additional CO_2.

3.3 Tunable reduction of CO_2–organocayalyzed selective formylation and methylation of amines.[98]

The *N*-formylation and *N*-methylation reaction appear to proceed by a general Lewis base catalyzed reaction mechanism, in which hydrosilanes or CO_2 need to be activated by the basic catalyst. In the catalytic protocol with internal phosphonium salt **42c**, low yields of both formylated and methylated products were obtained in the presence of the less expensive PMHS. To explore a catalysts which can tolerate polymeric PMHS and inert CO_2, the spotlight is put on the phosphonium methylcarbonate salts. In the previous study, the phosphonium methylcarbonate salts decompose to CO_2 and phosphonium methoxide after heating.[99] It was envisioned that the methoxy anion could present better activity than phenolate anion towards the reaction. On the other hand, the phosphonium methylcarbonate salt ($[Ph_3PCH_3][CH_3OCO_2]$) **45** is commercially available and can also be prepared from phosphines and dimethylcarbonate (DMC) according to literature.[100] It was firstly reported as a CO_2 surrogate in the preparation of propylene oxide in 2006,[101] and then it has been employed in the transesterification[102] and Henry reaction,[99] as well as vinylation reagents in the Wittig reaction.[100] PMHS was selected to be reducing agent to meet the challenge. *N*-methylaniline was chosen as model substrate to evaluate the activity of the catalyst towards the methylation reaction with 4 equiv. PMHS, CO_2 as carbon source at 1 bar and 70 °C (Table 7). In the absence of catalyst, no conversion was observed (entry 1). A moderate yield of 53% and good selectivity of *N*-methylated product **30a** was obtained in the presence of the catalyst (entry 2). In CH_3CN, *N*-methylaniline gave the *N*-methylated product **30a** and *N*-formylated product **12a** in the yield of 20% and 6%, respectively (entry 3). In EtOAc and CH_2Cl_2, **11a** failed to convert to either **30a** or **12a** (entries 4–5). Due to the polymeric properties, PMHS was less active than non-polymeric silanes, thus excessive amount were normally required. Full conversion was achieved by increasing PMHS to 10 equiv. and **30a** was obtained in a good yield of 87%. A comparable yield of 83% **30a** was obtained by replacing THF with the biomass-derived chemical 2-methyltetrahydrofuran (entry 7). To further optimize the reaction condition of *N*-methylation, halving catalyst loading led to lower yield of methylated product **30a** and selectivity (entry 8). After that,

reaction temperature was raised to 80 °C and decreased to 60 °C and 50 °C, respectively. Unfortunately, lower yields were observed in this case (entries 9–11).

Table 7. Reaction conditions optimization for the conversion of *N*-methylaniline (**11a**) with CO_2 to methylated product **30a**.

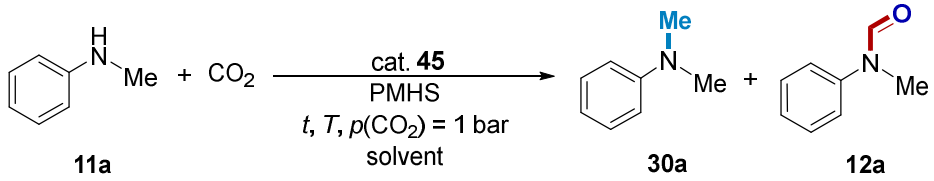

11a **30a** **12a**

Entry	Catalyst (mol %)	PMHS (equiv.)	Solvent	Temperature (°C)	Yield **30a** (%)	Yield **12a** (%)
1	0	4	THF	70	0	0
2	10	4	THF	70	53	0
3	10	4	MeCN	70	20	6
4	10	4	EtOAc	70	0	0
5	10	4	CH_2Cl_2	70	0	0
6	10	10	THF	70	87	0
7	10	10	Me-THF	70	83	10
8	5	10	THF	70	62	30
9	10	10	THF	80	72	0
10	10	10	THF	60	82	17
11	10	10	THF	50	55	38

Reaction conditions: *N*-methylaniline **11a** (0.233 mmol, 1 equiv.), PMHS (4–10 equiv.), catalyst **45**: 0–10 mol%, $p(CO_2)$ = 1 bar, 50–70 °C for 16 h, solvent: 2 mL. Yield was determined by ^{1}H-NMR using mesitylene as the internal standard.

The scope of the reaction was next investigated by testing a variety of substituted secondary and primary amines (Scheme 20). In this case, although a reaction time of 16 hours was required to achieve an appropriate yield for most substrates, the transformation was finished within 4 hours for a few of substrates. *p*-Methoxy-*N*-methylaniline (**11b**) gave the corresponding dimethylaniline derivative **30b** in 72% yield after 16 h, while 71% of *o*-methoxy-*N,N*-dimethylaniline **30c** was isolated after only 4 hours. The bromo-substituted *N*-methylaniline gave the product **30d** in good yield of 77%. The methylated product of *p*-acetyl-*N*-methylaniline (**30e**) was isolated in 42% yield. *N*-benzyl- and *N*-allyl-anilines were converted to their corresponding products **30f** and **30l** in excellent yields (82% and 89%). Tetrahydroquinoline afforded the methylated product **30h** in a yield of 76% in 4 hours.

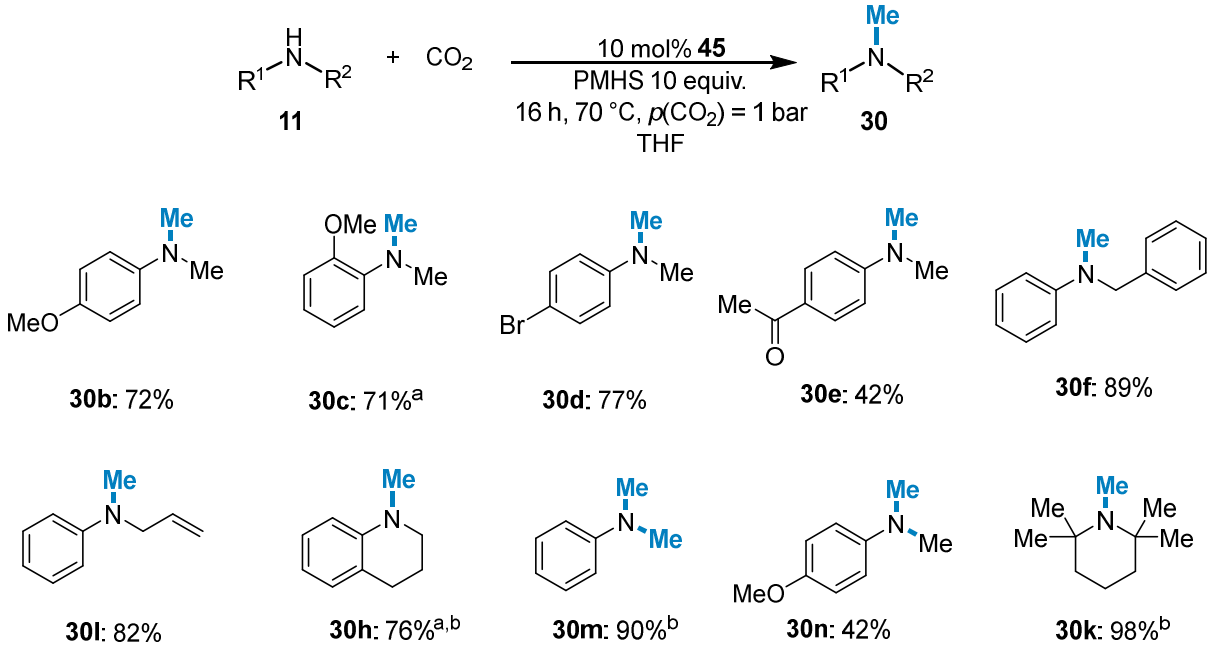

Scheme 20. Selected examples of substrates of *N*-methylation reaction. Isolated yields are given. [a] 4 h. [b] Yield was determined by ^{1}H NMR, mesitylene as the internal standard.

In comparison with secondary anilines, primary anilines normally exhibit less nucleophilicity and form multiple reduction products, but with this catalytic system they were also converted. Aniline **11m** and *p*-methoxyaniline **11n** afforded the dimethylanilines in 90% and 42%, respectively. Surprisingly, the sterically hindered substrates 2,2,6,6-tetramethylpiperidine successfully converted to methylated product pempidine **30k**, which is a ganglion-blocking drug.

Subsequently, the *N*-formylation of *N*-methylaniline was explored with the catalyst **45** (Scheme 21). It was found in the screening for *N*-formylation that *N*-formylated product is unfavored in the presence of PMHS at various temperature. As a result, we had to screen different silanes for *N*-formylation reaction. Finally, $(MeO)_3SiH$ afforded the *N*-formylated product in 95% yield and outstanding selectivity (Scheme 16). With the optimal conditions in hand, the scope and limitations of $[Ph_3PCH_3][CH_3OCO_2]$ **45** for the catalytic conversion of amines to their formylated products were studied at 70 °C for 4–24 hours in the presence of $(MeO)_3SiH$. Contrary to the methylation reaction, the hindered *o*-methoxy-*N*-methylaniline **11c** needed 24 h to be converted to the corresponding formylated product, but *p*-methoxyaniline **11b** achieved higher yield in only 4 hours. Bromo-substituted aniline **11d** afforded the corresponding *N*-methylformamides **12d** in good yield in 4 h while nitro-substituted anilines **11m** led to a low yield of 13%. *N*-substituted anilines were also

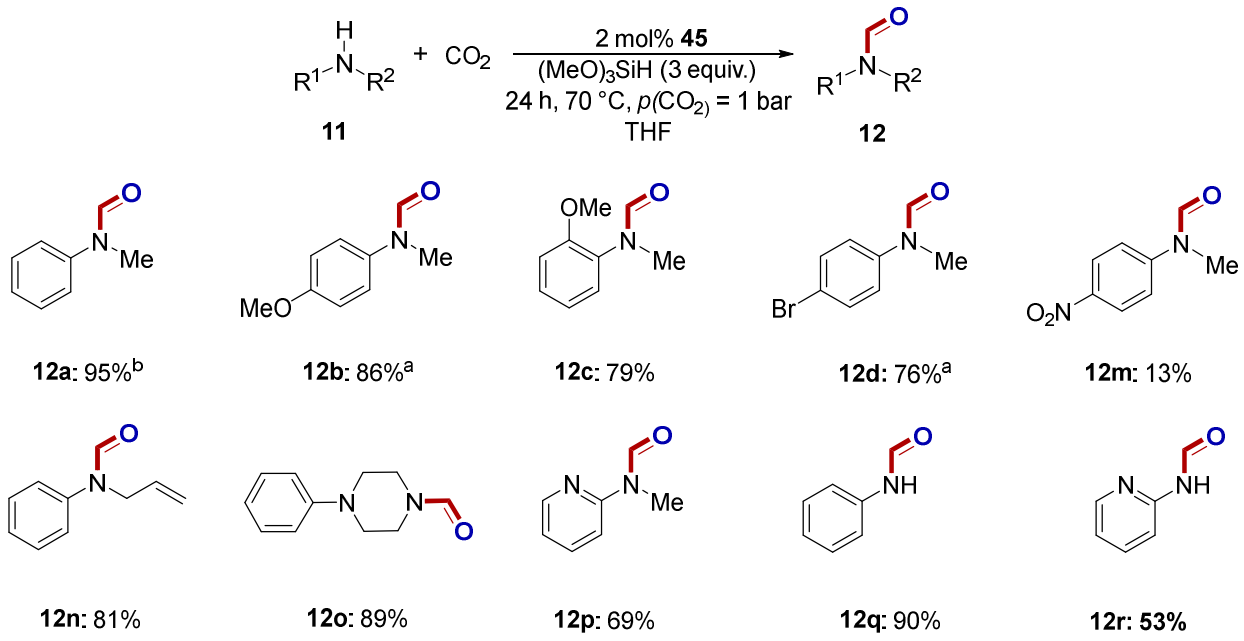

Scheme 21. Selected examples of substrates of *N*-formylation reaction. Isolated yields are given. [a] 4 h. [b] Yield was determined by ^{1}H NMR, mesitylene as the internal standard.

tolerated, *N*-allyl-substituted anilines **11n** was successfully converted to the formylated product **12n** in 81% yield after 24 h. Piperazine derivative **11o** afforded the formylated product **12o** in the yield of 89%. A moderate yield of 69% of the formylated product **12p** was obtained from the pyridine-substituted amine. Aniline **11q** and pyridine-2-amine **11r** were selected as representative substrates of primary anilines. An excellent yield 90% of *N*-formanilide **12q** was obtained from aniline, while 53% of the *N*-formylated-pyridine-2-amine **12r** was isolated.

The excellent conversion and selectivity of aniline to *N*-phenylformamide (**12q**) encouraged us to study the possibility of the benzimidazole formation by monoformylation of the *o*-phenylendiamin **25a** followed by the intramolecular condensation with an amino group present in the molecule. Therefore, the reaction was performed under the same reaction conditions for the formylation of aniline without other additives (Scheme 22). To our surprise, 83% of benzimidazole **27a** was isolated from 1,2-diaminobenzene and CO_2 in one step. Then, diverse substrates were investigated under the reaction conditions. *p*-Methoxy-1,2-diaminobenzene **25b** afforded the desired product **27b** in the yield of 47%. For *N*-disubstituted substrates 1-*N*-methylbenzene-1,2-diamine **25c** and *N*-phenyl-*o*-phenylenediamine **27d** were evaluated in this protocol: 61% and 70% of the desired products **27c** and **27d** were obtained, respectively. The lower yields were due to the formation of the monoformylation byproduct of the primary amino group that is less nucleophilic than the secondary amino group. Moreover, quinazoline derivative **27e** was obtained from 25e in the yield of 64%.

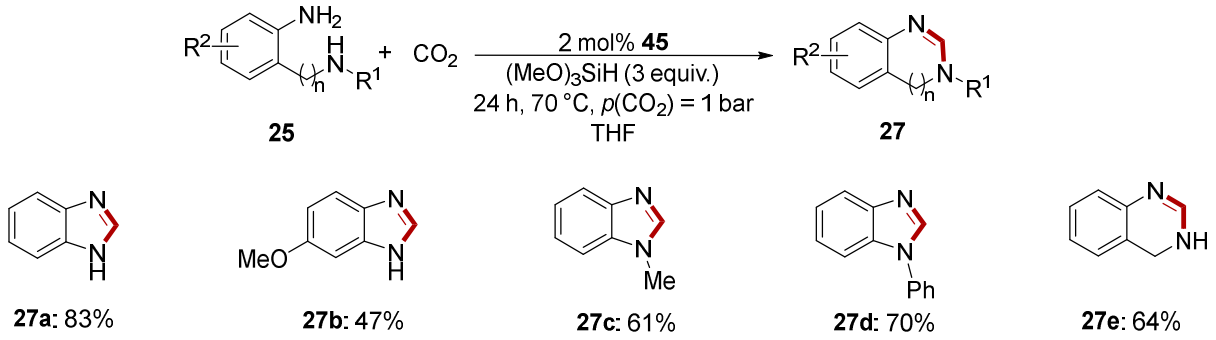

Scheme 22. Selected examples of substrates for the synthesis of benzoheterocycles **27** from diamines **25** and CO_2 under reductive condition.

To gain insights into the mechanism of this chemoselective reaction, control experiments were performed to explore the possible intermediates in the *N*-formylation and *N*-methylation reaction. The same control experiments with internal phosphonium salt catalyst **42c** were performed. Initially, trimethoxysilane reacted with CO_2 in the presence of catalyst $[Ph_3PCH_3][CH_3OCO_2]$ **45** affording the silyl formate in 29% yield. The resulting reaction mixture was purged with argon to replace the remaining CO_2. *N*-methylaniline **11a** was added and reacted at 70 °C for 6 hours affording *N*-methylformanilide **12a** in 69% yield. Without catalyst, the silyl formate was not obtained, and as expected, no product was observed upon addition of *N*-methylaniline. Then to reveal the pathways of *N*-methylation reaction, the conversion of *N*-formamide to the *N*-methylamine was tested using PMHS in the presence and absence of catalyst under the reaction conditions. In both cases, the product could not be obtained, thus the path I (Scheme 12) was dismissed.

Once the different routes for the formation of products were established, we became interested in understanding the role of the catalyst in this reaction and the different selectivity observed for the reducing agents. Initially, a stoichiometric mixture of trimethoxysilane and catalyst $[Ph_3PCH_3][CH_3OCO_2]$ **45** was prepared, heated up to 70 °C and analyzed by NMR spectroscopy (Figures 6 and 7). The characteristic signal at δ(Si–*H*)= 4.07 ppm in trimethoxysilane and the signal at $\delta(CO_3CH_3)$= 3.37 ppm for the catalyst are not observed in the mixture (Figure 6c). Instead, a new signal at $\delta(HCO_2^-)$= 8.58 ppm was observed in the mixture of trimethoxysilane and the catalyst. The signals at –78.60 ppm in the ^{29}Si NMR (Figure 7b), respectively indicate the formation of $Si(OMe)_4$. The signal at around 3.30 ppm (marked as *) can be addressed to a methoxy anion which is probably formed due to the decomposition of $[Ph_3PMe][CO_3Me]$ to CO_2 and $[Ph_3PMe][OMe]$. The results show the total conversion of the methylcarbonate anion and silane and the formation of formate and tetramethoxysilane, which demonstrates that the catalyst reacts stoichiometrically with the silane, supporting the hypothesis that the reaction is initiated in this step.

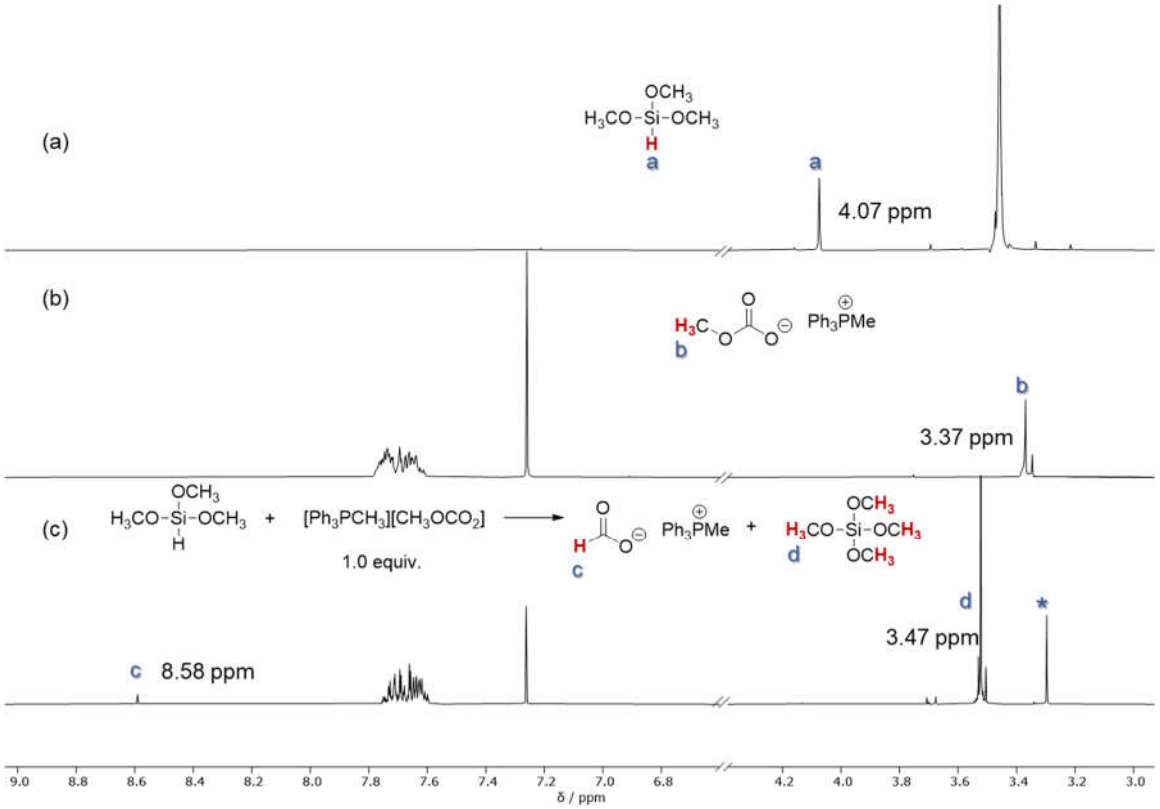

Figure 6. The ^{1}H NMR spectra for the control experiments. a) Section of the ^{1}H NMR of trimeoxysilane. b) Section of the ^{1}H NMR of the catalyst **45**. c) Section of the ^{1}H NMR of a 1:1 mixture trimeoxysilane and $[Ph_3PCH_3][CO_3Me]$ after 16 h at 70°C. * Methoxy anion.

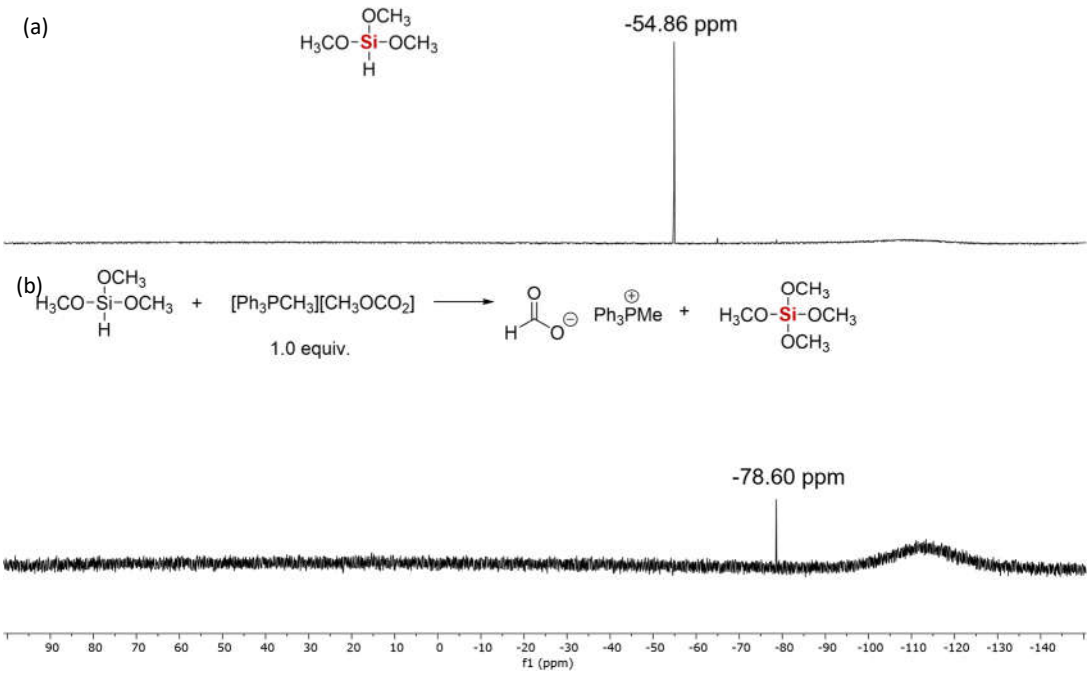

Figure 7. The ^{29}Si NMR spectra for the control experiments. a) ^{29}Si NMR of trimeoxysilane. b) ^{29}Si NMR of a 1:1 mixture trimeoxysilane and $[Ph_3PCH_3][CO_3Me]$ after 16 h at 70°C. * Methoxy anion.

Altogether, the mechanism presented was proposed (Scheme 23). The methylcarbonate anion attacks the silane forming a linear carbonate (A) that facilitates the attack of the hydride to the carbonyl center. As a result, a tetrahedral intermediate (B) is formed. In the absence of CO_2, this intermediate can suffer a rearrangement giving the formate anion and tetramethoxysilane. In presence of CO_2, the methoxy group attacks the CO_2 molecule, regenerating the catalyst and giving the silyl formate, which further reacts with the amine through path I or II giving the corresponding products.

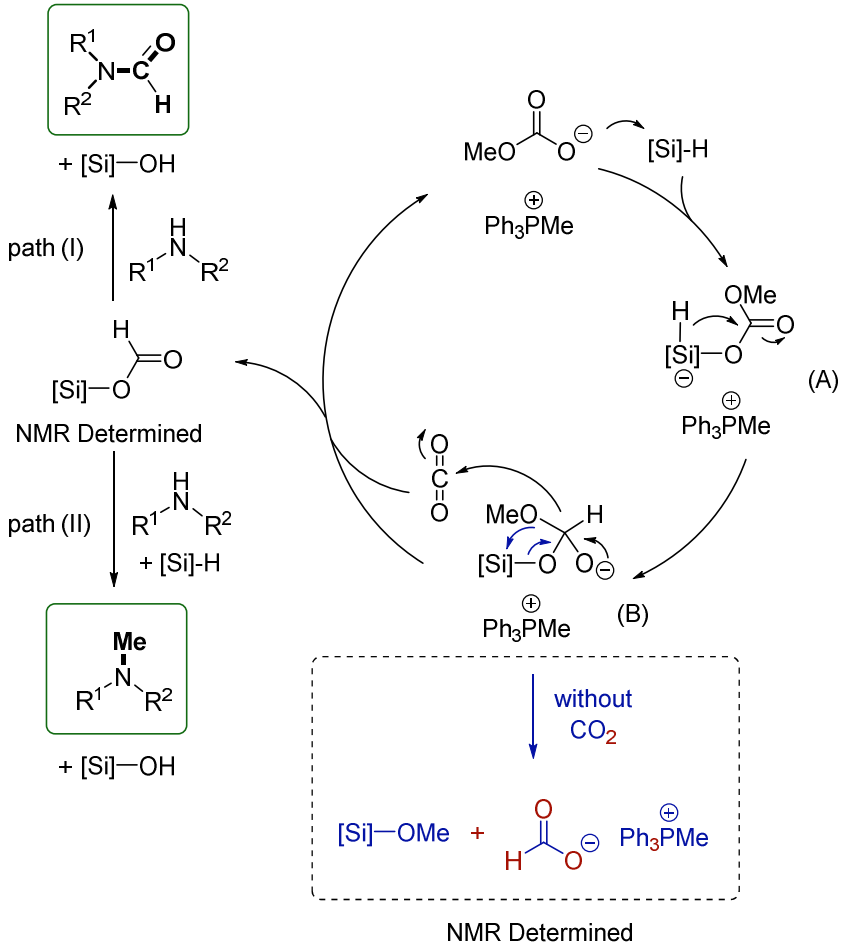

Scheme 23. Proposed mechanism for the selective reduction of CO_2 to formamides and methylamines with phosphonium methylcarbonate salts.

4 Summary

In this work, a series of new phosphonium salt catalysts were prepared and employed in the reductive and non-reductive fixation of CO_2. In the first part, a bifunctional phosphonium salt and two bifunctional phosphonium salts bearing perfluorinated side chains were prepared. These compounds are suitable for the synthesis of cyclic carbonates from epoxides and CO_2 even under mild conditions (23 °C, 0.1 MPa). In addition, the antitussive agent dropropizine was synthesized via cyclic carbonate as intermediate. Recycling experiments were performed for fluorinated catalysts. The bifunctional catalyst bearing a hydroxyalkyl moiety was recycled five times. A decrease in product yield from 90% to 37% during this process

was observed, which could be assigned to the decomposition of the catalyst to the corresponding phosphine oxide. The recycling of the catalyst containing a phenolic moiety was also performed. The analysis of the reisolated catalyst revealed the partial formation of an internal phosphonium salt which is catalytically inactive under the reaction conditions. However, this type of internal phosphonium salt can be used as a Lewis base catalyst for the CO_2 reductive coupling with amines.

In the second part, internal phosphonium salts were prepared and introduced as an efficient catalyst for switchable *N*-methylation and *N*-formylation reaction from CO_2 and amines in the presence of *n*-hexylsilane. The reaction outcome could be tuned by altering the reaction temperature and solvent. The methylation reaction was performed at 70 °C while the formylation reaction was performed solvent-free at room temperature. The catalyst exhibited wide substrate applicability, 22 examples of secondary and primary amines converted to corresponding methylated products in up to 99% and 25 examples of secondary and primary amines. The pharmaceutical molecule Sertraline converted to the corresponding methylated and formylated products successfully. The scale-up reactions were also performed. The control experiments and NMR studies showed that the silane is first activated by the phenolate anion. Notably, the methylation and formylation reaction follow two different pathways. The formylation proceeds via a silylformate intermediate while methylation proceeds via a bis silylacetal.

In the final part, a phosphonium methylcarbonate salt was studied for the selective reduction of CO_2 with amines. Among them, methyltriphenylphosphonium methylcarbonate showed to be efficient for the 6-electron reduction of CO_2 with PMHS affording the *N*-methylated product. Under the optimized conditions, 15 primary and secondary amines and anilines were converted in yields up to 98%. The *N*-formylation of amines was also studied. After performing a silane screening, trimethoxysilane was found to be a selective reducing agent for formation of formamides. 15 substrates were converted and the desired products were obtained in yields up to 94%. Additionally, this procedure was evaluated for the one-step synthesis of benzoheterocycles from diamines. Under the reaction conditions the catalyzed formation of the amidine group by formylation of amines followed by intramolecular condensation was achieved, affording 5 benzimidazole derivatives in yields up to 83%. Mechanistic studies support the reaction of the silane with CO_2 for the formation of silylformate, which in the case of trimethoxysilane gives the formylated product. In the presence of PMHS this intermediate undergoes a further reduction and gives the methylated product through the formation of the aminal. Experiments support that the reaction is initiated by the reaction between the methylcarbonate anion with the silane. The silylcarbonate formed reacts with CO_2 regenerating the catalyst and giving the silylformate as a result. This novel catalytic cycle provides a new perspective for CO_2 mediated reaction.

5 References

[1] a) https://www.co2.earth/; b) S. Paraschiv, L. S. Paraschiv, *Energy Rep.* **2020**, *6*, 237−242.

[2] a) C. Hepburn, E. Adlen, J. Beddington, E. A. Carter, S. Fuss, N. Mac Dowell, J. C. Minx, P. Smith, C. K. Williams, *Nature* **2019**, *575*, 87−97; b) https://www.iea.org/data-and-statistics/data-tools/greenhouse-gas-emissions-from-energy-data-explorer.

[3] a) B. C. O'Neill, M. Oppenheimer, R. Warren, S. Hallegatte, R. E. Kopp, H. O. Pörtner, R. Scholes, J. Birkmann, W. Foden, R. Licker, K. J. Mach, P. Marbaix, M. D. Mastrandrea, J. Price, K. Takahashi, J.-P. van Ypersele, G. Yohe, *Nat. Clim. Change* **2017**, *7*, 28−37; b) S.-a. Robinson, *WIREs Climate Change* **2020**, *11*, e653.

[4] a) M. Aresta, A. Dibenedetto, A. Angelini, *Chem. Rev.* **2014**, *114*, 1709−1742; b) L. I. Eide, M. Batum, T. Dixon, Z. Elamin, A. Graue, S. Hagen, S. Hovorka, B. Nazarian, P. H. Nøkleby, G. I. Olsen, P. Ringrose, R. A. Vieira, in *Energies, Vol. 12*, **2019**; c) T. T. d. Cruz, J. A. Perrella Balestieri, J. M. de Toledo Silva, M. R. N. Vilanova, O. J. Oliveira, I. Ávila, *Int. J. Greenhouse Gas Control* **2021**, *108*, 103309; d) K. Arning, J. Offermann-van Heek, A. Linzenich, A. Kaetelhoen, A. Sternberg, A. Bardow, M. Ziefle, *Energy Policy* **2019**, *125*, 235−249.

[5] a) E. Kawai, A. Ozawa, B. D. Leibowicz, *Appl. Energy* **2022**, *328*, 120183; b) J. Nyári, M. Magdeldin, M. Larmi, M. Järvinen, A. Santasalo-Aarnio, *J. CO2 Util.* **2020**, *39*, 101166; c) X. Jiang, X. Nie, X. Guo, C. Song, J. G. Chen, *Chem. Rev.* **2020**, *120*, 7984−8034; d) E. J. C. Lopes, A. P. C. Ribeiro, L. M. D. R. S. Martins, *Catalysts* **2020**, *10*, 479; e) B. Grignard, S. Gennen, C. Jérôme, A. W. Kleij, C. Detrembleur, *Chem. Soc. Rev.* **2019**, *48*, 4466−4514; f) V. Aomchad, À. Cristòfol, F. Della Monica, B. Limburg, V. D'Elia, A. W. Kleij, *Green Chem.* **2021**, *23*, 1077−1113; g) I. Sullivan, A. Goryachev, I. A. Digdaya, X. Li, H. A. Atwater, D. A. Vermaas, C. Xiang, *Nat. Catal.* **2021**, *4*, 952−958.

[6] D. Hidalgo, J. M. Martín-Marroquín, *Renew. Sustain. Energy Rev.* **2020**, *132*, 110057.

[7] T. Galimova, M. Ram, D. Bogdanov, M. Fasihi, S. Khalili, A. Gulagi, H. Karjunen, T. N. O. Mensah, C. Breyer, *J. Clean. Prod.* **2022**, *373*, 133920.

[8] Q. Liu, L. Wu, R. Jackstell, M. Beller, *Nat. Commun.* **2015**, *6*, 5933.

[9] a) W. Leitner, *Angew. Chem. Int. Ed.* **1995**, *34*, 2207−2221; b) L. Fan, C. Xia, P. Zhu, Y. Lu, H. Wang, *Nat. Commun.* **2020**, *11*, 3633; c) D. Wei, R. Sang, P. Sponholz, H. Junge,

M. Beller, *Nat. Energy* **2022**, *7*, 438−447.

[10] D. Yu, Y. Zhang, *Proc. Natl. Acad. Sci. U.S.A* **2010**, *107*, 20184−20189.

[11] S. Jin, Z. Hao, K. Zhang, Z. Yan, J. Chen, *Angew. Chem. Int. Ed.* **2021**, *60*, 20627−20648.

[12] a) S. Navarro-Jaén, M. Virginie, J. Bonin, M. Robert, R. Wojcieszak, A. Y. Khodakov, *Nat. Rev. Chem.* **2021**, *5*, 564−579; b) S. Xie, W. Zhang, X. Lan, H. Lin, *ChemSusChem* **2020**, *13*, 6141−6159.

[13] a) F. D. Bobbink, S. Das, P. J. Dyson, *Nat. Protoc.* **2017**, *12*, 417−428; b) X. Jiang, Z. Huang, M. Makha, C.-X. Du, D. Zhao, F. Wang, Y. Li, *Green Chem.* **2020**, *22*, 5317−5324.

[14] a) S. Maji, A. Das, S. K. Mandal, *Chem. Sci.* **2021**, *12*, 12174−12180; b) Y. Li, X. Fang, K. Junge, M. Beller, *Angew. Chem. Int. Ed.* **2013**, *52*, 9568−9571; c) E. Blondiaux, J. Pouessel, T. Cantat, *Angew. Chem. Int. Ed.* **2014**, *53*, 12186−12190.

[15] a) H. Wu, W. Dai, S. Saravanamurugan, H. Li, S. Yang, *Green Chem.* **2020**, *22*, 5822−5832; b) R. Yao, Y. Li, J. Wang, J. Chen, Y. Xu, *J. Catal.* **2023**, *418*, 78−89.

[16] a) P. Ríos, A. Rodríguez, J. López-Serrano, *ACS Catal.* **2016**, *6*, 5715−5723; b) M. Sharif, R. Jackstell, S. Dastgir, B. Al-Shihi, M. Beller, *ChemCatChem* **2017**, *9*, 542−546.

[17] a) H. Büttner, J. Steinbauer, T. Werner, *ChemSusChem* **2015**, *8*, 2655−2669; b) T. Werner, H. Büttner, *ChemSusChem* **2014**, *7*, 3268−3271; c) M. Liu, X. Wang, Y. Jiang, J. Sun, M. Arai, *Catal. Rev.* **2019**, *61*, 214−269.

[18] S. Pulla, C. M. Felton, P. Ramidi, Y. Gartia, N. Ali, U. B. Nasini, A. Ghosh, *J. CO2 Util.* **2013**, *2*, 49−57.

[19] M. Xu, A. R. Jupp, M. S. E. Ong, K. I. Burton, S. S. Chitnis, D. W. Stephan, *Angew. Chem. Int. Ed.* **2019**, *58*, 5707−5711.

[20] S.-E. Dechent, A. W. Kleij, G. A. Luinstra, *Green Chem.* **2020**, *22*, 969−978.

[21] C. Wulf, M. Reckers, A. Perechodjuk, T. Werner, *ACS Sustain. Chem. Eng.* **2020**, *8*, 1651−1658.

[22] M. Chehrazi, B. K. Moghadas, *J. CO2 Util.* **2022**, *61*, 102030.

[23] S. Dabral, T. Schaub, *Adv. Synth. Catal.* **2019**, *361*, 223−246.

[24] R. K. Parsapur, S. Chatterjee, K.-W. Huang, *ACS Energy Lett.* **2020**, *5*, 2881−2885.

[25] H. Kolbe, *Liebigs Ann.* **1860**, *113*, 125−127.

[26] S. Subramanian, Y. Song, D. Kim, C. T. Yavuz, *ACS Energy Lett.* **2020**, *5*, 1689−1700.

[27] a) A. Sharma, A. Kumar, S. A. H. Abdel Monaim, Y. E. Jad, A. El-Faham, B. G. de la Torre, F. Albericio, *Biopolymers* **2018**, *109*, e23110; b) M. Petrowsky, M. Ismail, D. T.

Glatzhofer, R. Frech, *J. Phys. Chem. B* **2013**, *117*, 5963−5970.

[28] a) L. Panza, F. Compostella, D. Imperio, *Carbohydr. Res.* **2019**, *472*, 50−57; b) F. Siragusa, E. Van Den Broeck, C. Ocando, A. J. Müller, G. De Smet, B. U. W. Maes, J. De Winter, V. Van Speybroeck, B. Grignard, C. Detrembleur, *ACS Sustain. Chem. Eng.* **2021**, *9*, 1714−1728; c) K. A. Maltby, M. Hutchby, P. Plucinski, M. G. Davidson, U. Hintermair, *Chem. Eur. J.* **2020**, *26*, 7405−7415; d) B. M. Stadler, C. Wulf, T. Werner, S. Tin, J. G. de Vries, *ACS Catal.* **2019**, *9*, 8012−8067.

[29] a) A. Gomez-Lopez, F. Elizalde, I. Calvo, H. Sardon, *Chem. Commun* **2021**, *57*, 12254−12265; b) H. Chen, P. Chauhan, N. Yan, *Green Chem.* **2020**, *22*, 6874−6888.

[30] J. Nemirowsky, *J. Prakt. Chem.* **1883**, *28*, 439−440.

[31] M. Selva, A. Caretto, M. Noè, A. Perosa, *Org. Biomol. Chem.* **2014**, *12*, 4143−4155.

[32] Q. Li, W. Zhang, N. Zhao, W. Wei, Y. Sun, *Catal. Today* **2006**, *115*, 111−116.

[33] F. Doro, P. Winnertz, W. Leitner, A. Prokofieva, T. E. Müller, *Green Chem.* **2011**, *13*, 292−295.

[34] a) F. D. Bobbink, W. Gruszka, M. Hulla, S. Das, P. J. Dyson, *Chem. Commun* **2016**, *52*, 10787−10790; b) M. Honda, M. Tamura, K. Nakao, K. Suzuki, Y. Nakagawa, K. Tomishige, *ACS Catal.* **2014**, *4*, 1893−1896.

[35] a) L. Guo, K. J. Lamb, M. North, *Green Chem.* **2021**, *23*, 77−118; b) H. Buttner, J. Steinbauer, C. Wulf, M. Dindaroglu, H. G. Schmalz, T. Werner, *ChemSusChem* **2017**, *10*, 1076−1079; c) Y. Yang, Y. Guo, J. Yuan, H. Xie, C. Gao, T. Zhao, Q. Zheng, *ACS Sustain. Chem. Eng.* **2022**, *10*, 7990−8001; d) Y.-Y. Zhang, G.-W. Yang, R. Xie, L. Yang, B. Li, G.-P. Wu, *Angew. Chem. Int. Ed.* **2020**, *59*, 23291−23298.

[36] H. Zhou, W.-Z. Zhang, C.-H. Liu, J.-P. Qu, X.-B. Lu, *J. Org. Chem.* **2008**, *73*, 8039−8044.

[37] J. Sun, W. Cheng, Z. Yang, J. Wang, T. Xu, J. Xin, S. Zhang, *Green Chem.* **2014**, *16*, 3071−3078.

[38] a) S. Liu, N. Suematsu, K. Maruoka, S. Shirakawa, *Green Chem.* **2016**, *18*, 4611−4615; b) J. Steinbauer, A. Spannenberg, T. Werner, *Green Chem.* **2017**, *19*, 3769−3779; c) J. Steinbauer, C. Kubis, R. Ludwig, T. Werner, *ACS Sustain. Chem. Eng.* **2018**, *6*, 10778−10788; d) Y. Hu, Z. Wei, A. Frey, C. Kubis, C.-Y. Ren, A. Spannenberg, H. Jiao, T. Werner, *ChemSusChem* **2021**, *14*, 363−372.

[39] F. Della Monica, A. W. Kleij, *Catal. Sci. Technol.* **2020**, *10*, 3483−3501.

[40] S. Liang, H. Liu, T. Jiang, J. Song, G. Yang, B. Han, *Chem. Commun* **2011**, *47*,

2131−2133.

[41] T. Werner, N. Tenhumberg, *J. CO2 Util.* **2014**, *7*, 39−45.

[42] S. Kaneko, S. Shirakawa, *ACS Sustain. Chem. Eng.* **2017**, *5*, 2836−2840.

[43] C. Terazzi, K. Laatz, J. von Langermann, T. Werner, *ACS Sustain. Chem. Eng.* **2022**, *10*, 13335−13342.

[44] Y. Tsutsumi, K. Yamakawa, M. Yoshida, T. Ema, T. Sakai, *Org. Lett.* **2010**, *12*, 5728−5731.

[45] H. Zhou, G.-X. Wang, W.-Z. Zhang, X.-B. Lu, *ACS Catal.* **2015**, *5*, 6773−6779.

[46] H. Buettner, J. Steinbauer, C. Wulf, M. Dindaroglu, H.-G. Schmalz, T. Werner, *ChemSusChem* **2017**, *10*, 1076−1079.

[47] a) Y. Hu, J. Steinbauer, V. Stefanow, A. Spannenberg, T. Werner, *ACS Sustain. Chem. Eng.* **2019**, *7*, 13257−13269; b) P. Goodrich, H. Q. N. Gunaratne, J. Jacquemin, L. Jin, Y. Lei, K. R. Seddon, *ACS Sustain. Chem. Eng.* **2017**, *5*, 5635−5641; c) S. Yue, P. Wang, X. Hao, *Fuel* **2019**, *251*, 233−241; d) Y. Hao, D. Yuan, Y. Yao, *ChemCatChem* **2020**, *12*, 4346−4351.

[48] a) M. Schou, C. Halldin, *J. Label. Compd. Radiopharm.* **2012**, *55*, 460−462; b) A. Del Vecchio, F. Caille, A. Chevalier, O. Loreau, K. Horkka, C. Halldin, M. Schou, N. Camus, P. Kessler, B. Kuhnast, F. Taran, D. Audisio, *Angew. Chem. Int. Ed.* **2018**, *57*, 9744−9748.

[49] J. Bruffaerts, N. von Wolff, Y. Diskin-Posner, Y. Ben-David, D. Milstein, *J. Am. Chem. Soc.* **2019**, *141*, 16486−16493.

[50] I. M. Downie, M. J. Earle, H. Heaney, K. F. Shuhaibar, *Tetrahedron* **1993**, *49*, 4015−4034.

[51] S. Kobayashi, K. Nishio, *J. Org. Chem.* **1994**, *59*, 6620−6628.

[52] R. Saladino, G. Botta, S. Pino, G. Costanzo, E. Di Mauro, *Chem. Soc. Rev.* **2012**, *41*, 5526−5565.

[53] D. Cheng, M. Wang, L. Tang, Z. Gao, X. Qin, Y. Gao, D. Xiao, W. Zhou, D. Ma, *Angew. Chem. Int. Ed.* **2022**, *61*, e202202654.

[54] N. Ortega, C. Richter, F. Glorius, *Org. Lett.* **2013**, *15*, 1776−1779.

[55] J. Zhu, Y. Zhang, Z. Wen, Q. Ma, Y. Wang, J. Yao, H. Li, *Chem. Eur. J.* **2023**, *29*, e202300106.

[56] C. Freudenreich, J. P. Samama, J. F. Biellmann, *J. Am. Chem. Soc.* **1984**, *106*, 3344−3353.

[57] C. Das Neves Gomes, O. Jacquet, C. Villiers, P. Thuéry, M. Ephritikhine, T. Cantat, *Angew. Chem. Int. Ed.* **2012**, *51*, 187−190.

[58] G. Li, J. Chen, D.-Y. Zhu, Y. Chen, J.-B. Xia, *Adv. Synth. Catal.* **2018**, *360*, 2364−2369.

[59] O. Jacquet, C. Das Neves Gomes, M. Ephritikhine, T. Cantat, *J. Am. Chem. Soc.* **2012**, *134*, 2934−2937.

[60] S. Das, F. D. Bobbink, S. Bulut, M. Soudani, P. J. Dyson, *Chem. Commun* **2016**, *52*, 2497−2500.

[61] B.-X. Leong, Y.-C. Teo, C. Condamines, M.-C. Yang, M.-D. Su, C.-W. So, *ACS Catal.* **2020**, *10*, 14824−14833.

[62] C. C. Chong, R. Kinjo, *Angew. Chem. Int. Ed.* **2015**, *54*, 12116−12120.

[63] V. B. Saptal, G. Juneja, B. M. Bhanage, *New J. Chem.* **2018**, *42*, 15847−15851.

[64] X.-F. Liu, R. Ma, C. Qiao, H. Cao, L.-N. He, *Chem. Eur. J.* **2016**, *22*, 16489−16493.

[65] X.-F. Liu, X.-Y. Li, C. Qiao, H.-C. Fu, L.-N. He, *Angew. Chem. Int. Ed.* **2017**, *56*, 7425−7429.

[66] Z. Yu, Z. Li, L. Zhang, K. Zhu, H. Wu, H. Li, S. Yang, *Green Chem.* **2021**, *23*, 5759−5765.

[67] T.-X. Zhao, G.-W. Zhai, J. Liang, P. Li, X.-B. Hu, Y.-T. Wu, *Chem. Commun* **2017**, *53*, 8046−8049.

[68] M. Hulla, F. D. Bobbink, S. Das, P. J. Dyson, *ChemCatChem* **2016**, *8*, 3338−3342.

[69] a) Y. Hu, J. Song, C. Xie, H. Wu, Z. Wang, T. Jiang, L. Wu, Y. Wang, B. Han, *ACS Sustain. Chem. Eng.* **2018**, *6*, 11228−11234; b) W. Zhao, X. Chi, H. Li, J. He, J. Long, Y. Xu, S. Yang, *Green Chem.* **2019**, *21*, 567−577.

[70] a) L. Hao, H. Zhang, X. Luo, C. Wu, Y. Zhao, X. Liu, X. Gao, Y. Chen, Z. Liu, *J. CO2 Util.* **2017**, *22*, 208−211; b) A. Kumar, P. Sharma, N. Sharma, Y. Kumar, D. Mahajan, *RSC Adv.* **2021**, *11*, 25777−25787.

[71] a) Y. Yang, M. Cui, *Eur. J. Med. Chem.* **2014**, *87*, 703−721; b) M. V. Fawaz, A. F. Brooks, M. E. Rodnick, G. M. Carpenter, X. Shao, T. J. Desmond, P. Sherman, C. A. Quesada, B. G. Hockley, M. R. Kilbourn, R. L. Albin, K. A. Frey, P. J. H. Scott, *ACS Chem. Neurosci.* **2014**, *5*, 718−730.

[72] O. Jacquet, C. Das Neves Gomes, M. Ephritikhine, T. Cantat, *ChemCatChem* **2013**, *5*, 117−120.

[73] Z. Zhang, Q. Sun, C. Xia, W. Sun, *Org. Lett.* **2016**, *18*, 6316−6319.

[74] M. Hulla, S. Nussbaum, A. R. Bonnin, P. J. Dyson, *Chem. Commun* **2019**, *55*,

13089−13092.

[75] X. Li, J. Zhang, Y. Yang, H. Hong, L. Han, N. Zhu, *J. Organomet. Chem.* **2021**, 122079.

[76] Y. Sun, K. Gao, *J. Org. Chem.* **2023**, *88*, 7463−7468.

[77] J. Chatterjee, F. Rechenmacher, H. Kessler, *Angew. Chem. Int. Ed.* **2013**, *52*, 254−269.

[78] a) E. M. Isin, C. S. Elmore, G. N. Nilsson, R. A. Thompson, L. Weidolf, *Chem Res Toxicol* **2012**, *25*, 532−542; b) D. J. McCarthy, C. Halldin, J. D. Andersson, M. Edward Pierson, in *Annual Reports in Medicinal Chemistry, Vol. 44* (Ed.: J. E. Macor), Academic Press, **2009**, p. 501−513; c) G. Antoni, B. Långström, in *Positron Emission Tomography: Basic Sciences* (Eds.: D. L. Bailey, D. W. Townsend, P. E. Valk, M. N. Maisey), Springer London, London, **2005**, p. 223−236.

[79] U. o. A. M. H. Qureshi，Top 200 small molecule drugs by sales in 2022, https://njardarson.lab.arizona.edu/content/top-pharmaceuticals-poster.

[80] E. Curti, D. de Britto, S. P. Campana-Filho, *Macromol. Biosci.* **2003**, *3*, 571−576.

[81] M. L. Di Gioia, A. Leggio, A. Le Pera, A. Liguori, A. Napoli, C. Siciliano, G. Sindona, *J. Org. Chem.* **2003**, *68*, 7416−7421.

[82] M. Selva, A. Perosa, *Green Chem.* **2008**, *10*, 457−464.

[83] H. Seo, A.-C. Bédard, W. P. Chen, R. W. Hicklin, A. Alabugin, T. F. Jamison, *Tetrahedron* **2018**, *74*, 3124−3128.

[84] S. H. Pine, *J. Chem. Educ.* **1968**, *45*, 118.

[85] a) I. Sorribes, K. Junge, M. Beller, *Chem. Eur. J.* **2014**, *20*, 7878–7883; b) K. Beydoun, T. vom Stein, J. Klankermayer, W. Leitner, *Angew. Chem. Int. Ed.* **2013**, *52*, 9554−9557.

[86] D.-Y. Zhu, L. Fang, H. Han, Y. Wang, J.-B. Xia, *Org. Lett.* **2017**, *19*, 4259−4262.

[87] Z. Yang, B. Yu, H. Zhang, Y. Zhao, G. Ji, Z. Ma, X. Gao, Z. Liu, *Green Chem.* **2015**, *17*, 4189−4193.

[88] Y. Li, X. Cui, K. Dong, K. Junge, M. Beller, *ACS Catal.* **2017**, *7*, 1077−1086.

[89] a) Y. Zhang, H. Zhang, K. Gao, *Org. Lett.* **2021**, *23*, 8282−8286; b) H. Zhang, Y. Zhang, K. Gao, *Org. Chem. Front.* **2023**, *10*, 2491−2497.

[90] H. Niu, L. Lu, R. Shi, C.-W. Chiang, A. Lei, *Chem. Commun* **2017**, *53*, 1148−1151.

[91] M. Hulla, P. J. Dyson, *Angew. Chem. Int. Ed.* **2020**, *59*, 1002−1017.

[92] C. Zhang, Y. Lu, R. Zhao, W. Menberu, J. Guo, Z.-X. Wang, *Chem. Commun* **2018**, *54*, 10870−10873.

[93] a) S. Liu, Y. Kumatabara, S. Shirakawa, *Green Chem.* **2016**, *18*, 331−341; b) S. Fang, Z.

Liu, T. Wang, *Angew. Chem. Int. Ed.* **2023**, *62*, e202307258.

[94] a) J. Steinbauer, L. Longwitz, M. Frank, J. Epping, U. Kragl, T. Werner, *Green Chem.* **2017**, *19*, 4435−4445; b) Y. Toda, Y. Komiyama, A. Kikuchi, H. Suga, *ACS Catal.* **2016**, *6*, 6906−6910.

[95] D. Bianchi, A. Bosetti, P. Cesti, P. Golini, *Tetrahedron Lett.* **1992**, *33*, 3231−3234.

[96] M. Borsa, G. Tonon, S. Malandrino, **1987**, *US4699911A*.

[97] A. S. Stalsmeden, J. L. B. Vazquez, K. van Weerdenburg, R. Rae, P.-O. Norrby, N. Kann, *ACS Sustainable Chem. Eng.* **2016**, *4*, 5730–5736.

[98] C. Ren, C. Terazzi, T. Werner, *Green Chem.* **2024**, *26*, 439−447.

[99] M. Fabris, M. Noè, A. Perosa, M. Selva, R. Ballini, *J. Org. Chem.* **2012**, *77*, 1805−1811.

[100] L. Cattelan, M. Noè, M. Selva, N. Demitri, A. Perosa, *ChemSusChem* **2015**, *8*, 3963−3966.

[101] A. Berkessel, M. Brandenburg, *Org. Lett.* **2006**, *8*, 4401−4404.

[102] M. Hatano, Y. Tabata, Y. Yoshida, K. Toh, K. Yamashita, Y. Ogura, K. Ishihara, *Green Chem.* **2018**, *20*, 1193−1198.

6 Appendix

My contributions to publications are given.

Publication 1: Y. Hu, Z. Wei, A. Frey, C. Kubis, C.-Y. Ren, A. Spannenberg, H. Jiao, and T. Werner, *ChemSusChem* **2020**, *14*, 363−372.

"*Catalytic, Kinetic, and Mechanistic Insights into the Fixation of CO_2 with Epoxides Catalyzed by Phenol-Functionalized Phosphonium Salts*"

In this work, I did a small part of the experiments. My overall contribution to this work is approximately 5%.

Publication 2: C. Ren, A. Spannenberg, T. Werner, *Asian J. Org. Chem.* **2022**, *11*, e202200156.

"*Synthesis of Bifunctional Phosphonium Salts Bearing Perfluorinated Side Chains and Their Application in the Synthesis of Cyclic Carbonates from Epoxides and CO_2*"

In this work, I did all the part of the experiments. The manuscript was written by me. My overall contribution to this work is approximately 80%.

Publication 3: C. Ren, A. Spannenberg, T. Werner, *ACS Sustainable Chemistry & Engineering.* **2024**, accepted.

*"*Phosphonium salt catalyzed *N*-methylation and *N*-formylation of amines with CO_2*"*

In this work, I did all the part of the experiments. The manuscript was written by me. My overall contribution to this work is approximately 80%.

Publication 4: C. Ren, C. Terazzi and T. Werner, *Green Chem.* **2024**, *26*, 439−447.

"Tunable reduction of CO_2 – organocatalyzed selective formylation and methylation of amines"

A large part of experiments and manuscript were carried out and written by me by me. My overall contribution is approximately 60%.

6.1 Catalytic, Kinetic, and Mechanistic Insights into the Fixation of CO_2 with Epoxides Catalyzed by Phenol-Functionalized Phosphonium Salts

Y. Hu, Z. Wei, A. Frey, C. Kubis, C.-Y. Ren, A. Spannenberg, H. Jiao, and T. Werner*
ChemSusChem **2020**, *14*, 363−372.

DOI: 10.1002/cssc.202002267

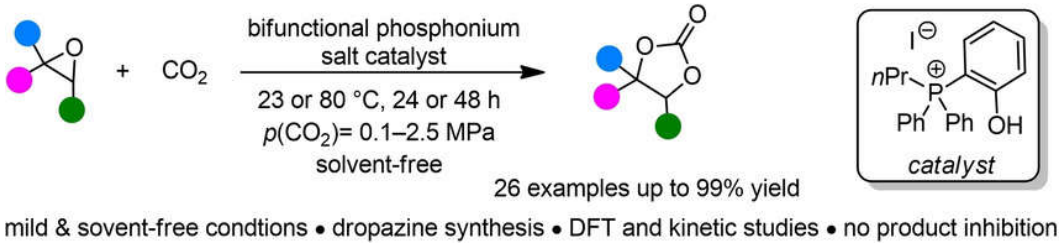

Abstract: A series of hydroxy-functionalized phosphonium salts were studied as bifunctional catalysts for the conversion of CO_2 with epoxides under mild and solvent-free conditions. The reaction in the presence of a phenol-based phosphonium iodide proceeded via a first order rection kinetic with respect to the substrate. Notably, in contrast to the aliphatic analogue, the phenol-based catalyst showed no product inhibition. The temperature dependence of the reaction rate was investigated, and the activation energy for the model reaction was determined from an Arrhenius-plot (*E*a=39.6 kJmol^{-1}). The substrate scope was also evaluated. Under the optimized reaction conditions, 20 terminal epoxides were converted at room temperature to the corresponding cyclic carbonates, which were isolated in yields up to 99%. The reaction is easily scalable and was performed on a scale up to 50 g substrate. Moreover, this method was applied in the synthesis of the antitussive agent dropropizine starting from epichlorohydrin and phenylpiperazine. Furthermore, DFT calculations were performed to rationalize the mechanism and the high efficiency of the phenol-based phosphonium iodide catalyst. The calculation confirmed the activation of the epoxide via hydrogen bonding for the iodide salt, which facilitates the ring-opening step. Notably, the effective Gibbs energy barrier regarding this step is 97 kJmol^{-1} for the bromide and 72 kJmol^{-1} for the iodide salt, which explains the difference in activity.

VIP *Very Important Paper*

Catalytic, Kinetic, and Mechanistic Insights into the Fixation of CO_2 with Epoxides Catalyzed by Phenol-Functionalized Phosphonium Salts

Yuya Hu,[a] Zhihong Wei,[a, b] Anna Frey,[a] Christoph Kubis,[a] Chang-Yue Ren,[a] Anke Spannenberg,[a] Haijun Jiao,[a] and Thomas Werner*[a]

Dedicated to Paul Kamer, a great scientist and inspiring person.

A series of hydroxy-functionalized phosphonium salts were studied as bifunctional catalysts for the conversion of CO_2 with epoxides under mild and solvent-free conditions. The reaction in the presence of a phenol-based phosphonium iodide proceeded via a first order rection kinetic with respect to the substrate. Notably, in contrast to the aliphatic analogue, the phenol-based catalyst showed no product inhibition. The temperature dependence of the reaction rate was investigated, and the activation energy for the model reaction was determined from an Arrhenius-plot ($E_a = 39.6$ kJ mol^{-1}). The substrate scope was also evaluated. Under the optimized reaction conditions, 20 terminal epoxides were converted at room temperature to the corresponding cyclic carbonates, which were isolated in yields up to 99%. The reaction is easily scalable and was performed on a scale up to 50 g substrate. Moreover, this method was applied in the synthesis of the antitussive agent dropropizine starting from epichlorohydrin and phenylpiperazine. Furthermore, DFT calculations were performed to rationalize the mechanism and the high efficiency of the phenol-based phosphonium iodide catalyst. The calculation confirmed the activation of the epoxide via hydrogen bonding for the iodide salt, which facilitates the ring-opening step. Notably, the effective Gibbs energy barrier regarding this step is 97 kJ mol^{-1} for the bromide and 72 kJ mol^{-1} for the iodide salt, which explains the difference in activity.

Introduction

The use of CO_2 as a C_1 building block is receiving increasing attention from the scientific and industrial community due to economic and ecological considerations.[1] It is progressively regarded as an attractive, inexpensive, and abundant renewable feedstock rather than waste.[2] Furthermore, in a future CO_2 based circular economy it can be used as a platform to produce bulk chemicals and energy carriers through its transformation to fuels.[3] Nevertheless, due to its thermodynamic stability, the efficient activation and chemical fixation is still challenging.[4] This can be partially overcome by converting CO_2 with high-energy starting materials such as epoxides or hydrogen in the presence of a catalyst. Thus, it is crucial to develop new catalytic processes that allow the efficient transformation of CO_2 into valuable products. Promising transformations even on an industrial scale are the fixation of CO_2 into organic carbonates or polycarbonates (Scheme 1, A).[1b,5] These processes can be of significant advantage regarding economic and ecological considerations, for example, by saving fossil resources or lowering the carbon footprint of a process.[6]

The synthesis of five-membered cyclic carbonates **2** from CO_2 and epoxides **1** is of particular interest. It is an atom-economic reaction and an excellent example of green chemistry.[7] Moreover, cyclic carbonates are important materials that are used in various applications, for example, as intermediates in organic synthesis,[8] indirect CO_2 reductions to methanol,[9] green solvents,[10] electrolyte in lithium ion batteries,[11] polymer building blocks,[12] and even as additives in drugs and cosmetics.[13]

Metal-based systems including Al-salen[14] and triphenolat[15] complexes have been reported for the synthesis of cyclic carbonates.[16] In these binary catalytic systems, the Lewis-acidic metal complexes are often combined with an external nucleophile, typically a halide ion from an onium salt, to activate the epoxide (Scheme 1, B). The nucleophilic counter anion of the salt acts as a temporary relay, ring-opening the epoxide, which is activated by the Lewis-acidic metal center, and subsequently serving as a leaving group upon ring closure after CO_2 insertion. Catalytic systems that operate under near-ambient conditions (low CO_2 pressure and room temperature) are of interest in terms of advances towards sustainability.[17] In the past decade, the use of organocatalysts has attracted increasing attention in this research area.[18] A significant benefit

[a] Y. Hu, Dr. Z. Wei, A. Frey, Dr. C. Kubis, C.-Y. Ren, Dr. A. Spannenberg, Dr. H. Jiao, Dr. T. Werner
Leibniz Institute for Catalysis e. V.
Albert-Einstein-Straße 29a, 18059, Rostock (Germany)
E-mail: Thomas.Werner@catalysis.de
[b] Dr. Z. Wei
Institute of Molecular Science, Key Laboratory of Materials for Energy Conversion and Storage of Shanxi Province
Shanxi University
Taiyuan 030006 (P. R. China)

Supporting information for this article is available on the WWW under https://doi.org/10.1002/cssc.202002267

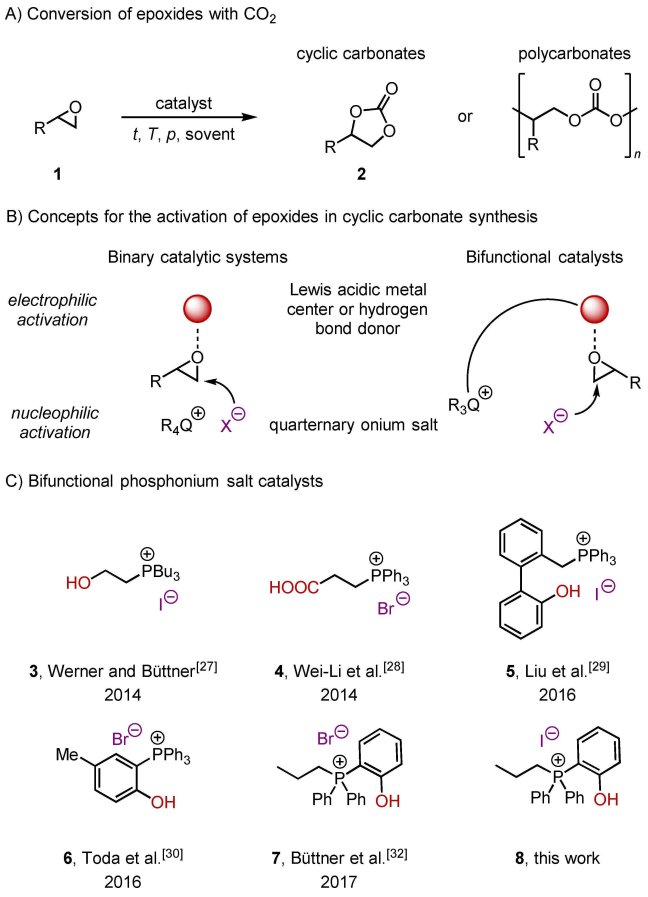

Scheme 1. Synthesis of cyclic and polycarbonates as well as concepts and selected catalysts for the conversion of epoxides with CO_2.

of this catalyst class is undoubtedly the metal-free carbon-based scaffold, which is associated with a high potential for structural modification, catalyst tuning, and immobilization.[19] In analogy to the metal-based systems, the combination of hydrogen bond donors and quaternary ammonium salts to activate the epoxide proved to be a promising concept in the field of organocatalyzed cyclic carbonate synthesis (Scheme 1, B).[20] Systems based on different hydrogen bond donor functionalities, such as alcohols,[21] carboxylic acids,[22] silanol,[23] phenols,[24] and (thio-)ureas,[25] were used in combination with external nucleophiles to catalyze the addition of CO_2 to epoxides to yield the corresponding cyclic carbonates. Even though great advances have been made it is still challenging to realize this reaction efficiently under low CO_2 pressures (1 atm) and reaction temperatures below 100 °C.[17]

It is generally recognized that bifunctional catalysts consisting of an electrophilic group and an internal nucleophile significantly accelerate the process through synergistic effects.[18,26] However, it was not until recently that bifunctional phosphonium salts emerged as potent class of organocatalysts (Scheme 1, C). In 2014 our group reported the use of bifunctional phosphonium salt catalyst **3** bearing an alcohol moiety as hydrogen bond donor. This catalyst allowed for the synthesis of cyclic carbonates at 90 °C and 1.0 MPa CO_2 pressure, yielding the desired products in up to 99% yield under solvent-free conditions.[27] More recently, we reported a mechanistic study on the use of bifunctional phosphonium salt **3**.[26a] This study clearly showed that the epoxide is activated by hydrogen bonding and that the order of reactivity in regard to the anion increased in the order $Cl^- < Br^- < I^-$. Significantly, the analysis of the kinetic data revealed that partial product inhibition hampered the overall efficiency of this catalyst. Also in 2014, Wei-Li et al. introduced carboxylic acid derivative **4** as a catalyst for the synthesis of cyclic carbonates at elevated temperatures and pressure (130 °C and 2.5 MPa).[28] In 2016, Liu et al. showed that biphenyl-derived phosphonium salt **5** enables the conversion of epoxides with CO_2 at 60 °C and low CO_2 pressure (1.0 atm).[29] In the same year, Toda et al. studied bifunctional tetraarylphosphonium salt **6**, which allowed for the synthesis of cyclic carbonate at atmospheric CO_2 pressure but high reaction temperatures of 120 °C in chlorobenzene as the solvent.[30] Very recently, they carefully investigated the impact of the electronic properties of the substituents on the catalyst efficiency.[31] The introduction of electron-donating groups significantly enhanced the catalytic activity, which allowed to reduce the reaction temperature to 60 °C. In 2017 our group reported the use of bifunctional phenolic phosphonium bromide **7** for the preparation of oleochemical carbonates at 80 °C and 2.5 MPa CO_2 pressure.[32] Based on our previous results we envisioned that the corresponding iodide **8** should show superior efficiency as catalyst in the synthesis of cyclic carbonates under mild and solvent free-conditions. Herein we report the synthesis and application of this catalyst as well as thorough kinetic investigations and DFT calculations to rationalize its superior performance and the reaction mechanism.

Results and Discussion

Catalyst screening

We chose the conversion of 1,2-butylene oxide (**1a**) with CO_2 to produce 1,2-butylene carbonate (**2a**) as a benchmark system to evaluate and compare to previously reported catalysts under uniform reaction conditions (Table 1). Our first-generation bifunctional phosphonium salt **3** (2 mol%) gave the desired product **2a** in 25% yield after 24 h at 23 °C and 1.0 MPa CO_2 pressure (Table 1, entry 1). In the presence of catalysts **5**, **6**, and **7** significantly lower conversions and yields $\leq$10% were achieved (entries 2–4). In contrast, phosphonium iodide **8** gave **2a** in 65% yield (entry 5).

This is remarkable since catalyst **7** was identified to be more efficient compared to **8** at higher temperature (100 °C) and CO_2 pressure (5.0 MPa) in the synthesis of oleochemical carbonates.[32] With increasing reaction temperature the obtained yield for **2a** equalizes (entries 6–9). Notably, in the presence of 5 mol% **8** an excellent yield >99% was achieved at 23 °C (entry 10). Even at a lower CO_2 pressure of 0.1 MPa **2a** was obtained in 71% yield (entry 11). The lower yield might be due to a lower CO_2 concentration in solution at this pressure, which can have a strong impact on the reaction rate.[33]

Table 1. Comparison of bifunctional phosphonium salts in the cycloaddition of CO_2 with epoxides.

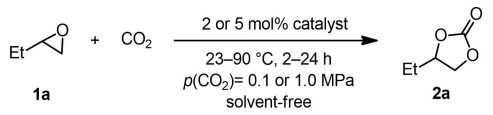

1a 2a

Entry	Catalyst	*Loading* [mol%]	*T* [°C]	*t* [h]	Yield[a] [%]	TON
1	**3**	2	23	24	25	13
2	**5**	2	23	24	2	1
3	**6**	2	23	24	2	1
4	**7**	2	23	24	10	5
5	**8**	2	23	24	65	33
6	**7**	2	45	6 (24)	60 (>99)	30
7	**8**	2	45	6 (24)	85 (>99)	43
8	**7**	2	90	2	89	45
9	**8**	2	90	2	96	48
10	**8**	5	23	24	>99	50
11[b]	**8**	5	23	24	71	36

Reaction conditions: 1.0 equiv. **1a** (1.00 g, 13.9 mmol), 2–5 mol% catalyst, 2–24 h, $p(CO_2) = 1.0$ MPa, solvent-free. [a] Yields were determined by ^{1}H NMR spectroscopy using mesitylene as internal standard. [b] $p(CO_2) = 0.1$ MPa. TON: turnover number.

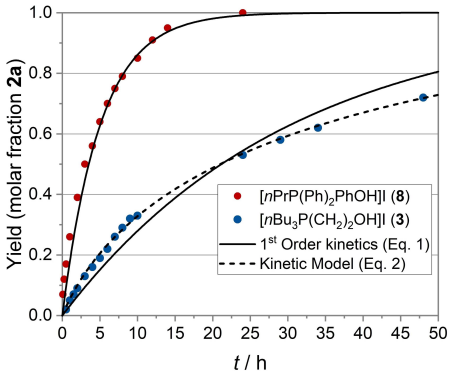

Figure 1. Comparison of a first-order kinetic fit and the kinetic model represented in Equation (2) for the conversion of epoxide **1a** with CO_2 in the presence of catalyst **3** and **8**. The observed selectivity was >99%. Reaction conditions: 1,2-butylene oxide (**1a**, 460 mmol), 2 mol% catalyst **3** or **8**, $p(CO_2) = 1.0$ MPa, 45 °C, 48 h.

$$\frac{dY}{dt} = k^{obs}(1 - Y) \quad (1)$$

$$\frac{dY}{dt} = \frac{k^{obs}(1 - Y)}{1 + K_{inh}[S]^0 Y} \quad (2)$$

Kinetic investigations

The efficiency of bifunctional phosphonium salts is closely related to the ability of activating the epoxide by hydrogen bonding.[20] Recently, we reported a detailed mechanistic study on alkyl-bridged bifunctional phosphonium salts as catalysts in cyclic carbonate synthesis.[26a] In this study the activation of epoxide **1a** by hydrogen bonding to catalyst **3** was proven by IR spectroscopy. Moreover, kinetic and IR studies revealed an interaction of **3** with the product **2a** leading to significant product inhibition. In the present case attempts failed to investigate the interaction of phenolic catalyst **8** with the epoxide or the carbonate by transmission IR spectroscopy due to an overlap of the OH-stretching vibration from the phenol moiety with bands of the C–H stretching modes. Unfortunately, also measurements in the attenuated total reflection (ATR) mode did not provide unambiguous results in this regard.[34]

However, to further investigate the difference in the activity of catalysts **3** and **8**, we performed kinetic measurements of the model reaction with 1,2-butylene oxide (**1a**) as the substrate at 23 and 45 °C. These experiments have been conducted at a CO_2 pressure of 1.0 MPa with a substrate content of 460 mmol and 2 mol% of catalyst. Product formation was monitored by the sampling of the liquid reaction mixture at distinct time intervals followed by ^{1}H NMR spectroscopic analyses. The selectivity of **2a** was consistently >99%. At 23 °C with **8** as a catalyst, an induction period was observed, which was attributed to the low solubility of **8** in the pure epoxide at room temperature.[34] For the catalyst system **3**, no induction period has been identified, but at higher conversions the catalytic performance is significantly lower compared to the phenolic catalyst **8**. In the next step, we performed these model reactions at 45 °C. Now, for the catalyst **8**, the yield versus time data can be described by a first-order kinetic model [Eq. (1)], in which Y is the yield and k^{obs} is the observable rate constant, as shown in Figure 1.

In contrast, for the reaction in the presence of **3** a kinetic model in which product inhibition was considered needs to be used [Eq. (2)]. This equation is based on a Michaelis-Menten model including a reversible product inhibition, which is valid for the case of a first order with respect to the substrate. The equilibrium constant K_{inh} of the product inhibition with the aliphatic catalyst **3** was calculated as 0.260 L mol^{-1} for the given initial substrate concentration $[S]^0$. The fact that the yield versus time data for **8** was best described with the first-order model indicates that product inhibition is not relevant for this system. The obtained observable rate constants k^{obs} were 0.197 h^{-1} (**8**) >0.0605 h^{-1} (**3**), reflecting the catalytic activity.[34] From these observations it can be concluded that both the absence of a significant product inhibition and an intrinsically higher activity for the catalytic system with catalyst **8** cause its better performance.

We were further interested in the temperature dependence of the reaction rate for the catalytic system with the phenolic catalyst **8**.[34] Therefore, additional experiments have been performed so that a temperature range of 35–90 °C was covered. Yield versus time data was analyzed using a first-order kinetic model (first-order with respect to the substrate concentration) providing observable rate constants (k^{obs}). An acceptable Arrhenius behavior was found between 35–65 °C (T = 308.15–338.15 K). Interestingly, at higher temperatures the values of the rate constant decreased, which might be attributed to a change in the solubility of CO_2 at higher temperatures.[33b] From an Arrhenius-plot a value for the activation energy was calculated with $E_a = 39.6$ kJ mol^{-1}, which is in agreement with previous reports (Figure 2).[35] A respective Eyring-plot allowed for the calculation of the enthalpy of activation, which gave a value of $\Delta H^{\ddagger} = 36.9$ kJ mol^{-1}.

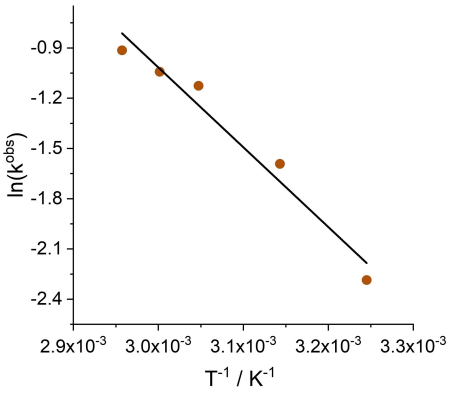

Figure 2. Arrhenius-plot for the estimation of the activation energy E_a of the conversion of epoxide **1a** with CO_2 in the presence of catalyst **8** over the temperature range of 35–65 °C (T = 308.15–338.15 K). Reaction conditions: 1,2-butylene oxide (**1a**, 460 mmol), 2 mol% catalyst **8**, $p(CO_2)$ = 1.0 MPa. $y = -476.5x + 13.277$, $R^2 = 0.9638$.

Substrate scope

Due to the observed superior efficiency of catalyst **8** we evaluated the substrate scope regarding the conversion of terminal epoxides **1** to the respective cyclic carbonates **2** at room temperature (Figure 3). Carbonates **2a–d** bearing aliphatic substituents were synthesized in good to excellent yields. Particularly, propylene carbonate (**2b**) has attracted much interest due to its applications as an electrolyte in lithium-ion batteries[11] and is regarded as one of the most sustainable alternative solvents in organic chemistry.[10a] Notably, the conversion of enantiomerically pure (*S*)-propylene oxide (*S*-**1b**) led to the corresponding cyclic carbonates *S*-**2b** in 94% yield and >99% enantiomeric excess (*ee*). Due to the lower polarity of epoxides **1c** and **1d** the solubility of the catalyst was reduced, and the addition of a solvent (*n*BuOH) was required to achieve 95 and 72% yield for **2c** and **2d**, respectively. The phenyl-substituted product **2e** was isolated in a yield of 74%. In this case acetophenone was found as a by-product that was derived from a Meinwald rearrangement.[36] This indicates that the conversion of styrene oxide (**1e**) proceeds at least partially via a cationic intermediate. This assumption is supported by the partial racemization, which was observed when (*R*)-styrene oxide (*R*-**1e**) was converted. In this case, carbonate *R*-**2e** was isolated in 74% yield and 83% *ee*. Furthermore, epichlorohydrin (**1f**) was converted to the respective carbonate **2f** in an excellent yield of 95% while morpholine derivative **2g** was obtained in 73% yield. After having established a general protocol for the conversion of monosubstituted epoxides under mild conditions, the catalyst system was applied in converting disubstituted terminal epoxides. Products **2h** and **2i** were obtained in yields of 86 and 85%, respectively, even though elevated reaction temperature (80 °C) and higher CO_2 pressure (2.5 MPa) were required.

Cyclic carbonates are frequently used as protecting groups for 1,2-diols.[37] The successful preparation of morpholine derivative **2g** prompted us to evaluate the synthesis of dropropizine *rac*-**10**, which is an antitussive agent typically employed as a racemic mixture in a number of commercial cough suppressant.[38] In general, it is prepared from the epoxides **1j** under acidic conditions or by direct amination of solketal, a 1,2-hydroxy-protected derivative of glycerol, via ruthenium-catalyzed hydrogen borrowing reaction and subsequent ketal hydrolysis.[39]

The intermediate epoxide *rac*-**1j** as well as enantiomerically pure *R*- and *S*-**1j** were obtained in yields up to 96% from phenylpiperazine (**9**) and the respective epichlorohydrin (**1f**) (Scheme 2). The subsequent conversion under the standard reaction conditions for terminal epoxides gave the respective carbonate *rac*-**2j** in 65% after 48 h. At 45 °C full conversion was achieved, and **2j** was isolated in >99% yield. The subsequent cleavage of the carbonate protecting group under basic conditions gave dropropizine *rac*-**10** in 95% yield. Notably, the formation and subsequent cleavage of the carbonate to obtain

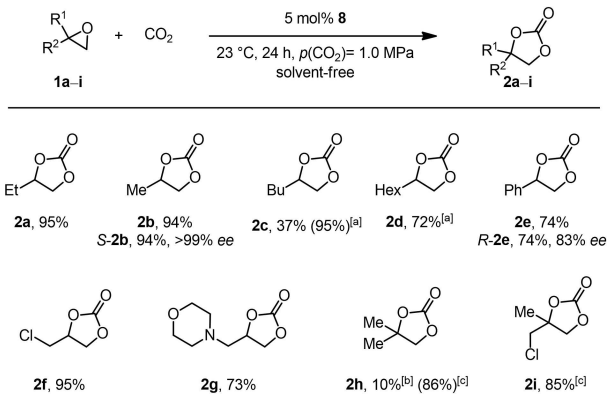

Figure 3. Substrate scope for the conversion of terminal epoxides **1** into the corresponding carbonates **2**. Reaction conditions: 1.0 equiv. **1** (1.00 g), 5 mol% **8**, 23 °C, 24 h, $p(CO_2)$ = 1.0 MPa, solvent-free. Isolated yields are given. [a] *n*-Butanol was employed as a solvent. [b] Yields were determined by ^{1}H NMR spectroscopy using mesitylene as internal standard. [c] 80 °C, $p(CO_2)$ = 2.5 MPa.

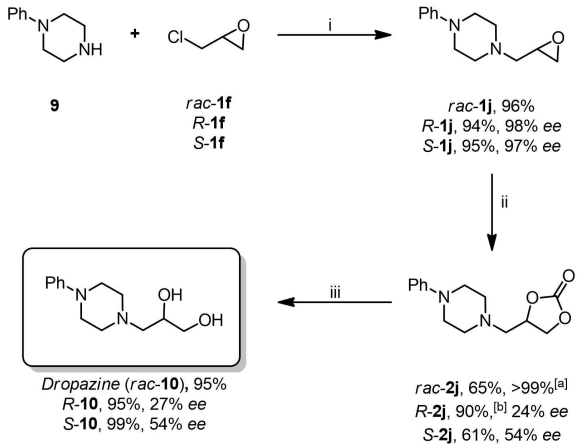

Scheme 2. Synthesis of dropropizine via cyclic carbonate **2j**. Reaction conditions: i) 23 °C, 1 h, H_2O then NaOH/H_2O, 75 °C, 15 min. ii) 5 mol% **8**, 23 °C, 48 h, $p(CO_2)$ = 1.0 MPa. iii) NaOH/H_2O, 3 h, 23 °C. [a] 45 °C. [b] 45 °C, 24 h.

dropropizine in a sequential one-pot reaction could also be achieved, leading to *rac*-**10** in 61% yield. We envisioned that also enantiomerically pure dropropizine should be accessible via this route. Notably, this protocol circumvents the acidic hydrolysis of the epoxide to the 1,2-diol, which might lead to racemization. The precursors *R*-**1j** and *S*-**1j** were readily accessible from (*R*)- and (*S*)-epichlorohydrin (*R*- and *S*-**1f**) and amine **9** in excellent yields and enantioselectivities of 94% (98% *ee*) and 95% (97% *ee*), respectively. The conversion of *R*-**1j** with CO_2 at 45 °C led to carbonate *R*-**2j** in excellent 90% yield. However, under these conditions partial racemization was observed, and *R*-**2j** was obtained in 24% *ee*. Thus, *S*-**2h** was converted at lower temperature (23 °C), which led to a significant improvement to 54% *ee* but a lower yield of 61%. The deprotection of carbonates *R*-**2j** and *S*-**2j** occurred stereoselectively as expected to yield enantiomerically enriched *R*-**10** and *S*-**10** in 95 and 99% yield, respectively.

As the major by-product in the manufacturing of biodiesel, glycerol is widely available.[40] Thus, the use of glycerol as the feedstock for the preparation of value-added products is an attractive goal. Moreover, the use of this biobased material can lead to a significant reduction in the carbon footprint, for example, in the synthesis of carbonates, compared to their production from fossil resources.[6a] Glycidol (**11c**) and its derivatives can be obtained from glycerol.[41] The respective carbonates show unique properties and find a range of applications, for example, as synthetic building blocks, monomers, and solvents.[10b,42] Hence, we were particularly interested in the preparation of cyclic carbonates **12a–j** from epoxides **11a–j** in the presence of catalyst **8** (Figure 4). Under the standard conditions the conversion of glycidyl ethers **11a** and **11b** did not lead to full conversion, and **12a** and **12b** were isolated in 56 and 58% yield, respectively. Hence, we adjusted the reaction time to 48 h, which led to full conversion and excellent isolated yields of 96 and 97%. The conversion of glycidol (**11c**), which is susceptible to polymerization,[43] gave glycerol carbonate **12c** in 82%. In addition, the highly fluorinated carbonates **12d** and **12e**, which can be used as electrolytes in lithium batteries,[44] were prepared in yields of 86 and 79% respectively. Furthermore, the unsaturated carbonates **12f** and **12g**, which are potential building blocks for homo- and copolymers with cyclic carbonate units in the backbone, were isolated in distinguished yields up to 99%.[45] Epoxide **11h**, containing a furfuryl moiety, can also be synthesized from renewables,[46] and the respective carbonate was isolated in 97% yield. Silyl-functionalized carbonates are often used as precursors for the synthesis of non-isocyanate polyhydroxyurethane hybrid materials.[47] They also find applications in industry due to their potential utilization as electrolytes[48] and in surface modification. Thus, we converted **11i** with CO_2 in the presence of catalyst **8** and were able to obtain **12i** in 93% under slightly modified conditions. Additionally, bisphenol diglycidyl ether (**11j**) was converted into the respective carbonate **12j** in 95% yield. This biscarbonate is a frequently used monomer for the synthesis of non-isocyanate polyurethanes (NIPUs).[49]

The synthesis of internal carbonates derived from epoxides and CO_2 is rather challenging and is often marginally studied in the evaluation of the substrate scope. Considering the high efficiency of catalyst **8** in the conversion of terminal epoxides under mild conditions we were interested in its performance regarding the conversion of internal epoxides **13** (Figure 5). Initially, the standard protocol [5 mol%, 23 °C, 24 h, $p(CO_2) = 1.0$ MPa] was tested for the conversion of cyclohexene oxide

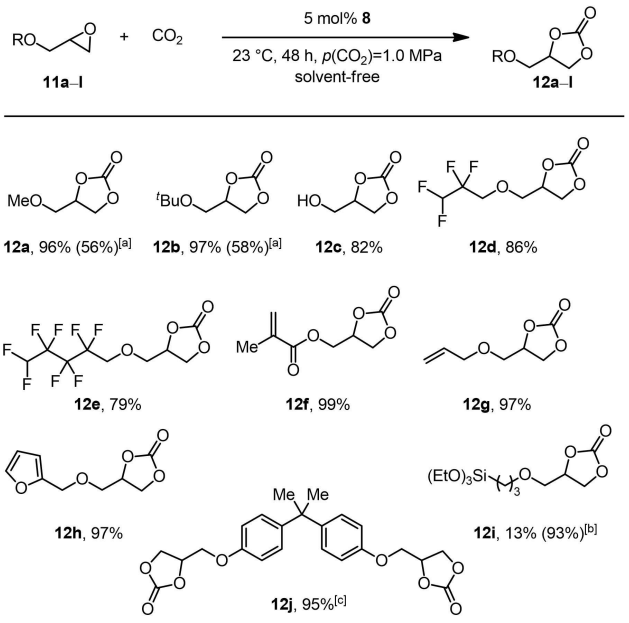

Figure 4. Substrate scope for the conversion of glycidol and its derivatives **11** into the corresponding carbonates **12**. Reaction conditions: 1.0 equiv. **11** (1.00 g), 5 mol% **8**, 23 °C, 48 h, $p(CO_2) = 1.0$ MPa, solvent-free. Isolated yields are given. [a] 24 h. [b] 2 mol% **8**, 90 °C, 4 h. [c] 10 mol% **8**, 45 °C, *n*-butanol as solvent.

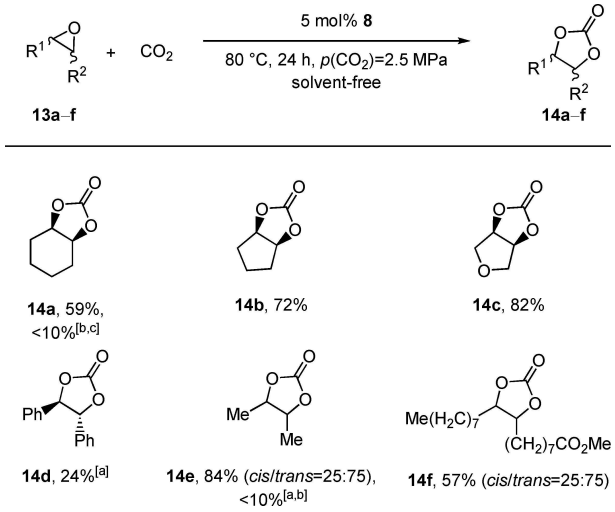

Figure 5. Substrate scope for the conversion of internal epoxides **13** into the corresponding carbonates **14**. Reaction conditions: 1.0 equiv. **13** (1.00 g), 5 mol% **8**, 80 °C, 24 h, $p(CO_2) = 2.5$ MPa, solvent-free. Isolated yields are given. [a] *n*-Butanol was employed as a solvent. [b] 23 °C, $p(CO_2) = 1.0$ MPa. [c] Yields were determined by ^{1}H NMR spectroscopy using mesitylene as the internal standard.

(**13a**). Under these conditions < 10% of the desired carbonate **14a** was obtained. Hence, the reaction temperature and CO_2 pressure were increased to 80 °C and 2.5 MPa, respectively. This led to significant improvement of the yield, and **14a** was obtained in 59%. Moreover, the conversion of epoxides **13b** and **13c** led to the corresponding cyclic carbonates **14b** and **14c** in 72 and 82% yield, respectively. Notably, the conversion of *cis*-stilbene oxide (**13d**) gave the *trans*-stilbene carbonate *trans*-**14d** in a selectivity of 99%. This indicates that the reaction proceeds via a cationic intermediate (S_N1-pathway), which is stabilized by the phenyl substituent.[34] This pathway leads to the thermodynamically more stable *trans*-product. Moreover, 1,2-diphenyl-ethan-1-one was observed as a by-product, which comes from the Meinwald rearrangement.[36] In contrast, the conversion of *cis*-**13e** and *cis*-methyl oleate (**13f**) gave the respective carbonates in yields up to 84% with a *cis*/*trans*-selectivity of 25:75. This can be attributed to the less pronounced stabilization of the cationic intermediate by hyperconjugation in the S_N1-pathway.

DFT calculations

On the basis of our findings and previous reports[50] we propose a three-step mechanism. The initial step is the ring-opening of epoxide **1a**. Subsequently, the positively charged carbon atom of CO_2 couples with the negatively charged oxygen atom to form a linear carbonate; alternatively, this step can also be considered as a nucleophilic attack of the negatively charged oxygen atom to the lowest unoccupied molecular orbital (LUMO) of CO_2. Finally, an intramolecular nucleophilic substitution leads to the formation of the desired cyclic carbonate and liberates the catalyst. Since the nucleophilic counterion has been found to have an important effect on the activity of the catalyst, both bromide salt **7** and iodide salt **8** were considered. On the basis of this proposal, we calculated the full Gibbs free-energy surface for the cycloaddition of CO_2 to epoxide **1a** catalyzed by phenol-derived phosphonium halides **7** and **8**, affording the five-membered cyclic carbonate **2a**. All computational details are given in the Supporting Information. Here we present the results for the more active catalyst **8**, while those for the less active bromide salt **7** can be found in the Supporting Information. The optimized structure **I** shows a hydrogen bonding (2.297 Å) interaction between the phenolic OH and the I^- counter ion. Notably, this interaction can also be seen in the crystal structure of catalyst **8** (Figure 6, O1A–H1A···I1A^i: O1A–H1A = 0.89(5) Å, H1A···I1A^i = 2.48(5) Å, O1A···I1A^i = 3.365(3) Å, O1A–H1A···I1A^i = 172(4)°, symmetry code: (i) $-1/2+x,y,1/2-z$).

For catalyst **8**, two possible pathways for the ring-opening at the methylene (C_β, Scheme 3, right) and methine carbon (C_α, Scheme 3, left) in the epoxide function were evaluated.

The structure of the intermediates in the catalytic cycle are shown in Scheme 3 while for clarity the optimized structures of transition states **TS1-α** to **TS3-α** as well as **TS1-β** to **TS3-β** are shown separately in Figure 7. The corresponding Gibbs free-energy profile for the opening at C_α and C_β is depicted in Figure 8. The initial step is the epoxide coordination to the phenol-derived phosphonium salt to form intermediate **II** via hydrogen bonding. The coordination is exergonic by 3 kJ mol^{-1}. This energy difference indicates dynamic equilibrium in favor of **II** (77%). The next step is the nucleophilic attack of I^- to the carbon of the epoxide with C–O bond cleavage and the formation of a C–I bond.

Notably, the ring-opening at C_β via transition state of **TS1-β** has an energy barrier of 68 kJ mol^{-1}, which is lower than that at C_α via transition state of **TS1-α** by 20 kJ mol^{-1}. This can be attributed to the steric interaction as estimated on the basis of the distortion energy of epoxide. Namely, the geometrical strain energy ΔE_{strain} of **1a** in **TS1-β** is 30.6 kJ mol^{-1} lower than that in

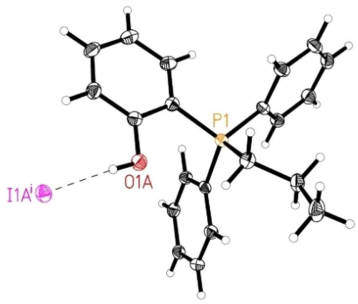

Figure 6. Molecular structure of catalyst **8** in the solid state. Displacement ellipsoids correspond to 30% probability. Lower occupancy sites are omitted for clarity. The intermolecular hydrogen bond is shown as dashed line.[51]

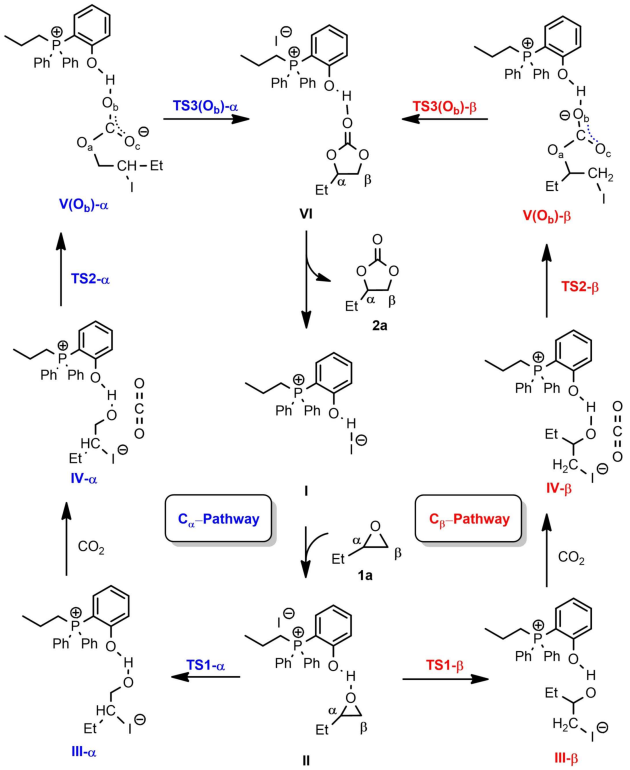

Scheme 3. Intermediates of the calculated catalytic cycle for ring-opening at the methylene (C_β, right) and methine carbon (C_α, left) at epoxide **1a**.

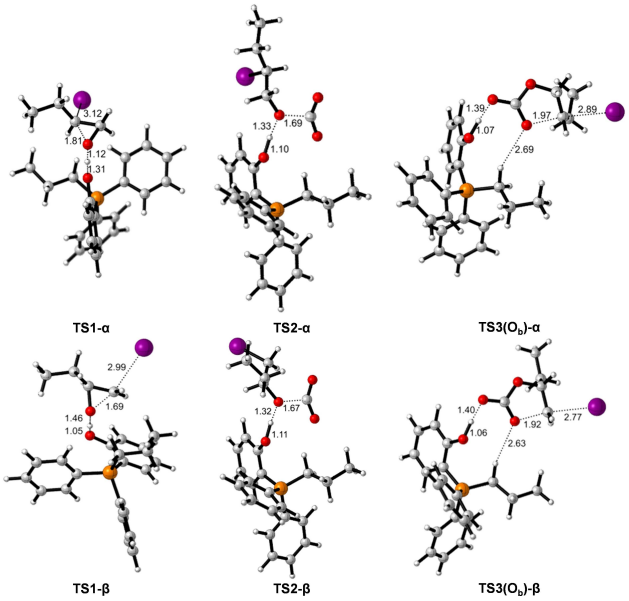

Figure 7. Optimized structures for transition states of **TS1-α** to **TS3-α** as well as **TS1-β** to **TS3-β**.

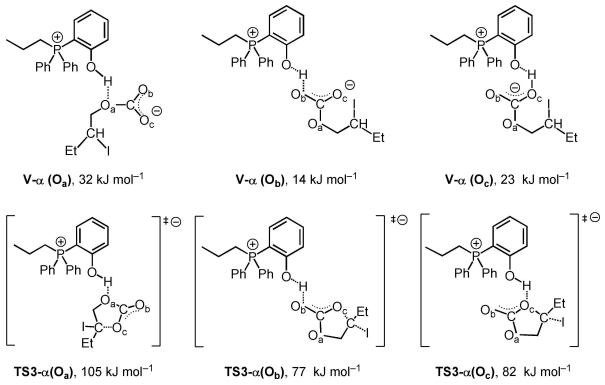

Figure 9. The three possibilities of the stabilized intermediates **Vα** (O_a, O_b, and O_c) and the transition states **TS3-α** (O_a, O_b, and O_c) in the C_α pathway. The structures of O_b hydrogen bonding interaction have the lowest energy.

TS1-α. The proton of the phenol group is transferred to the oxygen of iodo butanolate forming an ylide and iodo-butanol. The formation of **III** from **II** is endergonic by 15 and 9 kJ mol^{-1} for 2-iodobutan-1-ol (**III-α**) and 1-iodobutan-2-ol (**III-β**), respectively. The co-adsorption of CO_2 from **III-α** and **III-β** to form **IV-α** and **IV-β** is also endergonic by 14 and 26 kJ mol^{-1}, respectively. The energy barrier of C–O coupling via transition state of **TS2-α** and **TS2-β** is 40 and 57 kJ mol^{-1} from **III-α** and **III-β**, respectively. The formation of 2-iodobutyl carbonate anion **V-α** and 1-iodobutan-2-yl carbonate anion **V-β** in which O_b is interacting with the OH of phenol is endergonic by 2 and 9 kJ mol^{-1} from **III-α** and **III-β**, respectively.

For the last step (the ring-closure reaction), three possible pathways were calculated considering that three oxygen (O_a/O_b/O_c) in carbonate may interact with the OH group of phenol (Figure 9). For the α route, the interaction in **V-α** between 2-iodobutyl carbonate through O_a and O_c with OH of phenol is less favorable than that through O_b by 21 and 8 kJ mol^{-1}, respectively. This indicates the strong stabilization of the carboxylate anion through the hydrogen bonding between the OH-group of the phenol and O_b and O_c of the carboxylate moiety, respectively.

For the last step through the α route, the ring closure through the O_a, O_b, and O_c routes from the most stable **V-α** (O_b) via **TS3-α** to the carbonate–catalyst adduct **VI** has an energy barrier of 91, 63, and 68 kJ mol^{-1}, respectively. Notably, the formation of adduct **VI** is exergonic by 60 kJ mol^{-1}. For the β route, the interaction in **V-β** between 2-iodobutyl carbonate through O_b and O_c with OH of phenol is more favorable than that through O_a by 22 and 14 kJ mol^{-1}, respectively. The ring closure through the O_a, O_b, and O_c route from **V-β** (O_b) via **TS3-β** to form the adduct **VI** has an energy barrier of 78, 54, and 58 kJ mol^{-1}, respectively. The formation of cyclic carbonate from **V-β** (O_b) is exergonic by 61 kJ mol^{-1}. Notably, the release of the cyclic carbonate **2a** from the catalyst-carbonate adduct **VI** is exergonic by 14 kJ mol^{-1}. This confirms the experimental finding that in the presence of catalyst **8** no product inhibition takes place. Overall, the Gibbs free-energy profile shows that intermediate **II** is the resting state of the catalytic cycle. Interestingly, the ring-opening and ring-closing steps have very similar effective Gibbs energy barriers of 71 and 72 kJ mol^{-1}, respectively, indicating that both steps can be rate-determining.

For catalyst **7**, the Gibbs free-energy profile (Figure S22) shows that the interaction of epoxide with phenol-derived phosphonium to form intermediate $\mathbf{II_{Br}}$ through the H-bond is

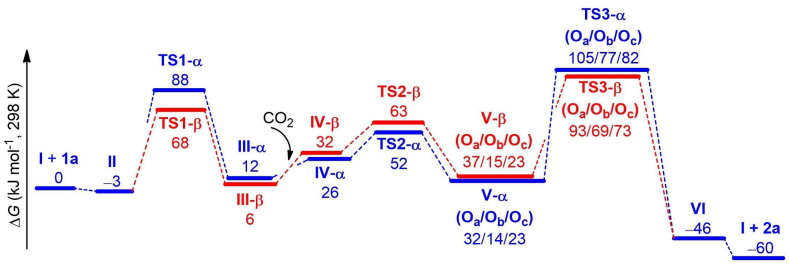

Figure 8. Calculated Gibbs free-energy profile for the addition of CO_2 to epoxide **1a** in the presence of catalyst **8** for the reaction at the methylene (C_β) and methine carbon (C_α).

endergonic by 27 kJ mol^{-1}. The large energy difference indicates dynamic equilibrium in favor of $\mathbf{I}_{Br}$ and **1a** (>99.99%) rather than $\mathbf{II}_{Br}$. For the ring-opening step, the β route is also more favorable than the α route. The energy barrier of ring-opening via **TS1-β$_{Br}$** is 97 kJ mol^{-1}, which is 5 kJ mol^{-1} lower than that via **TS1-α$_{Br}$**. It is worth noting that the formation of **III-β$_{Br}$** is highly exergonic by 22 kJ mol^{-1}, while the formation of **III-β$_{I}$** is slightly endergonic by 6 kJ mol^{-1}. This indicates that the reaction with both the Br^- catalyst **7** and the I^- catalyst **8** can compensate the increase of energy caused by ring-opening, and the formation of 1-bromobutan-2-ol is more thermodynamically preferred. The following C–O coupling via **TS2-β$_{Br}$** has an energy barrier of 51 kJ mol^{-1}. For the last step of ring-closing, the effective energy barrier via **TS3-β$_{Br}$(O$_b$)** from **III-β$_{Br}$** is 86 kJ mol^{-1}. In contrast to catalyst **8**, the rate-determining step for the reaction in the presence of catalyst **7** is clearly the ring-opening. The effective barrier regarding this step for the bromide salt **7** is 97 kJ mol^{-1}, which is higher than that for iodide salt **8** (72 kJ mol^{-1}) by 25 kJ mol^{-1}. This can reasonably explain the superior catalytic activity of **8** compared to catalyst **7**.

Conclusions

Bifunctional phenolic phosphonium salt catalysts showed superior efficiency in converting epoxides and CO_2 into value-added cyclic carbonates under mild and solvent-free conditions. The phenol-based phosphonium iodide **8** proved to be the most active catalyst. Notably, this catalyst showed high activity even at room temperature. Kinetic investigations revealed that the superior activity in comparison with the previously reported aliphatic catalyst **3** originates from a higher intrinsic activity as well as the absence of any product inhibition. In the model reaction the equilibrium constant K_{inh} of the product inhibition with the aliphatic catalyst was calculated as 0.260 L mol^{-1}. Moreover, the observable rate constants k^{obs} were determined as 0.197 h^{-1} (**8**) > 0.0605 h^{-1} (**3**), reflecting the catalytic activity. An apparent activation energy with a value of $E_a = 39.6$ kJ mol^{-1} was estimated for the benchmark reaction with catalyst **8**. The substrate scope was evaluated, and 20 terminal and 6 demanding internal epoxides were converted. Excellent results were achieved at room temperature for terminal epoxides while the conversion of internal epoxides required elevated reaction temperatures. Notably, catalyst **8** showed high functional group tolerance, and the desired cyclic carbonates were isolated in yields up to 99% even on multi-gram scale (up to 50 g substrate). Furthermore, this method was applied in the three-step synthesis of antitussive agent dropropizine starting from epichlorohydrin and phenylpiperazine. On the basis of the experimental findings the full Gibbs free-energy surfaces for the use of phenol-derived phosphonium halides **7** and **8** as catalysts in the model reaction were calculated. The calculation confirmed the activation of the epoxide via hydrogen bonding for the iodide salt, which facilitates the ring-opening step. Notably, the effective barrier regarding this step is 97 kJ mol^{-1} for the bromide and 72 kJ mol^{-1} for the iodide salt, which clearly explains the difference in activity. The DFT calculations also confirmed the experimental finding that no product inhibition occurs in the presence of the phenol-based phosphonium iodide. Interestingly, for catalyst **8** the ring-opening and ring-closing steps have similar effective Gibbs energy barriers of 71 and 72 kJ mol^{-1}, respectively, indicating that both steps can be rate-determining. In contrast, for catalyst **7** the rate-determining step is the epoxide opening with an effective Gibbs energy barrier of 97 kJ mol^{-1}.

Experimental Section

Synthesis of catalyst 8

2-(Diphenylphosphanyl)phenol:[52] Under argon a mixture of 2-iodophenol (660 mg, 3.00 mmol, 1.00 equiv.), $Pd(OAc)_2$ (6.7 mg, 0.029 mmol, 0.03 equiv.), and NaOAc (271 mg, 3.30 mmol, 1.10 equiv.) was dissolved in anhydrous dimethylacetamide (9.00 mL). After addition of diphenylphosphine (559 mg, 3.00 mmol, 1.00 equiv.) the reaction mixture was heated to 110 °C and stirred for 17 h. Subsequently, the reaction mixture was cooled to 23 °C and filtered over celite using CH_2Cl_2 as eluent. After removal of all volatiles under vacuum the crude product was purified by column chromatography (SiO_2, CH_2Cl_2) to yield the title compound (710 mg, 2.55 mmol, 83%) as a colorless solid. ^{1}H NMR (300 MHz, $CDCl_3$, 25 °C): $\delta = 6.26$–6.28 (br s, 1H), 6.88–7.03 (m, 3H), 7.29–7.39 (m, 11H) ppm. ^{31}P NMR (122 MHz, $CDCl_3$, 25 °C): $\delta = -28.62$ ppm.

(2-Hydroxyphenyl)diphenyl(propyl)phosphonium iodide (**8**):[32] In a pressure tube 1-iodopropane (2.17 g, 12.8 mmol) was added to 2-(diphenylphosphanyl)phenol (510 mg, 2.55 mmol). The tube was flushed with argon and sealed. Subsequently, the reaction mixture was stirred at 102 °C for 24 h. The crude product was filtered off and washed with Et_2O (4×50 mL) to yield **8** (1.06 g, 2.37 mmol, 93%) as a white solid. ^{1}H NMR (300 MHz, $CDCl_3$): $\delta = 1.14$ (td, $J = 7.3$, 1.9 Hz, 3H), 1.68–1.81(m, 2H), 3.08–3.18 (m, 2H), 6.84–6.92 (m, 1H), 6.94–7.01 (m, 1H), 7.53–7.69 (m, 9H), 7.75–7.82 (m, 2H), 7.96–8.01 (m, 1H), 10.78 (br s, 1H) ppm. ^{31}P NMR (122 MHz, $CDCl_3$) $\delta =$ 23.49 ppm.

Representative examples for the synthesis of cyclic carbonates

4-Methyl-1,3-dioxalan-2-one (**2a**):[53] A 45 cm^3 stainless-steel autoclave was charged with catalyst **8** (306 mg, 0.683 mmol, 5 mol%) and 1,2-epoxybutane (**1a**, 1.00 g, 13.9 mmol). The autoclave was purged with CO_2. Subsequently, the reaction mixture was stirred at 23 °C for 24 while $p(CO_2)$ was kept constant at 1.00 MPa. CO_2 was released slowly, and the reaction mixture was filtered over SiO_2 with EtOAc as eluent. After the removal of all volatiles under vacuum **2a** (1.53 g, 13.1 mmol, 95%) was obtained as a light-yellow oil. ^{1}H NMR (300 MHz, $CDCl_3$) $\delta = 1.03$ (t, $J = 7.4$ Hz, 3H), 1.66–1.93 (m, 2H), 4.09 (dd, $J = 8.4$, 7.0 Hz, 1H), 4.53 (dd, $J = 8.4$, 7.9 Hz, 1H), 4.61–4.74 (m, 1H) ppm.

4-(Methoxymethyl)-1,3-dioxalan-2-one (**12a**):[53] A 45 cm^3 stainless-steel autoclave was charged with 2-(methoxymethyl)oxirane (**11a**, 1.00 g, 11.4 mmol) and catalyst **8** (254 mg, 0.567 mmol, 5 mol%). The autoclave was purged with CO_2. Subsequently, the reaction mixture was stirred at 23 °C for 48 h while $p(CO_2)$ was kept constant at 1.00 MPa. CO_2 was released slowly, and the reaction mixture was filtered over SiO_2 with EtOAc as eluent. After the removal of all volatiles under vacuum **12a** (1.44 g, 10.9 mmol, 96%) was obtained as a yellow liquid. ^{1}H NMR (300 MHz, $CDCl_3$) $\delta = 3.43$ (s, 3H), 3.58

(dd, $J=10.9$, 3.8 Hz, 1H), 3.63 (dd, $J=3.9$ Hz, 1H), 4.39 (dd, $J=8.4$, 6.1 Hz, 1H), 4.50 (t, $J=8.3$ Hz, 1H), 4.75–4.87 (m, 1H) ppm.

cis-Tetrahydrofuro[3,4-d][1,3]dioxol-2-one (**14c**):[53] A 45 cm^3 stainless-steel autoclave was charged with 6-dioxabicyclo[3.1.0]hexane (**13c**, 1.00 g, 11.6 mmol) and catalyst **8** (261 mg, 0.582 mmol, 5 mol%). The autoclave was purged with CO_2. Subsequently the mixture was stirred at 80 °C for 24 h, while $p(CO_2)$ was kept constant at 2.50 MPa. The reactor was cooled with an ice bath below 20 °C and CO_2 was released slowly. The reaction mixture was filtered over SiO_2 with EtOAc as eluent. After the removal of all volatiles under vacuum the desired products **14c** (1.25 g, 9.61 mmol, 82%) was obtained as a colorless liquid.

Acknowledgements

This research was funded by the Leibniz Association within the scope of the Leibniz ScienceCampus Phosphorus Research Rostock (www.sciencecampus-rostock.de). C.-Y.R. is grateful for the financial support from Zunyi Medical University. Open access funding enabled and organized by Projekt DEAL.

Conflict of Interest

The authors declare no conflict of interest.

Keywords: CO_2 fixation · cyclic carbonates · homogeneous catalysis · mechanism · organocatalysts

[1] a) C. Hepburn, E. Adlen, J. Beddington, E. A. Carter, S. Fuss, N. Mac Dowell, J. C. Minx, P. Smith, C. K. Williams, *Nature* **2019**, *575*, 87–97; b) A. W. Kleij, M. North, A. Urakawa, *ChemSusChem* **2017**, *10*, 1036–1038; c) R. Wennersten, Q. Sun, H. Li, *J. Cleaner Prod.* **2015**, *103*, 724–736.
[2] a) M. Aresta, A. Dibenedetto, A. Angelini, *Chem. Rev.* **2013**, *114*, 1709–1742; b) J. Artz, T. E. Müller, K. Thenert, J. Kleinekorte, R. Meys, A. Sternberg, A. Bardow, W. Leitner, *Chem. Rev.* **2017**, *118*, 434–504; c) T. Sakakura, J.-C. Choi, H. Yasuda, *Chem. Rev.* **2007**, *107*, 2365–2387; d) F. M. Baena-Moreno, M. Rodriguez-Galan, F. Vega, B. Alonso-Farinas, L. F. V. Arenas, B. Navarrete, *Energy Sources Part A Recovery Util. Environ. Eff.* **2019**, *41*, 1403–1433.
[3] a) Z. Jiang, T. Xiao, V. L. Kuznetsov, P. P. Edwards, *Philos. Trans. R. Soc. London* **2010**, *368*, 3343–3364; b) R. Wennersten, Q. Sun, H. Li, *J. Cleaner Prod.* **2015**, *103*, 724–736; c) E. I. Koytsoumpa, C. Bergins, E. Kakaras, *J. Supercrit. Fluids* **2018**, *132*, 3–16.
[4] a) Q. Liu, L. Wu, R. Jackstell, M. Beller, *Nat. Commun.* **2015**, *6*, 5933; b) K. Müller, L. Mokrushina, W. Arlt, *Chem. Ing. Tech.* **2014**, *86*, 497–503.
[5] a) S. Dabral, T. Schaub, *Adv. Synth. Catal.* **2019**, *361*, 223–246; b) A. J. Kamphuis, F. Picchioni, P. P. Pescarmona, *Green Chem.* **2019**, *21*, 406–448.
[6] a) H. Büttner, C. Kohrt, C. Wulf, B. Schäffner, K. Groenke, Y. Hu, D. Kruse, T. Werner, *ChemSusChem* **2019**, *12*, 2701–2707; b) N. von der Assen, A. Bardow, *Green Chem.* **2014**, *16*, 3272–3280; c) N. von der Assen, J. Jung, A. Bardow, *Energy Environ. Sci.* **2013**, *6*, 2721–2734.
[7] P. Anastas, N. Eghbali, *Chem. Soc. Rev.* **2010**, *39*, 301–312.
[8] a) J. E. Gómez, À. Cristòfol, A. W. Kleij, *Angew. Chem. Int. Ed.* **2019**, *58*, 3903–3907; *Angew. Chem.* **2019**, *131*, 3943–3947; b) W. Guo, J. Gónzalez-Fabra, N. A. Bandeira, C. Bo, A. W. Kleij, *Angew. Chem. Int. Ed.* **2015**, *54*, 11686–11690; *Angew. Chem.* **2015**, *127*, 11852–11856; c) W. Guo, R. Kuniyil, J. E. Gómez, F. Maseras, A. W. Kleij, *J. Am. Chem. Soc.* **2018**, *140*, 3981–3987; d) L. C. Yang, Z. Q. Rong, Y. N. Wang, Z. Y. Tan, M. Wang, Y. Zhao, *Angew. Chem. Int. Ed.* **2017**, *56*, 2927–2931; *Angew. Chem.* **2017**, *129*, 2973–2977.
[9] a) X. Liu, J. G. de Vries, T. Werner, *Green Chem.* **2019**, *21*, 5248–5255; b) V. Zubar, Y. Lebedev, L. M. Azofra, L. Cavallo, O. El-Sepelgy, M. Rueping, *Angew. Chem. Int. Ed.* **2018**, *57*, 13439–13443; *Angew. Chem.* **2018**, *130*, 13627–13631; c) A. Kaithal, M. Holscher, W. Leitner, *Angew. Chem. Int. Ed.* **2018**, *57*, 13449–13453; *Angew. Chem.* **2018**, *130*, 13637–13641; d) E. Balaraman, C. Gunanathan, J. Zhang, L. J. W. Shimon, D. Milstein, *Nat. Chem.* **2011**, *3*, 609–614.
[10] a) C. M. Alder, J. D. Hayler, R. K. Henderson, A. M. Redman, L. Shukla, L. E. Shuster, H. F. Sneddon, *Green Chem.* **2016**, *18*, 3879–3890; b) B. Schäffner, F. Schäffner, S. P. Verevkin, A. Börner, *Chem. Rev.* **2010**, *110*, 4554–4581.
[11] J. P. Vivek, N. Berry, G. Papageorgiou, R. J. Nichols, L. J. Hardwick, *J. Am. Chem. Soc.* **2016**, *138*, 3745–3751.
[12] a) H. Blattmann, M. Fleischer, M. Bähr, R. Mülhaupt, *Macromol. Rapid Commun.* **2014**, *35*, 1238–1254; b) G. Rokicki, P. G. Parzuchowski, M. Mazurek, *Polym. Adv. Technol.* **2015**, *26*, 707–761; c) N. Yadav, F. Seidi, D. Crespy, V. D'Elia, *ChemSusChem* **2019**, *12*, 724–754; d) C. Carre, Y. Ecochard, S. Caillol, L. Averous, *ChemSusChem* **2019**, *12*, 3410–3430.
[13] J. H. Clements, *Ind. Eng. Chem. Res.* **2003**, *42*, 663–674.
[14] a) M. North, R. Pasquale, *Angew. Chem. Int. Ed.* **2009**, *48*, 2946–2948; *Angew. Chem.* **2009**, *121*, 2990–2992; b) M. North, S. C. Z. Quek, N. E. Pridmore, A. C. Whitwood, X. Wu, *ACS Catal.* **2015**, *5*, 3398–3402; c) M. North, B. Wang, C. Young, *Energy Environ. Sci.* **2011**, *4*, 4163–4170.
[15] a) C. J. Whiteoak, N. Kielland, V. Laserna, E. C. Escudero-Adán, E. Martin, A. W. Kleij, *J. Am. Chem. Soc.* **2013**, *135*, 1228–1231; b) C. J. Whiteoak, N. Kielland, V. Laserna, F. Castro-Gómez, E. Martin, E. C. Escudero-Adán, C. Bo, A. W. Kleij, *Chem. Eur. J.* **2014**, *20*, 2264–2275.
[16] a) J. W. Comerford, I. D. V. Ingram, M. North, X. Wu, *Green Chem.* **2015**, *17*, 1966–1987; b) C. Martin, G. Fiorani, A. W. Kleij, *ACS Catal.* **2015**, *5*, 1353–1370.
[17] a) H. Büttner, L. Longwitz, J. Steinbauer, C. Wulf, T. Werner, *Top. Curr. Chem.* **2017**, *375*, 50; b) R. R. Shaikh, S. Pornpraprom, V. D'Elia, *ACS Catal.* **2017**, *8*, 419–450.
[18] a) G. Fiorani, W. S. Guo, A. W. Kleij, *Green Chem.* **2015**, *17*, 1375–1389; b) M. Alves, B. Grignard, R. Méreau, C. Jerome, T. Tassaing, C. Detrembleur, *Catal. Sci. Technol.* **2017**, *7*, 2651–2684.
[19] B. List, *Chem. Rev.* **2007**, *107*, 5413–5415.
[20] M. Liu, X. Wang, Y. Jiang, J. Sun, M. Arai, *Catal. Rev.* **2019**, *61*, 214–269.
[21] a) C. Sperandio, J. Rodriguez, A. Quintard, *Org. Biomol. Chem.* **2020**, *18*, 2637–2640; b) M. E. Wilhelm, M. H. Anthofer, M. Cokoja, I. I. E. Markovits, W. A. Herrmann, F. E. Kühn, *ChemSusChem* **2014**, *7*, 1357–1360; c) T. Werner, N. Tenhumberg, H. Büttner, *ChemCatChem* **2014**, *6*, 3493–3500; d) Y. A. Rulev, Z. T. Gugkaeva, A. V. Lokutova, V. I. Maleev, A. S. Peregudov, X. Wu, M. North, Y. N. Belokon, *ChemSusChem* **2017**, *10*, 1152–1159; e) S. Arayachukiat, C. Kongtes, A. Barthel, S. V. C. Vummaleti, A. Poater, S. Wannakao, L. Cavallo, V. D'Elia, *ACS Sustainable Chem. Eng.* **2017**, *5*, 6392–6397; f) M. Alves, B. Grignard, S. Gennen, R. Mereau, C. Detrembleur, C. Jerome, T. Tassaing, *Catal. Sci. Technol.* **2015**, *5*, 4636–4643; g) S. Gennen, M. Alves, R. Méreau, T. Tassaing, B. Gilbert, C. Detrembleur, C. Jerome, B. Grignard, *ChemSusChem* **2015**, *8*, 1845–1849.
[22] a) N. Liu, Y.-F. Xie, C. Wang, S.-J. Li, D. Wei, M. Li, B. Dai, *ACS Catal.* **2018**, *8*, 9945–9957; b) J. Tharun, G. Mathai, A. C. Kathalikkattil, R. Roshan, J.-Y. Kwak, D.-W. Park, *Green Chem.* **2013**, *15*, 1673–1677.
[23] a) A. M. Hardman-Baldwin, A. E. Mattson, *ChemSusChem* **2014**, *7*, 3275–3278; b) J. Pérez-Pérez, U. Hernández-Balderas, D. Martínez-Otero, V. Jancik, *New J. Chem.* **2019**, *43*, 18525–18533.
[24] a) C. J. Whiteoak, A. Nova, F. Maseras, A. W. Kleij, *ChemSusChem* **2012**, *5*, 2032–2038; b) S. Sopeña, G. Fiorani, C. Martín, A. W. Kleij, *ChemSusChem* **2015**, *8*, 3248–3254.
[25] a) Y. Fan, M. Tiffner, J. Schorgenhumer, R. Robiette, M. Waser, S. R. Kass, *J. Org. Chem.* **2018**, *83*, 9991–10000; b) Y.-D. Li, D.-X. Cui, J.-C. Zhu, P. Huang, Z. Tian, Y.-Y. Jia, P.-A. Wang, *Green Chem.* **2019**, *21*, 5231–5237.
[26] a) J. Steinbauer, C. Kubis, R. Ludwig, T. Werner, *ACS Sustainable Chem. Eng.* **2018**, *6*, 10778–10788; b) T. Ema, Y. Miyazaki, J. Shimonishi, C. Maeda, J.-y. Hasegawa, *J. Am. Chem. Soc.* **2014**, *136*, 15270–15279; c) C. Maeda, T. Taniguchi, K. Ogawa, T. Ema, *Angew. Chem. Int. Ed.* **2015**, *54*, 134–138; *Angew. Chem.* **2015**, *127*, 136–140.
[27] T. Werner, H. Buettner, *ChemSusChem* **2014**, *7*, 3268–3271.
[28] D. Wei-Li, J. Bi, L. Sheng-Lian, L. Xu-Biao, T. Xin-Man, A. Chak-Tong, *Appl. Catal. A* **2014**, *470*, 183–188.
[29] S. Liu, N. Suematsu, K. Maruoka, S. Shirakawa, *Green Chem.* **2016**, *18*, 4611–4615.
[30] Y. Toda, Y. Komiyama, A. Kikuchi, H. Suga, *ACS Catal.* **2016**, *6*, 6906–6910.
[31] Y. Toda, Y. Komiyama, H. Esaki, K. Fukushima, H. Suga, *J. Org. Chem.* **2019**, *84*, 15578–15589.

[32] H. Büttner, J. Steinbauer, C. Wulf, M. Dindaroglu, H. G. Schmalz, T. Werner, *ChemSusChem* **2017**, *10*, 1076–1079.
[33] a) F. Blanchard, B. Carré, F. Bonhomme, P. Biensan, D. Lemordant, *Can. J. Chem.* **2003**, *81*, 385–391; b) P. D. Mantor, O. Ablb, K. Y. Song, R. Kobayashi, *J. Chem. Eng. Data* **1982**, *27*, 243–245; c) H. Büttner, J. Steinbauer, T. Werner, *ChemSusChem* **2015**, *8*, 2655–2669.
[34] *See Supporting Information for details*.
[35] a) J. Peng, S. Wang, H.-J. Yang, B. Ban, Z. Wei, L. Wang, B. Lei, *Fuel* **2018**, *224*, 481–488; b) A. Rehman, V. C. Eze, M. Resul, A. Harvey, *Ind. Eng. Chem. Res.* **2019**, *37*, 35–42.
[36] M. W. Robinson, A. M. Davies, R. Buckle, I. Mabbett, S. H. Taylor, A. E. Graham, *Org. Biomol. Chem.* **2009**, *7*, 2559–2564.
[37] V. Laserna, G. Fiorani, C. J. Whiteoak, E. Martin, E. Escudero-Adán, A. W. Kleij, *Angew. Chem. Int. Ed.* **2014**, *53*, 10416–10419; *Angew. Chem.* **2014**, *126*, 10584–10587.
[38] D. Bianchi, A. Bosetti, P. Cesti, P. Golini, *Tetrahedron Lett.* **1992**, *33*, 3231–3234.
[39] a) M. Borsa, G. Tonon, S. Malandrino, **1987**, *US4699911 A*; b) A. S. Stalsmeden, J. L. B. Vazquez, K. van Weerdenburg, R. Rae, P.-O. Norrby, N. Kann, *ACS Sustainable Chem. Eng.* **2016**, *4*, 5730–5736.
[40] a) F. Ma, M. A. Hanna, *Bioresour. Technol.* **1999**, *70*, 1–15; b) M. R. Monteiro, C. L. Kugelmeier, R. S. Pinheiro, M. O. Batalha, A. da Silva César, *Renewable Sustainable Energy Rev.* **2018**, *88*, 109–122.
[41] a) B. M. Bell, J. R. Briggs, R. M. Campbell, S. M. Chambers, P. D. Gaarenstroom, J. G. Hippler, B. D. Hook, K. Kearns, J. M. Kenney, W. J. Kruper, *Clean Soil Air Water* **2008**, *36*, 657–661; b) R. M. Hanson, *Chem. Rev.* **1991**, *91*, 437–475; c) M. Pagliaro, R. Ciriminna, H. Kimura, M. Rossi, C. Della Pina, *Angew. Chem. Int. Ed.* **2007**, *46*, 4434–4440; *Angew. Chem.* **2007**, *119*, 4516–4522; d) M. Sutter, E. D. Silva, N. Duguet, Y. Raoul, E. Métay, M. Lemaire, *Chem. Rev.* **2015**, *115*, 8609–8651; e) K. Urata, *PharmaChem* **2010**, *9*, 7–10.
[42] a) A.-A. G. Shaikh, S. Sivaram, *Chem. Rev.* **1996**, *96*, 951–976; b) M. O. Sonnati, S. Amigoni, E. P. T. de Givenchy, T. Darmanin, O. Choulet, F. Guittard, *Green Chem.* **2013**, *15*, 283–306; c) D. C. Webster, *Prog. Org. Coat.* **2003**, *47*, 77–86.
[43] A. Sunder, R. Hanselmann, H. Frey, R. Mülhaupt, *Macromolecules* **1999**, *32*, 4240–4246.
[44] D. Nishikawa, T. Nakajima, Y. Ohzawa, M. Koh, A. Yamauchi, M. Kagawa, H. Aoyama, *J. Power Sources* **2013**, *243*, 573–580.
[45] N. Aoyagi, Y. Furusho, T. Endo, *Tetrahedron Lett.* **2013**, *54*, 7031–7034.
[46] Y. Hu, L. Qiao, Y. Qin, X. Zhao, X. Chen, X. Wang, F. Wang, *Macromolecules* **2009**, *42*, 9251–9254.
[47] a) H. Blattmann, R. Mülhaupt, *Macromolecules* **2016**, *49*, 742–751; b) Z. Hosgor, N. Kayaman-Apohan, S. Karatas, A. Gungor, Y. Menceloglu, *Adv. Polym. Technol.* **2012**, *31*, 390–400; c) Z. Hoşgör, N. Kayaman-Apohan, S. Karataş, Y. Menceloğlu, A. Güngör, *Prog. Org. Coat.* **2010**, *69*, 366–375; d) M. Kathalewar, A. Sabnis, G. Waghoo, *Prog. Org. Coat.* **2013**, *76*, 1215–1229.
[48] a) M. Philipp, R. Bernhard, H. A. Gasteiger, B. Rieger, *J. Electrochem. Soc.* **2015**, *162*, A1319–A1326; b) M. Philipp, R. Bhandary, F. J. Groche, M. Schönhoff, B. Rieger, *Electrochim. Acta* **2015**, *173*, 687–697.
[49] M. S. Kathalewar, P. B. Joshi, A. S. Sabnis, V. C. Malshe, *RSC Adv.* **2013**, *3*, 4110–4129.
[50] a) S. Foltran, R. Mereau, T. Tassaing, *Catal. Sci. Technol.* **2014**, *4*, 1585–1597; b) M. Alves, R. Mereau, B. Grignard, C. Detrembleur, C. Jerome, T. Tassaing, *RSC Adv.* **2016**, *6*, 36327–36335; c) H. Yang, X. Wang, Y. Ma, L. Wang, J. Zhang, *Catal. Sci. Technol.* **2016**, *6*, 7773–7782; d) K. R. Roshan, A. C. Kathalikkattil, J. Tharun, D. W. Kim, Y. S. Won, D. W. Park, *Dalton Trans.* **2014**, *43*, 2023–2031.
[51] Deposition Number 2024624 contains the supplementary crystallographic data for this paper. These data are provided free of charge by the joint Cambridge Crystallographic Data Centre and Fachinformationszentrum Karlsruhe Access Structures service www.ccdc.cam.ac.uk/structures.
[52] P. B. Kapadnis, E. Hall, M. Ramstedt, W. R. J. D. Galloway, M. Welch, D. R. Spring, *Chem. Commun.* **2009**, 538–540.
[53] J. Steinbauer, A. Spannenberg, T. Werner, *Green Chem.* **2017**, *19*, 3769–3779.

Manuscript received: September 23, 2020
Revised manuscript received: October 15, 2020
Accepted manuscript online: October 17, 2020
Version of record online: November 13, 2020

6.2 Synthesis of Bifunctional Phosphonium Salts Bearing Perfluorinated Side Chains and Their Application in the Synthesis of Cyclic Carbonates from Epoxides and CO_2

C. Ren, A. Spannenberg, and T. Werner* *Asian J. Org. Chem*, **2022**, *11*, e202200156.

DOI: 10.1002/ajoc.202200156

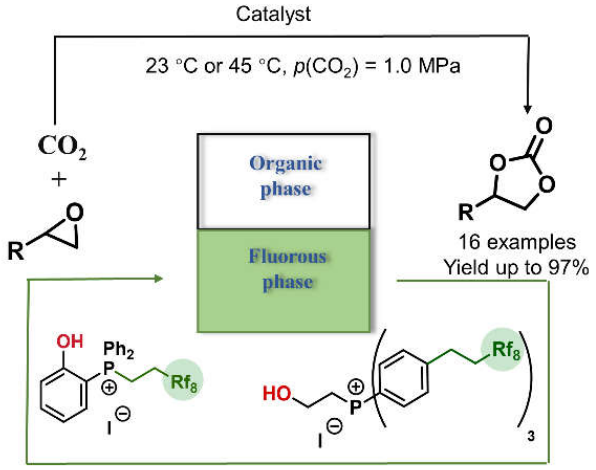

Abstract: The synthesis of three bifunctional phosphonium salts bearing perfluorinated side chains is reported. These compounds were employed as catalysts for the synthesis of cyclic carbonates from epoxides and CO_2. The most efficient catalyst comprised a phenolic substructure and allowed the synthesis of various carbonates at room temperature and a CO_2 pressure as low as 0.1 MPa. The reaction could be performed in perfluorodecalin which in some cases led to improved yields and facilitated the separation of the catalyst. Furthermore, the isolation from the reaction mixture and recyclability of two catalysts was evaluated. In total 16 cyclic carbonates were prepared in yields up to 97%.

ACES Asian Chemical Editorial Society

doi.org/10.1002/ajoc.202200156

ASIAN JOURNAL OF ORGANIC CHEMISTRY
Research Article

www.asianjoc.org

Synthesis of Bifunctional Phosphonium Salts Bearing Perfluorinated Side Chains and Their Application in the Synthesis of Cyclic Carbonates from Epoxides and CO_2

Changyue Ren,[a] Anke Spannenberg,[a] and Thomas Werner*[a, b]

Abstract: The synthesis of three bifunctional phosphonium salts bearing perfluorinated side chains is reported. These compounds were employed as catalysts for the synthesis of cyclic carbonates from epoxides and CO_2. The most efficient catalyst comprised a phenolic substructure and allowed the synthesis of various carbonates at room temperature and a CO_2 pressure as low as 0.1 MPa. The reaction could be performed in perfluorodecalin which in some cases led to improved yields and facilitated the separation of the catalyst. Furthermore, the isolation from the reaction mixture and recyclability of two catalysts was evaluated. However, the activity of the recycled catalysts gradually decreases due to partial decomposition. In total 16 cyclic carbonates were prepared in yields up to 97%.

Introduction

The utilization of CO_2 as a C1 building block in organic synthesis is of increasing importance and received great attention in recent years.[1] The global atmospheric CO_2 concentration has reached 417 ppm in 2021.[2] Thus, carbon capture and utilization (CCU) strategies to convert this readily available and cheap waste gas into valuable-added products are of great economic, social and ecological interest.[1g,3] CO_2 is used on industrial scale as a raw material, mainly to produce urea,[4] carbonates,[5] methanol,[6] and salicylic acid.[7] However, all of these valorization routes consume $<1\%$ of the annual global CO_2 emissions.[8]

A promising reaction that fulfills several of the 12 Green Chemistry Principles is the atom economic addition of CO_2 to epoxides **1** to produce cyclic carbonates **2** (Scheme 1).[9] Cyclic carbonates find applications as electrolytes in Li-ion batteries,[10] intermediates for fine chemicals and raw materials for the synthesis of polycarbonates.[11] They also provide a green alternative to produce non-isocyanate polyurethane (NIPU) in which the use of harmful isocyanates is avoided.[12]

Recently, bifunctional phosphonium salt catalysts bearing a phenol motif emerged as efficient catalysts for the addition of CO_2 to epoxides. These catalysts usually activate the epoxide via hydrogen bonding, lowering the activation barrier for the subsequent nucleophilic ring opening by the halogen anion.[1c,13]

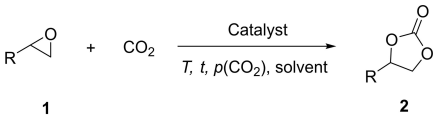

1 2

Scheme 1. Synthesis of cyclic carbonate **2** by coupling CO_2 with epoxides **1**.

In 2016, the group of Shirakawa reported that biphenyl-derived phosphonium salt **3** enables the conversion of epoxides with CO_2 at low CO_2 pressure (1.0 atm) (Scheme 2).[14] In the same year, Toda and coworkers studied bifunctional tetraarylphosphonium salt **4**, which also allowed for the synthesis of cyclic carbonate at atmospheric CO_2 pressure.[15] However, this catalyst requires reaction temperatures of 120 °C and chlorobenzene as the solvent. Subsequently, the same group studied the impact of the electronic properties of the substituents on the catalyst efficiency.[16] The introduction of electron-donating groups significantly enhanced the catalytic activity, which allowed to reduce the reaction temperature to 60 °C. In 2017 our group reported the use of bifunctional phenolic phosphonium bromide **5** for the preparation of oleochemical carbonates at 80 °C and 2.5 MPa CO_2 pressure.[17]

Changing the counter anion from Br^- to I^- allowed the synthesis of various terminal epoxides even at 23 °C.[18] The separation and recycling of homogenous catalysts is generally

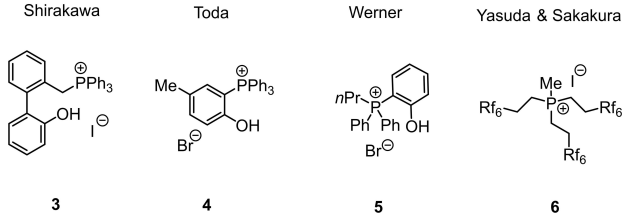

3 4 5 6

Scheme 2. Previously reported phosphonium salt catalysts **3**–**6** for the conversion of epoxides **1** with CO_2.

[a] C. Ren, Dr. A. Spannenberg, Prof. Dr. T. Werner
Leibniz Institute for Catalysis e.V. at the University of Rostock
Albert-Einstein-Straße 29a, 18059 Rostock (Germany)
E-mail: Thomas.Werner@catalysis.de

[b] Prof. Dr. T. Werner
Department of Chemistry
Paderborn University
Warburger Str. 100, D-33098 Paderborn (Germany)

Supporting information for this article is available on the WWW under https://doi.org/10.1002/ajoc.202200156

challenging. In some cases it is possible to separate the catalyst from the cyclic carbonate by distillation.[19] However, for higher boiling cyclic carbonates the thermal stress might lead to decomposition of the catalyst. The immobilization of the catalysts on heterogenous supports is one possible alternative. In this regard we previously reported the immobilization of bifunctional phosphonium salts bearing a phenol moiety on different supports.[20] Another possibility is the use of fluorinated catalysts and the separation of the catalyst from a biphasic system.[21] Yasuda and Sakakura reported the use of perfluorinated phosphonium salt **6** (–Rf_6= $C_6F_{13}C_2H_4$–) which allowed the facile separation of **6** in $scCO_2$ from the product phase.[22] Herein we report the synthesis of phenol based bifunctional phosphonium salts bearing perfluorinated side chains, their use in the synthesis of cyclic carbonates as well as studies on their recycling.

Results and Discussion

The fluorinated bifunctional organocatalysts **8, 9** and **11** with different fluorine contents (17%, 38% and 55%) were prepared by alkylation of the corresponding phosphine (Scheme 3). The conversion of **7** with perfluoroalkyl iodide (Rf_n, n = 2 and n = 8) gave the desired bifunctional salts **8** with a fluorine content of 17% and **9** with a fluorine content of 38% in 84% and 77% yield, respectively. Commercially available phosphine **10** with perflourinated side chains was alkylated with 2-iodoethanol. The desired salt **11** was obtained in a moderate yield of 64%.

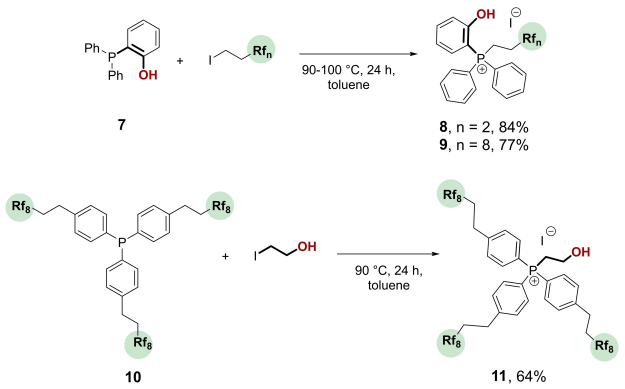

Scheme 3. Synthesis of the phosphonium salt catalysts.

Table 1. Comparison of phosphonium salts **8**, **9** and **11** as catalysts in the synthesis of carbonate **2a**.

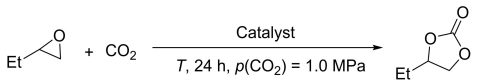

1a **2a**

Entry	Catalyst	T [°C]	Loading [mol%]	Yield [%][a]
1	**8**	23	2	58
2	**9**	23	2	55, 54[b]
3	**11**	23	2	< 5
4	**8**	23	5	95
5	**9**	23	5	98, 99,[b] 52[c]
6	**11**	23	5	30
7	**8**	45	5	99
8	**9**	45	5	99
9	**11**	45	5	93
10	**9**	60	1	98[d]

Reaction conditions: 1.0 equiv. epoxide **1a** (6.9 mmol), 2.0–5.0 mol% catalyst, 23–60 °C, 24 h, $p(CO_2)$ = 1.0 MPa, solvent-free. [a] Yields determined by ^{1}H NMR spectroscopy with mesitylene as internal standard. [b] Perfluorodecalin (1 mL) was used as solvent. [c] $p(CO_2)$ = 0.1 MPa. [d] 16 h.

The prepared catalysts were tested in the conversion of CO_2 with butylene oxide (**1a**) at low reaction temperatures (< 50 °C) under solvent-free conditions (Table 1). Even at room temperature the catalysts **8** and **9** (2 mol%) with a lower fluorine content led already to the desired product **2a** in moderate yields of 58% and 55% respectively (Entries 1 and 2). Interestingly, in the presence of catalyst **11** which has a fluorine content of 55% only traces of **2a** were observed (Entry 3). This might be explained by the low solubility of **11** in the epoxide **1a** which was observed at room temperature. Excellent yields of up to 98% were achieved by increasing the catalyst loading of **8** and **9** to 5 mol% (Entries 4 and 5). Notably, even at a low CO_2 pressure of 0.1 MPa **2a** was obtained in 52% at 23 °C in the presence of **9** (Entry 5). In the presence of **11** a yield of 30% was achieved (Entry 6). This agrees with previous studies in which catalysts with a phenolic hydroxyl group in the *ortho* position to the phosphonium moiety show higher activity compared to 2-hydroxyethyl-functionalized salts.[18] Excellent yields of > 90% were achieved with catalysts **8, 9** and **11** when the reaction temperature was increased to 45 °C (Table 1, entries 7–9). To further clarify the role of the hydroxyl group, we prepared an analog to catalyst **9** without this group. Under the condition of entry 5, only 3% yield was obtained in the presence of 5 mol% of this analog (see Supporting Information for details).

We were interested in the potential to separate the catalyst directly from the reaction mixture via a biphasic work-up using a suitable perfluorinated solvent. Thus, the solubility of the most active catalysts **8** and **9** in butylene carbonate (**2a**) and various perfluorinated solvents was investigated. Perfluorodecalin proved to be the most suitable solvent for the separation (see Supporting Information for details). Upon addition of toluene 70% of catalyst **9** is in the fluorous phase while the organic phase contains 30%. This result indicates the possibility of separating the catalyst from the reaction mixture by extraction with perfluorodecalin. As expected, the solubility of **8** in this solvent is much lower due to the low fluorine content of 17%. In this case 96% of the catalyst remained in the organic phase. Therefore, the performance of **9** was further investigated. At 23 °C the test reaction can also be performed at a lower CO_2 pressure (0.1 MPa) or in perfluorodecalin without loss of efficiency (Table 1, Entry 2). Compared to the solvent-free conditions a similar yield of 99% for **2a** was obtained in the presence of **9** (5 mol%) when perfluorodecalin was used as the solvent (Entry 5). At a reaction temperature of 60 °C full conversion to the desired product was achieved after 16 h with a reduced catalyst loading of 1 mol% (Entry 10). We obtained crystals of **9** which were suitable for X-ray crystallographic analysis (Figure 1). An intermolecular O–H···I hydrogen bond is observed in the crystal structure of **9** (O1–H1···I1: O1–H1 = 0.82(3) Å, H1···I1 = 2.57(3), O1···I1 = 3.381(2) Å, O1–H1···I1 =

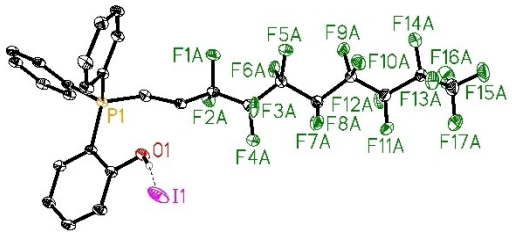

Figure 1. Molecular structure of catalyst **9** in the solid state (CCDC 2113188). Displacement ellipsoids correspond to 30% probability. Lower occupancy sites are omitted for clarity. The intermolecular hydrogen bond is shown as dashed line.[23]

168(3)°. The bond between the oxygen and hydrogen atom is shorter compared to the previously reported propyl-substituted analogue (0.89(5) Å), while the bond between the hydrogen and iodide counter ion is longer (2.48(5) Å).[18]

Subsequently we studied the scope and limitation of catalyst **9** in the conversion of epoxides **1** with CO_2 at room temperature (Scheme 4). Butylene oxide (**1a**) and propylene oxide (**1b**) gave the corresponding carbonates **2a** and **2b** in isolated yields of 93% and 91% respectively. The conversion of **1a** was also performed in perfluorodecalin which led to a comparable yield of 95%. Epoxide **1c** bearing a long alkyl chain gave the desired product **2c** in a moderate yield of 50%. At higher reaction temperature (45 °C) the isolated yield was increased to 94%. The reaction of epifluoro-(**1d**) and epichlorohydrin (**1e**) with CO_2 led to the corresponding cyclic carbonates in 78% and 85% respectively. At 45 °C styrene oxide (**1f**) was converted to carbonate **2f** in 91% yield while at room temperature only a low yield of 30% was obtained. Interestingly, 4-fluorophenyl substituted epoxide **1g** gave a yield of 60% which was further improved to 79% in the presence of perfluorodecalin as solvent. The more challenging 1,1-disubstituted terminal epoxide **1h** can be transformed to **2h** in 81% isolated yield under much milder conditions (45 °C, 1 MPa, 24 h), compared to the conditions published in a previous report (80 °C, 2.5 MPa, 24 h) utilizing a non-fluorous phosphonium salt catalyst.[18] Piperazine derivative **2i** is an intermediate in the synthesis of the antitussive dropropizine,[24] Conversion of **1i** at 45 °C gave this intermediate in 96% yield. Glycidyl ethers **1j**–**1o** represent a challenging class of substrates.[25] For their efficient conversion it was necessary to either extend the reaction time to 48 h or to increase the reaction temperature to 45 °C. Methyl glycidyl ether can be transformed to **2j** in 82% yield at 23 °C in 48 h, while the yield for *tert*-butyl glycidyl carbonate (**2k**) was improved from 64% to 97% when the reaction was performed at 45 °C instead of room temperature. Carbonate **2l**, a promising monomer for conducting polymers and coatings, was obtained in 77% yield at room temperature. *tert*-Butyldimethylsilyl ether **2m** was obtained in 94% yield. Fluoroalkyl-substituted carbonates are valuable products which can be used as electrolytes in lithium batteries.[26] The fluorous-tagged carbonates **2n** and **2o** are obtained from the corresponding glycidyl ethers in yields of 82% and 67% respectively. Finally, 41% yield was obtained at further elevated temperature and pressure for the very challenging cyclohexene oxide (**2p**).

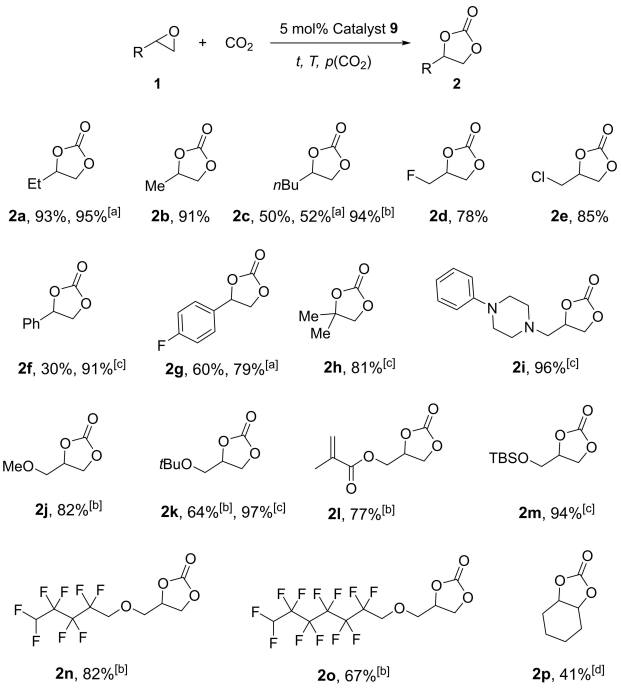

Scheme 4. Evaluation of the substrate scope with **9**. Reaction conditions: 1.0 equiv. epoxide **1** (500 mg), 5.0 mol% catalyst, 23 °C, 24 h, $p(CO_2)$ = 1.0 MPa, solvent-free, isolated yields are given. [a] 1 mL perfluorodecalin. [b] 48 h. [c] 45 °C [d] 60 °C, 2.5 MPa.

We studied the recyclability of catalyst **9** in the conversion of 4-fluorostyrene oxide (**1g**) at 23 °C. After 30 h reaction time toluene and more perfluorodecalin was added to dissolve the product **2g** and 73% of the catalyst was reisolated as a solid (Figure 2). In the second run the amount of substrate was adjusted to the amount of catalyst which was reisolated. Surprisingly the yield of **2g** dropped to 37%.

The ^{1}H NMR spectra of the recycled catalyst significantly changed compared to the spectra of the fresh catalyst **9** (Figure 3a vs. 3c). We postulated the formation of the zwitterionic compound **12** under the reaction conditions. This might occur either by the loss of hydrogen iodide or by the formation of the corresponding halohydrin which is a frequently observed side product in the synthesis of cyclic carbonates from epoxides in the presence of bifunctional onium salt catalysts.[13a,16] Thus, **12** was prepared and the ^{1}H NMR is shown in Figure 3d. ^{1}H NMR

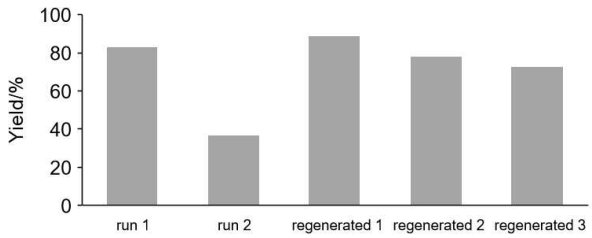

Figure 2. Recycling studies for catalyst **9**. Reaction conditions: **1g** (1.0 equiv), 5.0 mol% **9**, 23 °C, 30 h, 1.0 MPa CO_2, 1.0 mL perfluorodecalin. Yields were determined by ^{1}H NMR spectroscopy with mesitylene as internal standard.

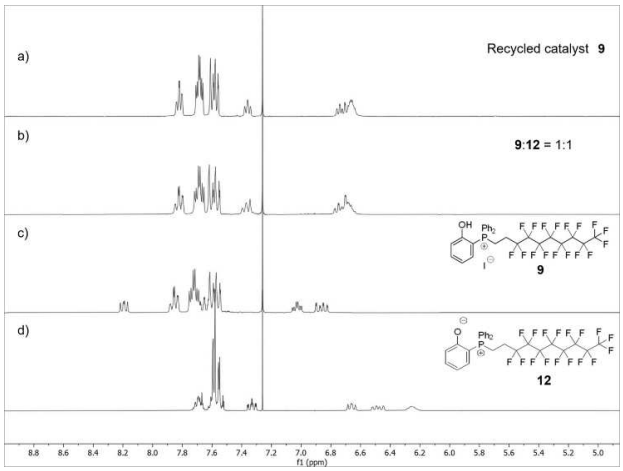

Figure 3. Sections of the ^{1}H NMR spectra of a) the recycled catalyst, b) a 1:1 mixture of **9** and **12**, c) catalyst **9**, d) compound **12**.

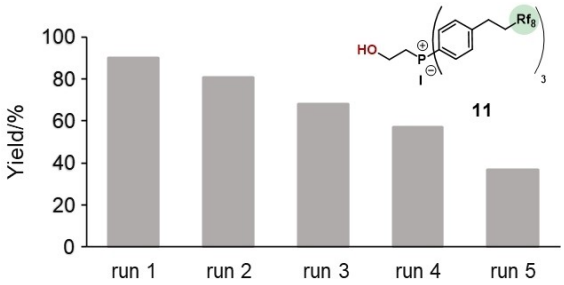

Figure 4. Recycling of catalyst **11**. Reaction conditions: **1a** (0.12 mmol), 5.0 mol% **11**, 45 °C, 24 h, 1.0 MPa CO_2, 0.5 mL perfluorodecalin. Yields of isolated products are given.

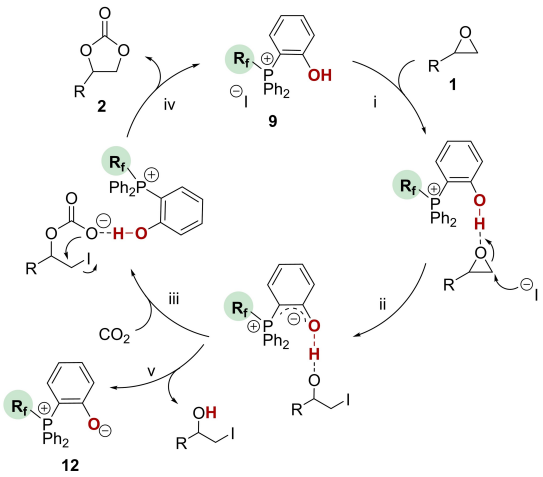

Scheme 5. Putative mechanism for coupling of epoxides **1** with CO_2 catalyzed by bifunctional phosphonium salt **9**.

spectra of several samples with different ratios of **9:12** were taken (Figure S4). The ^{1}H NMR spectra of the 1:1 mixture is comparable to the one of the recycled catalyst (Figure 3a vs. 3b). The elemental analysis of the recycled catalysts for iodide (calcd.: 8.05%, found.: 8.02%) supports this ratio. The initial activity of the catalyst was restored by treating the recycled catalyst with an aqueous solution of hydrogen iodide. Utilizing the regenerated catalyst in the third run led to a yield of 89% for **2g**. 69% of catalyst was reisolated and only 3% of the product was detected in the fluorous phase. The catalyst was recovered, regenerated and reused two more times with similar results.

Additionally, we tested the recyclability of **11** in the conversion of butylene oxide (**1a**) with CO_2 in perfluorodecalin. In the presence of 5.0 mol% **11** the desired product was obtained in 90% yield after 24 h at 45 °C and 1.0 MPa CO_2. At 45 °C the organic phase turned homogenous and allowed the reaction to proceed. After cooling the reaction mixture to 23 °C **11** directly precipitates from the reaction mixture. The product was removed by decantation. No signal was observed in the ^{31}P NMR of the product which indicates that the catalyst is not leaching to the product phase (Figure S6). Catalyst **11** and perfluorodecalin were directly used for the next run by simply adding new substrate. The isolated yield gradually decreased from 90% in the first run to 37% in the fifth run (Figure 4). The decrease in the catalytic activity can be addresses to the loss of iodoethanol and oxidation of **11** which is indicated by a peak shift in the ^{31}P NMR from 23.7 ppm for **11** to 27.9 ppm after the fifth run (Figure S5). While catalyst **11** is stable under air at room temperature heating **11** to 45 °C for 4 h led already to partial decomposition and a signal in the ^{31}P NMR at 28.0 ppm indicates the formation of the phosphine oxide.[27]

Based on our results and previous reports we propose the reaction mechanism shown in Scheme 5.[18] In the initial step catalyst **9** activates the epoxide via hydrogen bonding (Scheme 5, i). This is followed by the nucleophilic ring opening of the epoxide by iodide (ii). Subsequent CO_2 insertion leads to a linear carbonate intermediate (iii). An intramolecular nucleophilic substitution is then giving the product **2**, liberating the catalyst **9** (iii). The formation of halohydrins is a frequently observed side reaction in the synthesis of cyclic carbonates catalyzed by onium salts. This might lead to the observed formation of the species **12**. Toda reported that these type of zwitterionic phosphonium salts are capable forming cyclic carbonates from halohydrins and CO_2 at elevated temperatures (60 °C).[13b] However, no reaction was observed at a lower reaction temperature of 25 °C which is in agreement with our results in the catalyst recycling experiments.

Conclusion

Three bifunctional phosphonium salts bearing perfluorinated side chains were prepared in up to 84% yield by simple alkylation. These compounds are suitable for the synthesis of cyclic carbonates from epoxides and CO_2 even under mild conditions (23 °C, 0.1 MPa). The most active catalyst is based on a phenolic substructure. Under the optimized reaction conditions (5 mol% cat., 23 °C or 45 °C, 1.0 MPa) 15 terminal epoxides were converted to the corresponding cyclic carbonates in yields up to 96%. The reaction can be performed in perfluorodecalin which led in some cases to improved yields. To

the best of our knowledge, this is the first example for the coupling of epoxides with CO_2 employing a biphasic fluorous system. The catalyst can be easily separated by precipitation from the biphasic reaction mixture. Recycling experiments were performed for two of the catalysts. The bifunctional catalyst bearing a hydroxyalkyl moiety was recycled five times. A decrease in product yield from 90% to 37% during this process was observed which could be assigned to the decomposition of the catalyst to the corresponding phosphine oxide. The recycling of the catalyst containing a phenolic moiety was also performed. The analysis of the reisolated catalyst revealed the partial formation of a zwitterionic species which is catalytically inactive under the reaction conditions. However, this species can be converted to the active catalyst by regeneration with hydrogen iodide.

Experimental Section

(3,3,4,4,5,5,6,6,7,7,8,8,9,9,10,10,10-heptadecafluorodecyl)(2-hydroxyphenyl)diphenyl-phosphonium iodide (9) : A mixture of **7** (1.39 g, 5.00 mmol), 1,1,1,2,2,3,3,4,4,5,5,6,6,7,7,8,8-heptadecafluoro-10-iododecane (3.44 g, 6.00 mmol) and toluene (8 mL) was stirred for 24 h at 90 °C in a pressure tube. Subsequently, all volatiles were removed in vacuo. The obtained solid was washed with Et_2O (2× 100 mL) to yield **9** (3.27 g, 3.84 mmol, 77%) as a colorless solid. ^{1}H NMR (300 MHz, $CDCl_3$) δ = 10.41 (s, 1H), 8.14 (dd, J = 7.6, 6.0 Hz, 1H), 7.92–7.78 (m, 2H), 7.78–7.66 (m, 4H), 7.66–7.51 (m, 5H), 7.10–6.97 (m, 1H), 6.97–6.83 (m, 1H), 3.54–3.32 (m, 2H), 2.63–2.32 (m, 2H) ppm. ^{13}C NMR (75 MHz, $CDCl_3$) δ = 161.68 (d, J = 2.6 Hz), 138.31, 135.52 (d, J = 3.0 Hz), 134.10 (d, J = 9.1 Hz), 133.11 (d, J = 10.1 Hz), 130.77 (d, J = 12.8 Hz), 121.65 (d, J = 13.1 Hz), 119.23 (d, J = 7.1 Hz), 117.99, 116.81, 101.35, 100.15, 25.58, 17.20, 16.80 (d, J = 59.5 Hz) ppm. $C_{28}H_{19}F_{17}OP$, m/z (ESI) 725 (M^+).

tris(4(3,3,4,4,5,5,6,6,7,7,8,8,9,9,10,10,10-heptadecafluorodecyl)pheny-l)(2-hydroxyethyl)phosphonium iodide (11): A Schlenk flask was charged with **10** (3.20 g, 2.00 mmol), 2-iodoethanol (344 mg, 2.00 mmol) and toluene (15 mL). The flask was constantly purged with argon and the reaction mixture was stirred for 24 h at 90 °C. Subsequently, all volatiles were removed in vacuo. The obtained solid was washed with Et_2O (2×50 mL) to yield **11** (2.06 g, 1.27 mmol, 64%) as a colorless solid. ^{1}H NMR (400 MHz, $CDCl_3$) δ = 7.81–7.70 (m, 6H), 7.53 (dd, J = 8.3, 3.1 Hz, 6H), 4.29 (t, J = 6.7 Hz, 1H), 4.07 (dd, J = 19.7, 6.3 Hz, 2H), 3.86–3.79 (m, 2H), 3.09–2.98 (m, 6H), 2.44 (dt, J = 18.4, 9.5 Hz, 6H). ^{31}P NMR (162 MHz, $CDCl_3$) δ = 23.68. ^{13}C NMR (75 MHz, CD_2Cl_2) δ = 147.23, 147.19, 134.32, 134.17, 130.41, 130.24, 128.49, 117.29, 116.11, 32.23, 31.94, 31.64, 26.93, 26.54 ppm. HRMS (ESI) Calcd. for $C_{50}H_{29}OF_{51}P$ 1645.0940. Found: 1645.1142.

General procedure for the synthesis of various cyclic carbonates 2 using 9: A 45 cm^3 stainless-steel autoclave was charged with catalyst **9** (5.0 mol%) and epoxide **1** (500 mg, 1.00 equiv). The autoclave was purged with CO_2 and the pressure kept constant at 1.0 or 2.5 MPa. The reaction mixture was stirred at 23 °C–60 °C for 24 or 48 h. Subsequently the CO_2 was released slowly. The crude mixture was diluted with EtOAc (30 mL) and filtered over SiO_2 with cyclohexane/ethyl acetate = 10:1. The carbonates **2** were obtained after all volatiles were removed in vacuo.

4-Ethyl-1,3-dioxolan-2-one (2a):[18] According to the GP, 1,2-epoxybutane (**1a**, 500 mg, 6.95 mmol), **9** (296 mg, 0.347 mmol) and CO_2 were converted at 23 °C, 1.0 MPa for 24 h to yield **2b** (749 mg, 6.45 mmol, 93%) as a light-yellow oil. ^{1}H NMR (300 MHz, $CDCl_3$) δ = 4.69–4.57 (m, 1H), 4.49 (t, J = 8.1 Hz, 1H), 4.08–4.00 (m, 1H), 1.82–1.64 (m, 2H), 0.97 (t, J = 7.5 Hz, 3H). ^{13}C NMR (75 MHz, $CDCl_3$) δ = 155.19, 78.09, 69.06, 26.87, 8.43 ppm.

4-Methyl-1,3-dioxolan-2-one (2b):[18] According to the GP, 1,2-epoxypropane (**1b**, 500 mg, 8.61 mmol), **9** (296 mg, 0.430 mmol) and CO_2 were converted 23 °C, 1.0 MPa for 24 h to yield **2b** (797 mg, 7.81 mmol, 91%) as a light-yellow oil. ^{1}H NMR (300 MHz, $CDCl_3$) δ = 4.91–4.74 (m, 1H), 4.58–4.47 (m, 1H), 4.05–3.94 (m, 1H), 1.45 (d, J = 7.0 Hz, 3H) ppm. ^{13}C NMR (75 MHz, $CDCl_3$) δ = 155.13, 73.65, 70.72, 19.40 ppm.

4-Butyl-1,3-dioxolan-2-one (2c):[18] According to the GP, 1,2-butyloxirane (**1c**, 500 mg, 4.99 mmol), **9** (213 mg, 0.250 mmol) and CO_2 were converted 23 °C, 1.0 MPa for 48 h to yield **2c** (675 mg, 4.68 mmol, 94%) as a light-yellow oil. ^{1}H NMR (300 MHz, $CDCl_3$) δ = 4.76–4.64 (m, 1H), 4.56–4.47 (m, 1H), 4.06 (dd, J = 8.4, 7.2 Hz, 1H), 1.89–1.60 (m, 2H), 1.51–1.29 (m, 4H), 0.91 (t, J = 7.0 Hz, 3H) ppm. ^{13}C NMR (75 MHz, $CDCl_3$) δ = 155.20, 77.16, 69.50, 33.66, 26.53, 22.35, 13.89 ppm.

4-(Fluoromethyl)-1,3-dioxolan-2-one (2d):[18] According to the GP, epifluorohydrin (**1d**, 500 mg, 6.57 mmol), **9** (280 mg, 0.329 mmol) and CO_2 were converted 23 °C, 1.0 MPa for 24 h to yield **2d** (595 mg, 5.12 mmol, 78%) as a light-yellow oil. ^{1}H NMR (400 MHz, $CDCl_3$) δ = 4.98–4.89 (m, 1H), 4.74 (dd, J = 11.8, 2.3 Hz, 1H), 4.62 (dd, J = 11.2, 2.3 Hz, 1H), 4.55–4.52 (m, 1H), 4.44 (dd, J = 11.2, 3.1 Hz, 1H) ppm. ^{13}C NMR (101 MHz, $CDCl_3$) δ = 154.66, 82.22, 80.47, 74.62 (d, J = 19.6 Hz), 64.96 (d, J = 7.1 Hz) ppm.

4-(Chloromethyl)-1,3-dioxolan-2-one (2e):[18] According to the GP, epichlorohydrin (**1e**, 500 mg, 5.40 mmol), **9** (231 mg, 0.270 mmol) and CO_2 were converted 23 °C, 1.0 MPa for 24 h to yield **2e** (620 mg, 4.54 mmol, 85%) as a light-yellow oil. ^{1}H NMR (300 MHz, $CDCl_3$) δ = 5.04–4.89 (m, 1H), 4.65–4.53 (m, 1H), 4.41 (dd, J = 8.9, 5.8 Hz, 1H), 3.85–3.67 (m, 2H) ppm. ^{13}C NMR (75 MHz, $CDCl_3$) δ = 154.27, 74.35, 67.10, 43.71 ppm.

4-Phenyl-1,3-dioxolan-2-one (2f):[18] According to the GP, styrene oxide (**1f**, 500 mg, 4.16 mmol), **9** (178 mg, 0.208 mmol) and CO_2 were converted 45 °C, 1.0 MPa for 24 h to yield **2f** (625 mg, 3.81 mmol, 91%) as a colorless solid. ^{1}H NMR (300 MHz, $CDCl_3$) δ = 7.41–7.33 (m, 3H), 7.31–7.26 (m, 2H), 5.60 (t, J = 8.0 Hz, 1H), 4.77–4.67 (m, 1H), 4.30–4.22 (m, 1H) ppm. ^{13}C NMR (75 MHz, $CDCl_3$) δ = 154.95, 135.90, 129.82, 129.33, 125.98, 78.09, 71.26.ppm.

4-(4-Fluorophenyl)-1,3-dioxolan-2-one (2g):[19b] According to the GP, 2-(4-fluorophenyl)oxirane (**1g**, 500 mg, 3.62 mmol), **9** (154 mg, 0.181 mmol) and CO_2 were converted 23 °C, 1.0 MPa for 24 h to yield **2g** (516 mg, 2.83 mmol, 79%) as colorless solid. ^{1}H NMR (300 MHz, $CDCl_3$) δ = 7.40–7.32 (m, 2H), 7.18–7.09 (m, 2H), 5.71–5.61 (m, 1H), 4.79 (dd, J = 8.7, 8.1 Hz, 1H), 4.32 (dd, J = 8.7, 7.8 Hz, 1H) ppm. ^{13}C NMR (75 MHz, $CDCl_3$) δ = 163.56 (d, J = 248.7 Hz), 154.68, 131.73 (d, J = 3.3 Hz), 128.13 (d, J = 8.6 Hz), 116.50 (d, J = 22.0 Hz), 77.53, 71.22 ppm.

4,4-Dimethyl-1,3-dioxolan-2-one (2h):[18] According to the GP, 2,2-dimethyloxiran (**1h**, 500 mg, 6.93 mmol), **9** (296 mg, 0.347 mmol) and CO_2 were converted 45 °C, 1.0 MPa for 24 h to yield **2h** (654 mg, 5.63 mmol, 81%) as a light-yellow oil. ^{1}H NMR (300 MHz, $CDCl_3$) δ = 4.14 (s, 2H), 1.52 (s, 6H) ppm. ^{13}C NMR (75 MHz, $CDCl_3$) δ = 154.72, 81.80, 75.51, 26.19 ppm.

4-((4-Phenylpiperazin-1-yl)methyl)-1,3-dioxolan-2-one (2i)):[18] According to the GP, 1-(oxiran-2-ylmethyl)-4-phenylpiperazine (**1i**, 500 mg, 2.29 mmol), **9** (97.7 mg, 0.115 mmol) and CO_2 were converted 45 °C, 1.0 MPa for 24 h to yield **2i** (575 mg, 2.19 mmol, 96%) as a colorless solid. ^{1}H NMR (300 MHz, $CDCl_3$) δ = 7.28–7.24 (m, 2H), 6.89 (dd, J = 18.0, 7.5 Hz, 3H), 4.93–4.79 (m, 1H), 4.61–4.49 (m, 1H), 4.27 (dd, J = 8.5, 7.1 Hz, 1H), 3.19 (t, J = 5.0 Hz, 4H), 2.73 (dd, J =

12.0, 5.5 Hz, 6H) ppm. ^{13}C NMR (75 MHz, $CDCl_3$) δ = 154.82, 151.61, 127.27, 120.63, 116.54, 75.12, 68.20, 60.12, 54.58, 49.22 ppm.

4-(Methoxymethyl)-1,3-dioxalan-2-one (2j):[18] According to the GP, 2-(methoxymethyl)oxirane (**1j**, 500 mg, 5.67 mmol), **9** (242 mg, 0.284 mmol) and CO_2 were converted 23 °C, 1.0 MPa for 48 h to yield **2j** (618 mg, 5.67 mmol, 82%) as a light-yellow oil. ^{1}H NMR (300 MHz, $CDCl_3$) δ = 4.87–4.73 (m, 1H), 4.49 (t, J = 8.3 Hz, 1H), 4.37 (dd, J = 8.4, 6.1 Hz, 1H), 3.67–3.53 (m, 2H), 3.42 (s, 3H) ppm. ^{13}C NMR (75 MHz, $CDCl_3$) δ = 155.02, 75.07, 71.59, 66.30, 59.78 ppm.

4-(*tert*-Butoxymethyl)-1,3-dioxolan-2-one (2k):[18] According to the GP, 2-(tert-butoxymethyl)oxirane (**1k**, 500 mg, 3.84 mmol), **9** (164 mg, 0.192 mmol) and CO_2 were converted 45 °C, 1.0 MPa for 24 h to yield **2k** (650 mg, 3.73 mmol, 97%) as a light-yellow oil. ^{1}H NMR (400 MHz, $CDCl_3$) δ = 4.80–4.71 (m, 1H), 4.49–4.41 (m, 1H), 4.39–4.31 (m, 1H), 3.60 (dd, J = 10.4, 4.4 Hz, 1H), 3.53–3.46 (m, 1H), 1.17 (s, 9H) ppm. ^{13}C NMR (101 MHz, $CDCl_3$) δ = 155.24, 75.26, 73.86, 66.54, 61.27, 27.28 ppm.

2-(Oxo-1,3-dioxolan-4-yl)methyl methacrylate (2l):[18] According to the GP, oxiran-2-ylmethyl methacrylate (**1l**, 500 mg, 3.52 mmol), **9** (150 mg, 0.176 mmol) and CO_2 were converted 23 °C, 1.0 MPa for 48 h to yield **2l** (501 mg, 2.70 mmol, 77%) as a light-yellow oil. ^{1}H NMR (300 MHz, $CDCl_3$) δ = 6.20–6.12 (m, 1H), 5.70–5.63 (m, 1H), 5.03–4.93 (m, 1H), 4.58 (t, J = 8.6 Hz, 1H), 4.47–4.39 (m, 1H), 4.38–4.28 (m, 2H), 1.95 (s, 3H) ppm. ^{13}C NMR (75 MHz, $CDCl_3$) δ = 166.76, 154.56, 135.25, 127.45, 73.92, 66.19, 63.55, 18.27 ppm.

4-(((*tert*-Butyldimethylsilyl)oxy)methyl)-1,3-dioxolan-2-one (2m):[19b] According to the GP, tert-butyl-dimethyl-(oxiran-2-ylmethoxy)silane (**1m**, 500 mg, 2.65 mmol), **9** (113 mg, 0.133 mmol) and CO_2 were converted 45 °C, 1.0 MPa for 24 h to yield **2m** (580 mg, 2.50 mmol, 94%) as a colorless solid. ^{1}H NMR (300 MHz, $CDCl_3$) δ = 4.79–4.67 (m, 1H), 4.55–4.38 (m, 2H), 3.91 (dd, J = 11.7, 3.5 Hz, 1H), 3.72 (dd, J = 11.6, 2.8 Hz, 1H), 0.89 (s, 9H), 0.09 (s, 6H) ppm. ^{13}C NMR (75 MHz, $CDCl_3$) δ 155.07, 76.18, 60.00, 62.57, 25.80, 18.30, −5.37, −5.42 ppm.

4-(((2,2,3,3,4,4,5,5-Octafluoropentyl)oxy)methyl)-1,3-dioxolan-2-one (2n):[18] According to the GP, 4-(((2,2,3,3,4,4,5,5-octafluoropentyl)oxy)methyloxirane (**1n**, 500 mg, 1.82 mmol), **9** (77.8 mg, 0.091 mmol) and CO_2 were converted 23 °C, 1.0 MPa for 48 h to yield **2n** (473 mg, 1.49 mmol, 82%) as a light-yellow oil. ^{1}H NMR (400 MHz, $CDCl_3$) δ = 6.26–5.83 (m, 1H), 4.90–4.77 (m, 1H), 4.52 (td, J = 8.5, 0.5 Hz, 1H), 4.39 (ddd, J = 8.5, 6.1, 0.9 Hz, 1H), 4.16–3.96 (m, 2H), 3.96–3.87 (m, 1H), 3.84 (d, J = 11.0, 3.6, 1.1 Hz, 1H).^{13}C NMR (101 MHz, $CDCl_3$) δ = 154.68, 115.49, 110.24, 107.71, 105.35, 74.59, 71.71 68.58 (t, J = 25.7 Hz), 65.85 ppm.

4-(((2,2,3,3,4,4,5,5,6,6,7,7-Dodecafluoroheptyl)oxy)methyl)-1,3-dioxolan-2-one (2o) According to the GP, 4-((2,2,3,3,4,4,5,5,6,6,7,7-dodecafluoropentyl)oxy)methyloxirane (**1o**, 500 mg, 1.35 mmol), **9** (57.6 mg, 0.0675 mmol) and CO_2 were converted 23 °C, 1.0 MPa for 48 h to yield **2o** (373 mg, 0.901 mmol, 67%) as a light-yellow oil. ^{1}H NMR (300 MHz, $CDCl_3$) δ = 6.06 (tt, J = 51.9, 5.2 Hz, 1H), 4.90–4.77 (m, 1H), 4.52 (t, J = 8.5 Hz, 1H), 4.39 (dd, J = 8.5, 6.2 Hz, 1H), 4.16–3.97 (m, 2H), 3.95–3.81 (m, 2H) ppm. ^{13}C NMR (75 MHz, $CDCl_3$) δ = 154.55, 111.08, 110.56, 107.61, 104.32, 74.46, 71.60, 68.89, 68.51, 68.13, 65.71 ppm.

Hexahydrobenzo[*d*][1,3]dioxol-2-one (2p):[18] According to the GP, 7-oxabicyclo[4.1.0]heptane (**1p**, 500 mg, 5.09 mmol), **9** (217 mg, 0.254 mmol) and CO_2 (2.5 MPa) were converted 60 °C, 2.5 MPa for 24 h at 60 °C for 24 h to yield **2p** (298 mg, 2.10 mmol, 41%) as a light-yellow oil. ^{1}H NMR (400 MHz, $CDCl_3$) δ = 4.73–4.61 (m, 2H), 1.92–1.84 (m, 4H), 1.66–1.55 (m, 2H), 1.46–1.35 (m, 2H). ^{13}C NMR (101 MHz, $CDCl_3$) δ = 155.47, 75.85, 26.85, 19.24 ppm.

Procedure for the recycling of homogeneous catalyst 9: A 45 cm^3 stainless-steel autoclave was charged with catalyst **9** (245 mg, 5.80 mmol, 5.0 mol%), epoxide **1g** (800 mg, 1.0 equiv) and perfluorodecalin (1 mL). The autoclave was purged with CO_2 and kept constant at 1.0 MPa. The reactor was stirred at 23 °C for 30 h. Subsequently the CO_2 was released slowly. Toluene (10 mL) and perfluorodecalin (4 mL) were added. The organic phase was separated from the perfluorinated phase and precipitated catalyst. The catalyst **9** was reisolated from the perfluorinated phase by evaporation, washed with toluene (2×5 mL) and diethyl ether and reused in the next run. Combining all the eluate with organic phase and remove all the volatiles from the organic phase in vacuo the product **2g** was obtained as colorless solid. The yield was determined directly by ^{1}H NMR spectroscopy using mesitylene as internal standard. The catalyst was regenerated by treating with 5.0 mol% HI aqueous (56 wt. %) solution.

Procedure for the recycling of homogeneous catalyst 11: A 45 cm^3 stainless-steel autoclave was charged with catalyst **11** (246 mg, 6.00 µmol, 5.0 mol%), epoxide **1** (200 mg, 0.120 mmol, 1.0 equiv) and perfluorodecalin (0.5 mL). The autoclave was purged with CO_2 and kept constant at 1.0 MPa. The reactor was stirred at 45 °C for 30 h. Subsequently the CO_2 was released slowly. Toluene (0.2 mL) was added to facilitate the phase separation. The organic phase was separated from the perfluorinated phase and the precipitated catalyst. After removal of all volatiles from the organic phase in vacuo the product **2a** was obtained as light-yellow oil. The perfluorinated phase including catalyst **11** was directly used in the next run without further purification.

2-((3,3,4,4,5,5,6,6,7,7,8,8,9,9,10,10,10-Heptadecafluorodecyl)diphenylphosphonio)phenolate (12) A flask was charge with the phosphonium salt **11** (341 mg, 0.400 mmol), MeOH (0.8 mL). Then 10% NaOH aq (0.5 mL) was added, and the reaction mixture was stirred for 0.5 h at room temperature. The mixture was treated with H_2O (10 mL) and the aqueous layer was extracted with $CHCl_3$ (20 mL×3). The organic layers were combined, dried over Na_2SO_4, filtered, and concentrated to give the **12** as a colorless solid (208 mg, 0.287 mmol, 72%). ^{1}H NMR (300 MHz, $CDCl_3$) δ 7.76–7.65 (m, 2H), 7.64–7.49 (m, 8H), 7.37–7.29 (m, 1H), 6.66 (dd, J = 8.7, 6.3 Hz, 1H), 6.54–6.41 (m, 1H), 6.25 (d, J = 6.3 Hz, 1H), 3.42–3.21 (m, 2H), 2.84–2.51 (m, 2H). ^{13}C NMR (75 MHz, $CDCl_3$) δ 137.12, 133.70, 133.54, 133.40, 132.72 (d, J = 9.5 Hz), 129.69 (d, J = 12.2 Hz), 128.09, 122.71, 121.79, 110.65, 96.98, 26.21, 17.78, 17.36 (d, J = 63.4 Hz).^{31}P NMR (122 MHz, $CDCl_3$) δ 20.26 ppm.

Acknowledgements

C. Ren is grateful for the financial support from Zunyi Medical University. Open Access funding enabled and organized by Projekt DEAL.

Conflict of Interest

The authors declare no conflict of interest.

Data Availability Statement

Research data are not shared.

Keywords: CO_2 valorization · cyclic carbonates · bifunctional phosphonium salts · perfluorinated catalyst · organocatalysis

[1] a) S. Dabral, T. Schaub, *Adv. Synth. Catal.* **2019**, *361*, 223–246; b) B. Grignard, S. Gennen, C. Jérôme, A. W. Kleij, C. Detrembleur, *Chem. Soc. Rev.* **2019**, *48*, 4466–4514; c) Q. Liu, L. Wu, R. Jackstell, M. Beller, *Nat. Commun.* **2015**, *6*, 5933; d) J. Ye, T. Ju, H. Huang, L. Liao, D. Yu, *Acc. Chem. Res.* **2021**, *54*, 2518–2531; e) X. Jiang, X. Nie, X. Guo, C. Song, J. Che, *Chem. Rev.* **2020**, *120*, 7984–8034; f) Z.-Z. Yang, L.-N. He, Y.-N. Zhao, B. Li, B. Yu, *Energy Environ. Sci.* **2011**, *4*, 3971–3975; g) S. Kar, A. Goeppert, G. K. S. Prakash, *Acc. Chem. Res.* **2019**, *52*, 2892–2903.

[2] *Earth System Research Laboratory Global Monitoring Division*, https://research.noaa.gov/article/ArtMID/587/ArticleID/2764/Coronavirus-response-barely-slows-rising-carbon-dioxide, **2021**, (accessed 7 July 2021).

[3] a) A. Kätelhön, R. Meys, S. Deutz, S. Suh, A. Bardow, *Proc. Natl. Acad. Sci. USA* **2019**, *116*, 11187–11194; b) A. Al-Mamoori, A. Krishnamurthy, A. A. Rownaghi, F. Rezaei, *Energy Technol.* **2017**, *5*, 834–849.

[4] H. Wang, Z. Xin, Y. Li, in *Chemical Transformations of Carbon Dioxide* (Eds.: X.-F. Wu, M. Beller), Springer International Publishing, Cham, **2018**, pp. 177–202.

[5] H. Büttner, L. Longwitz, J. Steinbauer, C. Wulf, T. Werner, *Top. Curr. Chem.* **2017**, *375*, 50.

[6] S.-T. Bai, G. De Smet, Y. Liao, R. Sun, C. Zhou, M. Beller, B. U. W. Maes, B. F. Sels, *Chem. Soc. Rev.* **2021**, *50*, 4259–4298.

[7] I. Stanescu, L. E. K. Achenie, *Chem. Eng. Sci.* **2006**, *61*, 6199–6212.

[8] M. Aresta, A. Dibenedetto, A. Angelini, *Chem. Rev.* **2014**, *114*, 1709–1742.

[9] a) V. Aomchad, À. Cristòfol, F. Della Monica, B. Limburg, V. D'Elia, A. W. Kleij, *Green Chem.* **2021**, *23*, 1077–1113; b) H. Büttner, L. Longwitz, J. Steinbauer, C. Wulf, T. Werner, in *Chemical Transformations of Carbon Dioxide* (Eds.: X.-F. Wu, M. Beller), Springer International Publishing, Cham, **2018**, pp. 89–144; c) R. R. Shaikh, S. Pornpraprom, V. D'Elia, *ACS Catal.* **2018**, *8*, 419–450; d) C. N. Tounzoua, B. Grignard, C. Detrembleur, *Angew. Chem. Int. Ed.* **2022**, accepted manuscript, https://doi.org/10.1002/anie.202116066; e) K. A. Andrea, F. M. Kerton, *Polym. J.* **2021**, *53*, 29–46; f) L. Guo, K. J. Lamb, M. North, *Green Chem.* **2021**, *23*, 77–118.

[10] a) Y. Shim, *Phys. Chem. Chem. Phys.* **2018**, *20*, 28649–28657; b) M. Petrowsky, M. Ismail, D. T. Glatzhofer, R. Frech, *J. Phys. Chem. B* **2013**, *117*, 5963–5970.

[11] a) L. Panza, F. Compostella, D. Imperio, *Carbohydr. Res.* **2019**, *472*, 50–57; b) F. Siragusa, E. Van Den Broeck, C. Ocando, A. J. Müller, G. De Smet, B. U. W. Maes, J. De Winter, V. Van Speybroeck, B. Grignard, C. Detrembleur, *ACS Sustainable Chem. Eng.* **2021**, *9*, 1714–1728; c) K. A. Maltby, M. Hutchby, P. Plucinski, M. G. Davidson, U. Hintermair, *Chem. Eur. J.* **2020**, *26*, 7405–7415; d) B. M. Stadler, C. Wulf, T. Werner, S. Tin, J. G. de Vries, *ACS Catal.* **2019**, *9*, 8012–8067; e) J. N. Buckler, T. Meek, M. G. Banwell, P. D. Carr, *J. Nat. Prod.* **2017**, *80*, 2088–2093.

[12] a) A. Gomez-Lopez, F. Elizalde, I. Calvo, H. Sardon, *Chem. Commun.* **2021**, *57*, 12254–12265; b) H. Chen, P. Chauhan, N. Yan, *Green Chem.* **2020**, *22*, 6874–6888; c) C. Wulf, M. Reckers, A. Perechodjuk, T. Werner, *ACS Sustainable Chem. Eng.* **2020**, *8*, 1651–1658; d) B. Bizet, É. Grau, H. Cramail, J. M. Asua, *Polym. Chem.* **2020**, *11*, 3786–3799.

[13] a) J. Steinbauer, C. Kubis, R. Ludwig, T. Werner, *ACS Sustainable Chem. Eng.* **2018**, *6*, 10778–10788; b) J.-Q. Wang, J. Sun, W.-G. Cheng, K. Dong, X.-P. Zhang, S.-J. Zhang, *Phys. Chem. Chem. Phys.* **2012**, *14*, 11021–11026; c) C. Claver, M. B. Yeamin, M. Reguero, A. M. Masdeu-Bultó, *Green Chem.* **2020**, *22*, 7665–7706.

[14] S. Liu, N. Suematsu, K. Maruoka, S. Shirakawa, *Green Chem.* **2016**, *18*, 4611–4615.

[15] Y. Toda, Y. Komiyama, A. Kikuchi, H. Suga, *ACS Catal.* **2016**, *6*, 6906–6910.

[16] Y. Toda, Y. Komiyama, H. Esaki, K. Fukushima, H. Suga, *J. Org. Chem.* **2019**, *84*, 15578–15589.

[17] H. Büttner, J. Steinbauer, C. Wulf, M. Dindaroglu, H. G. Schmalz, T. Werner, *ChemSusChem* **2017**, *10*, 1076–1079.

[18] Y. Hu, Z. Wei, A. Frey, C. Kubis, C.-Y. Ren, A. Spannenberg, H. Jiao, T. Werner, *ChemSusChem* **2021**, *14*, 363–372.

[19] a) Y.-Y. Zhang, G.-W. Yang, R. Xie, L. Yang, B. Li, G.-P. Wu, *Angew. Chem. Int. Ed.* **2020**, *59*, 23291–23298; *Angew. Chem.* **2020**, *132*, 23491–23498; b) Y. Hu, J. Steinbauer, V. Stefanow, A. Spannenberg, T. Werner, *ACS Sustainable Chem. Eng.* **2019**, *7*, 13257–13269; c) P. Goodrich, H. Q. N. Gunaratne, J. Jacquemin, L. Jin, Y. Lei, K. R. Seddon, *ACS Sustainable Chem. Eng.* **2017**, *5*, 5635–5641; d) S. Yue, P. Wang, X. Hao, *Fuel* **2019**, *251*, 233–241; e) Y. Hao, D. Yuan, Y. Yao, *ChemCatChem* **2020**, *12*, 4346–4351.

[20] a) J. Steinbauer, L. Longwitz, M. Frank, J. Epping, U. Kragl, T. Werner, *Green Chem.* **2017**, *19*, 4435–4445; b) Y. Hu, S. Peglow, L. Longwitz, M. Frank, J. D. Epping, V. Brüser, T. Werner, *ChemSusChem* **2020**, *13*, 1825–1833.

[21] a) J.-M. Vincent, in *Biphasic Chemistry and The Solvent Case*, **2020**, pp. 57–98; b) B. Barabás, O. Fülöp, R. Molontay, G. Pályi, *ACS Sustainable Chem. Eng.* **2017**, *5*, 8108–8118; c) C. Liu, X. Li, Z. Jin, *Catal. Today* **2015**, *247*, 82–89; d) E. de Wolf, G. van Koten, B.-J. Deelman, *Chem. Soc. Rev.* **1999**, *28*, 37–41.

[22] L.-N. He, H. Yasuda, T. Sakakura, *Green Chem.* **2003**, *5*, 92–94.

[23] Deposition number CCDC 2113188 contains the supplementary crystallographic data for this paper. These data are provided free of charge by the joint Cambridge Crystallographic Data Centre and Fachinformationszentrum Karlsruhe Access Structures service www.ccdc.cam.ac.uk/structures.

[24] E. Barbayianni, G. Kokotos, *ChemCatChem* **2012**, *4*, 592–608.

[25] S. Subramanian, J. Oppenheim, D. Kim, T. S. Nguyen, W. M. H. Silo, B. Kim, W. A. Goddard, C. T. Yavuz, *Chem* **2019**, *5*, 3232–3242.

[26] a) K. Xu, *Chem. Rev.* **2014**, *114*, 11503–11618; b) Y. Zhu, M. D. Casselman, Y. Li, A. Wei, D. P. Abraham, *J. Power Sources* **2014**, *246*, 184–191.

[27] W. Chen, L. Xu, Y. Hu, A. B. Osuna, J. Xiao, *Tetrahedron* **2002**, *20*, 3889–3899.

Manuscript received: March 24, 2022
Revised manuscript received: July 6, 2022
Accepted manuscript online: July 11, 2022
Version of record online: August 18, 2022

6.3 Phosphonium Salt-Catalyzed *N*-methylation and *N*- formylation of Amines with CO_2

C. Ren, A. Spannenberg and T. Werner*, *ACS Sustainable Chemistry & Engineering.* **2024**, accepted.

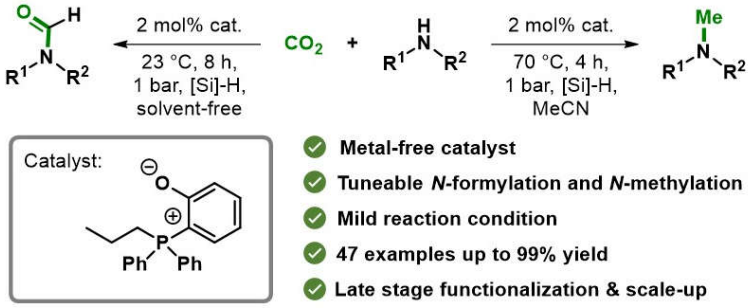

Abstract: The use of CO_2 as a C1 building block is of great relevance and a focus of current research. Herein, we report the synthesis of air-stable internal phosphonium salts and their application as catalysts in the *N*-methylation and *N*-formylation of amines utilizing CO_2. A series of catalysts was prepared and tested. Under the optimized reaction conditions the *N*-formylation of amines was achieved at 23 °C, 1 bar CO_2 pressure under solvent free conditions using equimolar amounts of *n*-hexylsilane as reducing agent. A modification of the reaction conditions led to a selectivity switch and the *N*-methylation was realized at 70 °C in acetonitrile using the same catalyst and reductant. In total, 22 amines were converted to corresponding *N*-methylated products in up to 99% yield. Moreover, 24 examples for the conversion to corresponding *N*-formylated products in up to 96% yield is reported. This reaction can be performed at gram-scale. Both the *N*-methylation and *N*-formylation reaction were also applied to the late-stage functionalization of the pharmaceutical Sertraline. NMR studies and control experiments revealed two different reaction pathways and intermediates for the *N*-methylation and *N*-formylation.

ACS Sustainable Chemistry & Engineering

pubs.acs.org/journal/ascecg

Research Article

Phosphonium-Salt-Catalyzed *N*-Methylation and *N*-Formylation of Amines with CO_2

Changyue Ren, Anke Spannenberg, and Thomas Werner*

Cite This: https://doi.org/10.1021/acssuschemeng.4c03464

Read Online

ACCESS | Metrics & More | Article Recommendations | Supporting Information

ABSTRACT: The use of CO_2 as a C_1 building block is of great relevance and is a focus of current research. Herein we report the synthesis of air-stable internal phosphonium salts and their application as catalysts in the *N*-methylation and *N*-formylation of amines utilizing CO_2. A series of catalysts were prepared and tested for these valuable transformations. Under the optimized reaction condition, the *N*-formylation of amines was achieved at 23 °C, 1 bar CO_2 pressure under solvent-free conditions using equimolar amounts of *n*-hexylsilane as reducing agent. A modification of the reaction conditions led to a selectivity switch, and the *N*-methylation was realized at 70 °C in acetonitrile using the same catalyst and reductant. In total, 22 amines were converted to the corresponding *N*-methylated products in up to 99% yield. Moreover, 25 examples of the conversion to the corresponding *N*-formylated products in up to 96% yield are reported. Both reactions can be performed at large scale. Both the *N*-methylation and *N*-formylation reactions were also applied to the late-stage functionalization of the pharmaceutical sertraline. NMR studies and control experiments revealed two different reaction pathways and intermediates for *N*-methylation and *N*-formylation.

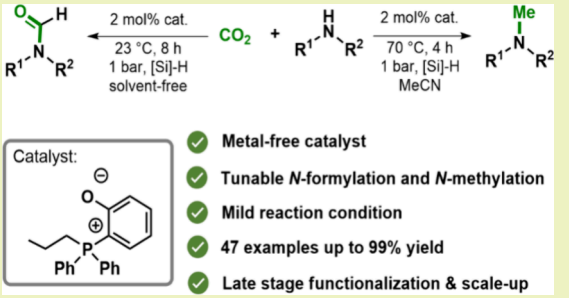

KEYWORDS: *CO_2, phosphonium salt, N-formylation, N-methylation, selective reduction*

INTRODUCTION

Carbon dioxide (CO_2) is a readily available, safe, and renewable carbon source, making it an attractive C_1 building block for the sustainable synthesis of organic molecules.[1−6] Methyl- and formyl-substituted amines represent core structures, e.g., in natural products, pharmaceuticals, and dyes.[7,8] The *N*-methylation reaction of amines is an important reaction in modulating biological functions of proteins and late-stage isotope labeling in the pharmaceutical industry.[9−14] Classical methodologies for *N*-formylation and *N*-methylation often require the use of a hazardous formylating reagent such as formaldehyde, chloral, or carbon monoxide[15,16] or alkylating agent such as methyl iodide, dimethyl sulfate, or dimethyl carbonate, respectively.[17−19] The catalytic reduction of CO_2 in the presence of secondary and primary amines avoids the need for these harmful reagents. This can be achieved by utilizing mild hydrides such as hydrosilanes or hydroboranes as reducing agents. In 2012 Cantat and co-workers reported the first examples of catalytic systems for the *N*-formylation of amines with CO_2 using triazabicyclodecene (TBD) as an organocatalyst and hydrosilanes as reducing agents.[20,21] Metal-based catalytic systems for the *N*-methylation of N−H bonds using CO_2 as a C_1 building block and hydrosilanes as reductants were consecutively reported in 2013 by the groups of Cantat and Beller, who employed Zn and Ru complexes as catalysts, respectively.[22,23] The reductive reaction of amines with CO_2 and hydrosilanes follows a complex network of interrelated reactions, which can lead to two-electron reductive product formamides or six-electron reductive product methylamines, and in a few cases four-electron reductive product aminals were also obtained (Scheme 1).[24] The selectivity depends on the catalyst loading, temperature, pressure of CO_2, amine, and solvent.[25−32] This opens the possibility of switching the selectivity to perform either transformation with one catalyst by modifying the reaction conditions. A number of metal-based catalysts and organocatalysts for the selective *N*-methylation and *N*-formylation of amines with CO_2 have been reported.[28,29,33−37] However, often high catalyst loadings, long reaction times, and/or high reaction temperatures are required.

Amine bases have been reported as organocatalysts for the transformations, such as 1,8-diazabicyclo[5.4.0]undec-7-en (DBU) in combination with polymethylhydrosiloxane (PMHS) as the reducing agent as well as 6-amino-2-picoline in combination with borane−trimethylamine.[25,33] The group of Dyson employed *N*-heterocyclic carbenes (NHCs) for the selective *N*-methylation and *N*-formylation of amines with CO_2 and silanes as reducing agents.[38] Organic salts such as

Received: April 25, 2024
Revised: June 16, 2024
Accepted: June 17, 2024

Scheme 1. Reaction of Amines with CO_2 under Reductive Conditions

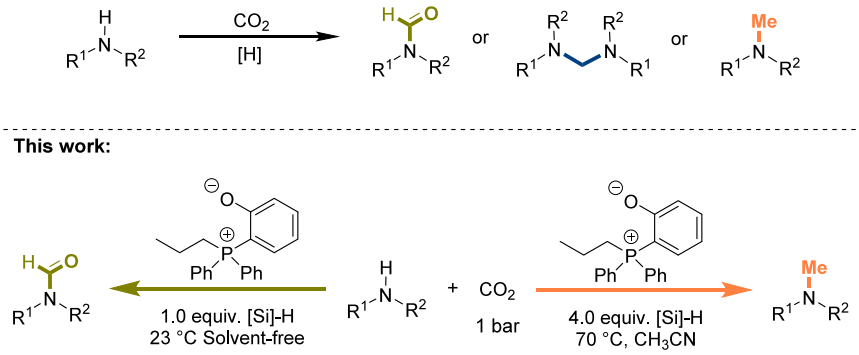

tetrabutylammonium fluoride (TBAF), acetylcholine-carboxylate, and phosphonium methylcarbonate have also been used as catalysts.[34,35,39] Moreover, a selectivity switch has been achieved utilizing zwitterionic salts such as glycine betaine and lecithin as catalysts.[28,29,36] Organocatalysts are desirable to circumvent the problematic availability, costs, and/or toxicity of metals.[40] Based on our work on the synthesis of bifunctional phosphonium salts for the coupling of CO_2 with epoxide to prepare cyclic carbonates,[41−45] we herein report the preparation of air-stable internal phosphonium salts and their use in selective reductive coupling of amines with CO_2 yielding *N*-methylated or *N*-formylated products.

RESULTS AND DISCUSSION

We envisioned that internal phosphonium salts **2** should be suitable catalysts for the *N*-methylation and *N*-formylation of amines with CO_2. A series of salts **2** were prepared based on previously reported phosphonium salts **1**.[42,44] Treating salts **1** with aqueous NaOH under previously reported condtions[47] led to bench-stable catalysts **2** in yields up to 93% (Scheme 2). After crystallization of **2b**, single crystals suitable for X-ray crystallographic analysis were obtained. The molecular structure of **2b** is shown in Scheme 2.

Scheme 2. Preparation of Internal Phosphonium Salts 2 from Salts 1 and Crystal Structure of 2b[a]

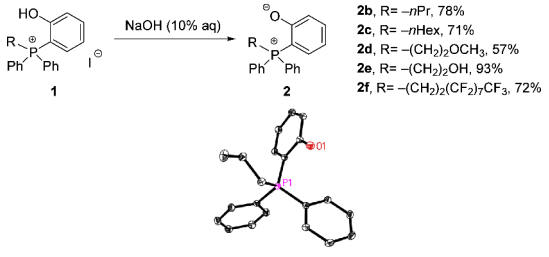

[a]Displacement ellipsoids correspond to 30% probability. Hydrogen atoms and the solvent molecule (H_2O) have been omitted for clarity.[46]

The prepared salts **2** (2 mol %) were evaluated as catalysts for the conversion of *N*-methylaniline (**3a**) with CO_2 and silane as reductants at 45 °C for 6 h (Table 1, entries 1−6). Catalysts **2a**−**2d** gave the methylated product **4a** in similar yields (72−76%). In all cases, the formylated product **5a** was also obtained in yields up to 21%. In contrast, catalysts **2e** and **2f** gave **4a** in significantly lower yields (entries 5 and 6). In the presence of salt **1b** instead of the catalyst **2b** or in the absence of **2b**, no conversion was observed (entries 7 and 8). Since the highest yield of 76% for the methylated product **4a** was achieved in the presence of catalyst **2b**, the reaction conditions were further optimized with **2b**. An increase of the reaction temperature to 70 °C led to full conversion, and **4a** was obtained in 99% yield (entry 9). Notably, at room temperature, the selectivity switched to the *N*-formylated product **5a**, which was obtained in 73% yield (entry 10). Various other silanes were screened at 70 °C and led to lower or no product formation (entries 11−16). Notably, shorter reaction times of 4 and 1 h still led to good yields of 98% and 90%, respectively (entries 17 and 18). A lower catalyst loading of 1 mol % **2b** gave the desired product **4a** in 89% yield (entry 19).

Under the optimal conditions, the scope and limitations of catalyst **2b** (2 mol %) in the conversion of amines **3** with CO_2 in the presence of *n*-hexylsilane to the methylated products **4** were further evaluated at 70 °C for 4 h (Scheme 3). *p*-Methoxy-*N*-methylaniline (**3b**) gave the corresponding dimethylaniline **4b** in a yield of 75%, while *o*-methoxy-substituted substrate **3c** gave the product **4c** in 99% yield. The reaction of 4-fluoro- and 4-bromo-*N*-methylaniline with CO_2 led to products **4d** and **4e** in 91% and 82% yield, respectively. 4-Iodo-*N*-methylaniline was converted to **4f** in 40% yield. Notably, the dehalogenation byproduct *N*-methylaniline (**3a**) was observed in 16% yield. **3g** bearing the electron-withdrawing acetyl group gave the desired product **4g** in a moderate yield of 43%, while the corresponding aminal was formed as byproduct in a yield of 15% (see the Supporting Information). The catalytic protocol was applicable to the conversion of various other secondary amines **3h**−**3k** with an *N*-benzyl, *N*-butyl, *N*-cyclohexyl, or *N*-allyl group, which led to the desired products **4h**−**4k** in excellent yields of up to 99%. The conversion of diphenylamines **3l** and **3m** gave the *N*-methylated products in moderate yields of 42% and 46%, respectively, while the reactions of tetrahydroquinoline (**3n**) and indole (**3o**) afforded **4n** and **4o** in good yields of up to 88%. *N*-Methylpyridin-2-amine (**3p**) gave the desired product **4p** in a moderate yield of 62%. The protocol was also applied to the conversion of benzyl- and alkyl-substituted amines **3q** and **3r**, leading to the desired products in 56% and 73% yield, respectively. 2,2,6,6-Tetramethylpiperidine (**3s**) and morpholine (**3t**) afforded the corresponding products pempidine (**4s**), a ganglion-blocking drug,[48] and **4t** in yields of 88% and 44%, respectively. Primary amines often afford multiple products in this type of reaction. However, aniline (**3u**) afforded the dimethylated product **4u** in a moderate yield of 66% as the main product under a slightly modified condition.

In the catalyst screening, the *N*-formylated product **5a** was obtained as the main product in 73% yield at 23 °C in the

https://doi.org/10.1021/acssuschemeng.4c03464
ACS Sustainable Chem. Eng. XXXX, XXX, XXX−XXX

Table 1. Catalyst Screening and Parameter Optimization for the Conversion of Methylaniline (3a) with CO_2 to *N*-Methylated Product 4a[a]

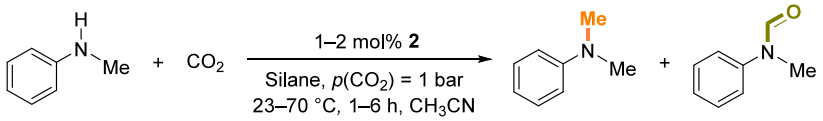

3a 4a 5a

entry	T (°C)	t (h)	catalyst	silane	yield of **4a** (%)	yield of **5a** (%)
1	45	6	**2a**	*n*-HexSiH$_3$	74	19
2	45	6	**2b**	*n*-HexSiH$_3$	76	15
3	45	6	**2c**	*n*-HexSiH$_3$	72	21
4	45	6	**2d**	*n*-HexSiH$_3$	72	18
5	45	6	**2e**	*n*-HexSiH$_3$	34	47
6	45	6	**2f**	*n*-HexSiH$_3$	59	32
7	45	6	**1b**	*n*-HexSiH$_3$	0	0
8	45	6	–	*n*-HexSiH$_3$	0	0
9	70	6	**2b**	*n*-HexSiH$_3$	99	0
10	23	6	**2b**	*n*-HexSiH$_3$	8	73
11	70	6	**2b**	PhSiH$_3$	24	0
12	70	6	**2b**	Ph$_2$SiH$_2$	93	0
13	70	6	**2b**	Ph$_3$SiH	0	0
14	70	6	**2b**	MePhSiH$_2$	57	8
15	70	6	**2b**	Me$_2$PhSiH	0	0
16	70	6	**2b**	PMHS	<5	4
17	70	4	**2b**	*n*-HexSiH$_3$	98	0
18	70	1	**2b**	*n*-HexSiH$_3$	90	4
19[b]	70	6	**2b**	*n*-HexSiH$_3$	89	0

[a]Reaction conditions: **3a** (0.47 mmol), silane (4.0 equiv), catalyst **2** (2 mol %), $p(CO_2)$ = 1 bar, 23–70 °C, CH_3CN (4 mL). Yields were determined by ^{1}H NMR analyses using mesitylene as the internal standard. [b]1 mol % catalyst.

presence of catalyst **2b** (Table 1, entry 10). We assumed that in general the *N*-formylation should be possible by adjusting the reaction conditions utilizing the same catalyst. Initially we studied the impact of the concentration of the reaction solution (Table 2, entries 1 and 2). With a lower amount of solvent, a similar yield of 71% was obtained (entry 1). However, under solvent-free conditions, an 87% yield was obtained (entry 2). The amount of silane was reduced to 1 equiv, which led to an 83% yield (entry 3). When the reaction time was prolonged to 8 h, full conversion was achieved, and **5a** was obtained in an excellent 96% yield (entry 4). The use of diphenylsilane as the reducing agent led to a slightly lower yield of 71% (entry 5).

Subsequently the scope and limitations of catalyst **2b** in the conversion of various amines **3** with CO_2 to formylated products **5** were investigated under the optimized conditions (Scheme 4). Except for insoluble substrates, all reactions were performed under solvent-free conditions. **3a** gave **5a** in an isolated yield of 82%. Both *p*-methoxy- (**3b**) and *o*-methoxy-*N*-methylaniline (**3c**) gave the corresponding formylated products **5b** and **5c** in yields of 85% and 81%, respectively. Halogen-substituted *N*-methylanilines **4d** and **4e** were also tolerated, leading to **5d** in 74% yield and **5e** in 62% yield. Anilines containing electron-withdrawing substituents are challenging substrates for metal-free catalytic protocols, and lower yields were previously reported.[21,29,35,49] The reaction of **3g** gave **5g** in a low yield of 32%. *N*-Benzyl, *N*-butyl, and *N*-allyl aniline derivatives (**3h**–**3j**) gave the desired products in yields up to 81%. *N*-Benzoylaniline (**3v**) gave only a 9% yield of formylated product **5v** even under more drastic conditions. In contrast, *N*-formylaniline (**3w**) afforded *N*,*N*-diformylaniline (**5w**) in 88% yield under the methylation condition. Notably, this indicates that formylated anilines are not intermediates in the methylation of anilines. Both tetrahydroquinoline (**3n**) and indole (**3o**) were tolerated, affording the corresponding formylated products **5n** and **5o** in good yield of 85%. Benzylic amines (**3q** and **3x**) and alkyl-substituted amines (**3r** and **3y**) could be converted to the desired formylated products in up to 96% yield. The reaction of morpholine (**3t**) afforded the desired product **5t** in an excellent yield of 95%. Adamantylamine (**3z**) and derivatives are drugs to treat Parkinson's disease and influenza.[50] *N*-Methyl-*N*-adamantyl1-amine (**3z**) was converted to the formylated product **5z** under the methylation conditions, and the product was isolated in 66% yield. Piperazine derivatives find wide applications as pharmaceuticals, and **3za** and **3zb** bearing a piperazine substructure gave excellent isolated yields of 92% and 90%, respectively. Under slightly modified conditions, the conversion of aniline (**3u**) led to the monoformylated product **5ua** in 76% yield, and at higher reaction temperatures the diformylated product **5ub** could be obtained in 70% yield.

From the application viewpoint, scale-up reactions were performed for both the *N*-methylation and *N*-formylation reactions (Scheme 5). **3h** (5 mmol) was converted to the desired *N*-methylated product **5h** in 82% yield (Scheme 5a). Moreover, 1 g of **3za** was converted with CO_2 at 45 °C for 24 h, and the desired product **5za** was isolated in 83% yield (Scheme 5b). The formation of the *N*-methylated product was not observed.

Furthermore, the **2b**-catalyzed *N*-methylation and *N*-formylation were applied to the late-stage functionalization of the antidepressant sertraline (**3zc**). Sertraline was converted to the *N*-methylated product in 76% yield. Moreover, sertraline was *N*-formylated, and the desired product was isolated in 58% yield (Scheme 6).

https://doi.org/10.1021/acssuschemeng.4c03464
ACS Sustainable Chem. Eng. XXXX, XXX, XXX−XXX

Scheme 3. *N*-Methylation of Amines 3 with CO_2[a]

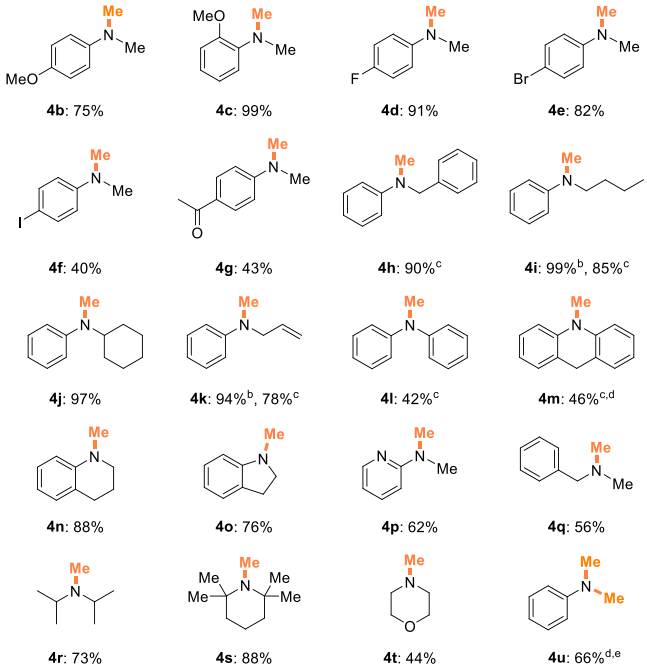

[a]Reaction conditions: Amine **3** (0.50 mmol), *n*-hexylsilane (4.0 equiv), **2b** (2 mol %), $p(CO_2)$ = 1 bar, 70 °C, CD_3CN (4 mL), 4 h. Yields were determined by ^1H NMR analyses with mesitylene as the internal standard. [b]2 h. [c]Isolated yield. [d]85 °C, 24 h. [e]8.0 equiv of *n*-hexylsilane.

Table 2. Optimization of the Reaction Conditions for the *N*-Formylation of 3a with CO_2[a]

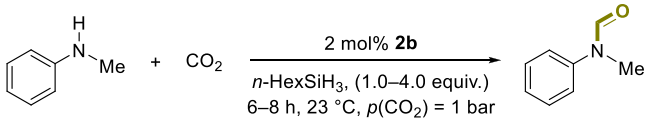

entry	*t* (h)	mL of solvent	silane (equiv)	yield of **5a** (%)
1	6	2	*n*-HexSiH$_3$ (4)	71
2	6	0	*n*-HexSiH$_3$ (4)	87
3	6	0	*n*-HexSiH$_3$ (1)	83
4	8	0	*n*-HexSiH$_3$ (1)	96
5	8	0	Ph_2SiH_2 (1)	71

[a]Reaction conditions: **3a** (0.47 mmol), *n*-hexylsilane, **2b** (2 mol %), $p(CO_2)$ = 1 bar, 23 °C, 6–8 h. Yields were determined by ^1H NMR analyses using mesitylene as the internal standard.

Several control experiments were performed to elucidate the possible mechanism of *N*-methylation and *N*-formulation with CO_2 in the presence of catalyst **2b**. The use of *n*-hexylsilane led to complex mixtures. Thus, diphenylsilane was employed for the control experiments since it showed comparable results in the *N*-methylation reaction (Table 1, entry 12) and *N*-formylation reaction (Table 2, entry 5). Initially a two-step control experiment was performed. Figure 1a shows a section of the ^1H NMR spectrum of diphenylsilane with the characteristic signal of δ(Si–*H*) = 4.93 ppm. In the first step, diphenylsilane

Scheme 4. *N*-Formylation of Amines 3 with CO_2[a]

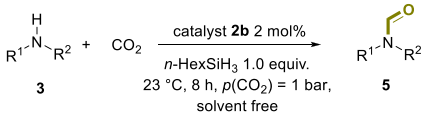

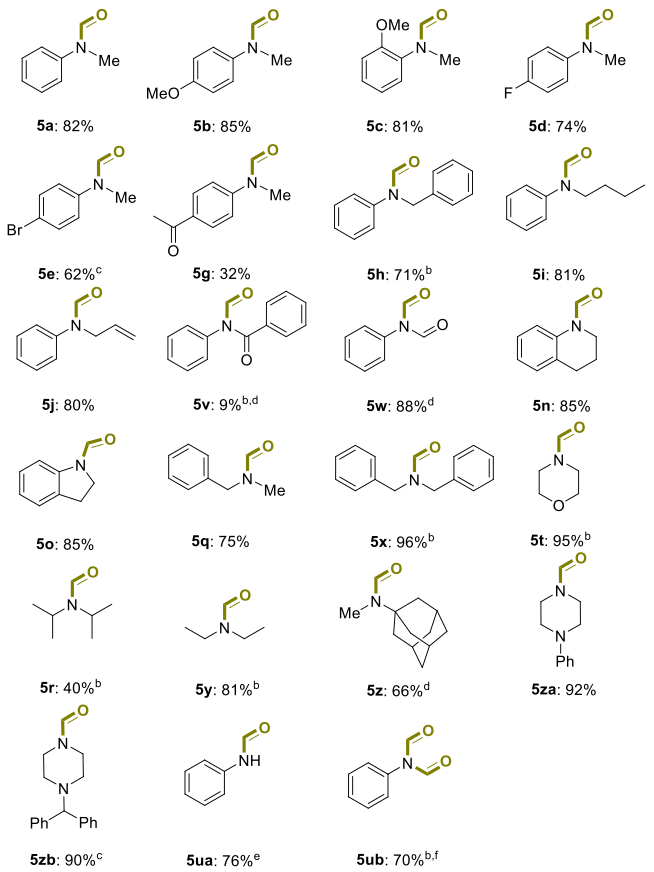

[a]Reaction conditions: Amine **3** (0.50 mmol), *n*-hexylsilane (1.0 equiv), **2b** (2 mol %), $p(CO_2)$ = 1 bar, 23 °C, 8 h, solvent-free. Isolated yields are given. [b]The yield was determined by ^1H NMR with mesitylene as the internal standard. [c]CH_3CN (0.5 mL). [d]*N*-Methylation conditions. [e]Amine (1.0 mmol), *n*-hexylsilane (2.0 equiv), 16 h, CH_3CN (4 mL). [f]*n*-Hexylsilane (4.0 equiv), **2b** (1 mol %), 70 °C, 24 h.

Scheme 5. Scale-Up Reactions: (a) Methylation of 3h; (b) Formylation of 3za

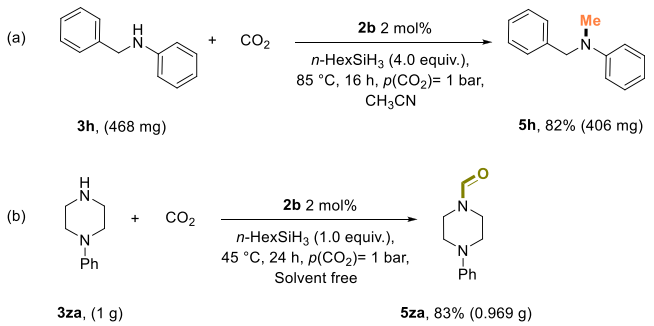

(2.0 equiv) and **2b** (2 mol %) were mixed under a CO_2 atmosphere (1 bar) at room temperature, resulting in a significant change in the ^1H NMR spectrum (Figure 1b). The characteristic signal at δ(Si–*H*) = 4.93 ppm was not observed after the reaction, and a new proton signal at $\delta(HCO_2)$ = 8.07

https://doi.org/10.1021/acssuschemeng.4c03464
ACS Sustainable Chem. Eng. XXXX, XXX, XXX−XXX

Scheme 6. Late-Stage Functionalization: *N*-Methylation and *N*-Formylation Reactions of Sertraline with CO_2

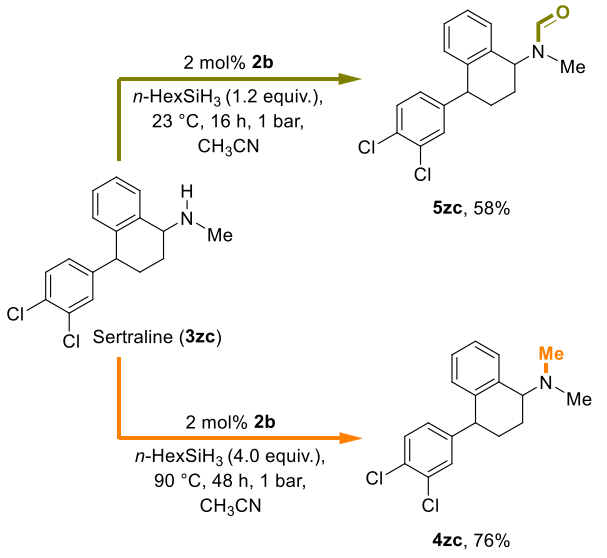

ppm appeared and was attributed to the formation of silyl formate **6**.[51] The signal at $\delta(C{=}O)$ = 163 ppm in the ^{13}C NMR spectrum also supports the formation of **6** (Figure S2). In the second step, *N*-methylamine (**3a**) was added to the mixture above and reacted under an argon atmosphere at room temperature for 16 h, giving *N*-methylformamide (**5a**) in 65% yield (Figure 1c). The ^1H NMR spectrum shows that the proton signal at $\delta(HCO_2)$ = 8.07 ppm disappeared and a new signal at δ = 8.50 ppm appeared, which can be attributed to the formation of *N*-methylformamide. As mentioned above, a similar yield of 71% for **5a** was obtained in the direct conversion of **3a** with CO_2 and diphenylsilane (Table 2, entry 5). Notably, in the absence of catalyst **2b**, neither the formation of the silyl formate nor the formation of the formylated product was observed. These results indicate an initial hydrosilylation of CO_2 catalyzed by **2b** to form a silyl formate, which subsequently reacts with the amine **3a** to form the *N*-formylated product **5a**.

Subsequently, we turned our attention to the *N*-methylation of amines with CO_2. In previously reported work, the dominant mechanism for the *N*-methylation proceeds via the hydrogenation of a formylated intermediate leading to the *N*-methylated product.[30,35,52] To investigate this possibility, **5a** was converted with diphenylsilane and CO_2 under the standard methylation conditions (Scheme 7). However, under these conditions, the formation of the methylated product **4a** was not observed. This clearly indicates that the pathway of *N*-methylation in the presence of **2b** does not proceed as previously reported via an *N*-formylated intermediate.

To identify possible intermediates of the *N*-methylation reaction, diphenylsilane was converted with CO_2 (1 bar) at 70 °C for 4 h in the presence of 2 mol % **2b** (Scheme 8a). In contrast to the reaction at 23 °C, the formation of formate **6** was not observed. Instead, dimethoxysilane (**7**), silyl acetal **8**, and siloxane **9** were detected as the main products (see the Supporting Information for details).[28] In the absence of catalyst **2b**, the formation of **7**, **8**, and **9** was not observed. We assumed

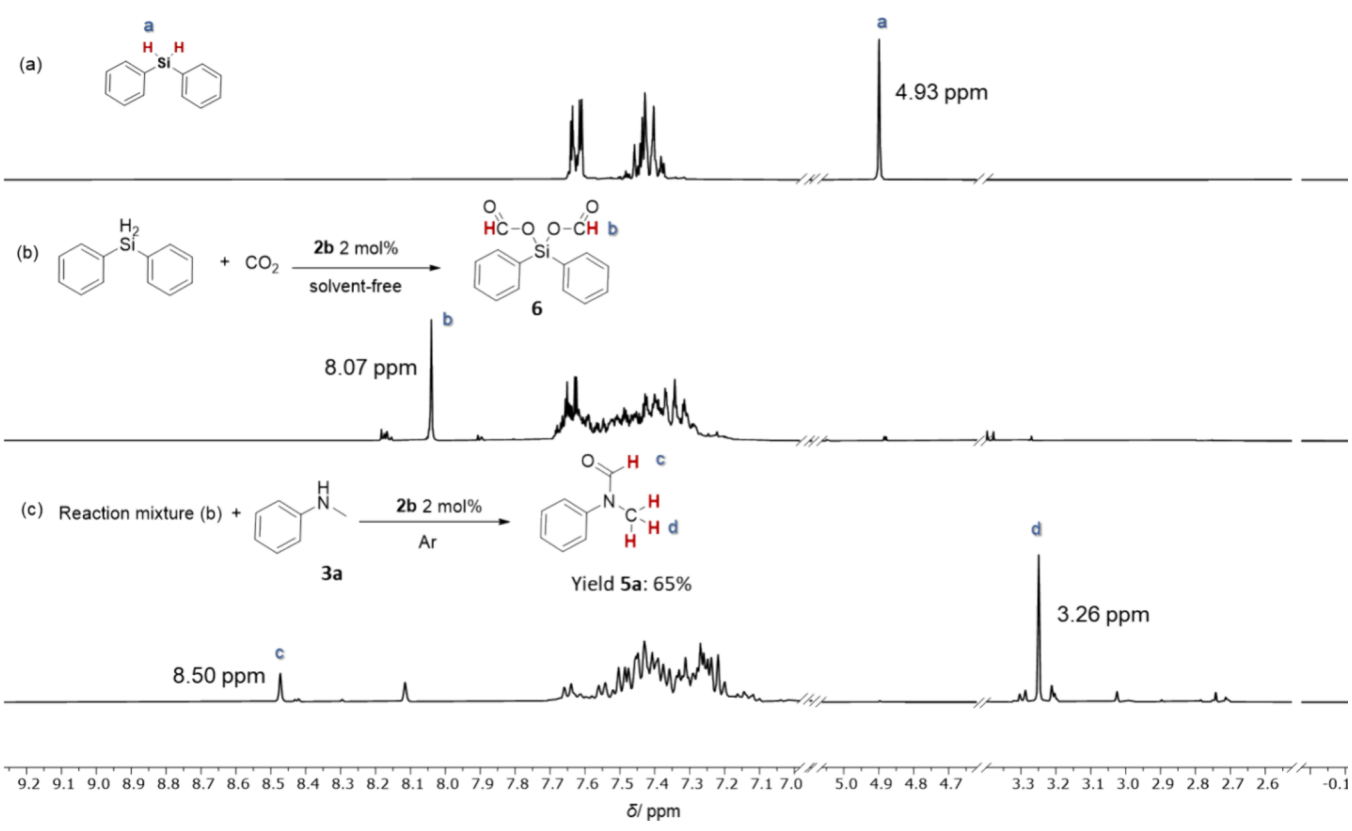

Figure 1. ^1H NMR spectra of diphenylsilane and control experiments in CD_3CN. (a) Section of the ^1H NMR spectrum of diphenylsilane. (b) Section of the ^1H NMR spectrum of diphenylsilane (2 equiv) and CO_2 with 2 mol % **2b** (1 bar, 23 °C, solvent-free, 16 h). (c) Section of the ^1H NMR spectrum of the reaction solution from (b) and *N*-methylamine (1 equiv) after 16 h at 23 °C under Ar in CD_3CN at 23 °C for 16 h with mesitylene as an internal standard.

https://doi.org/10.1021/acssuschemeng.4c03464
ACS Sustainable Chem. Eng. XXXX, XXX, XXX−XXX

Scheme 7. Reaction of 5a under the *N*-Methylation Conditions

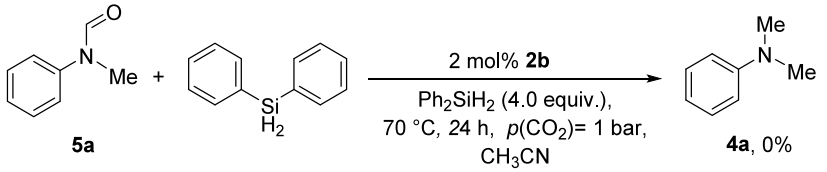

Scheme 8. Control Experiments for Mechanistic Studies of the *N*-Methylation Reaction: (a) Reaction of Diphenylsilane with CO_2 in the Presence of Catalyst 2b; (b) Reaction of 3a in Solution (a) under Argon; (c) Reaction of 3a in Solution (b) in the Presence of CO_2[a]

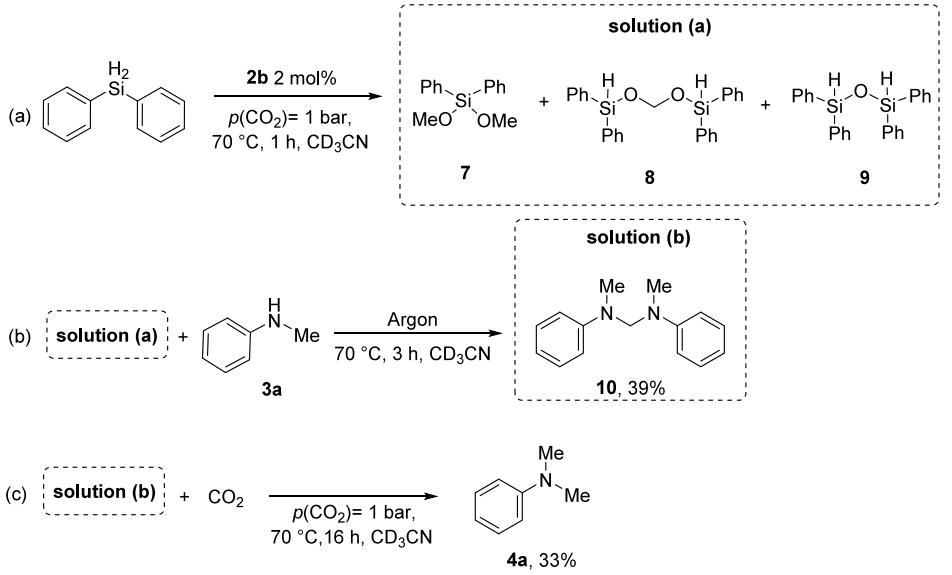

[a]Solution (a) is the reaction mixture from panel (a), and solution (b) is the reaction mixture from panel (b).

Scheme 9. Control Experiments for Mechanistic Study of the *N*-Methylation Reaction: (a) Reaction of Dimethoxysilane and Siloxane with 3a under Argon in the Presence of Catalyst 2b; (b) Reaction of Dimethoxysilane and Siloxane with 3a in the Presence of CO_2 and Catalyst 2b

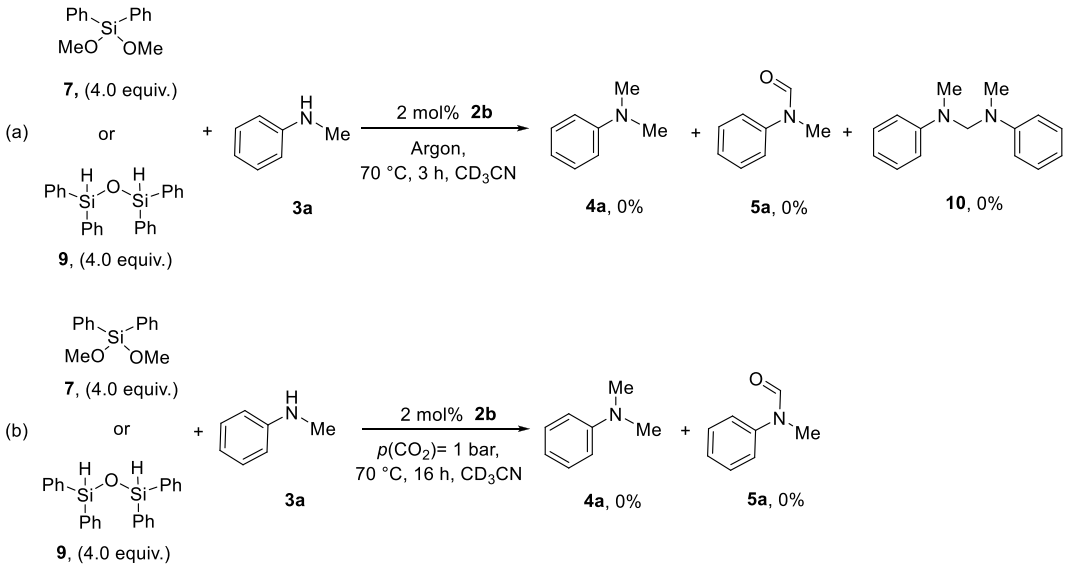

that silyl acetal **8** might be an intermediate of the reaction. Thus, **3a** was added to the reaction solution from Scheme 8a and reacted under argon (Scheme 8b). After 3 h, the aminal product **10** was obtained in 39% yield. This indicates that **8** is converted to **10**, which might be subsequently reduced to the product **4a** and **3a** in the next step. To convert **3a** to **4a** the addition of CO_2 would be required.[31] Indeed, when CO_2 (1 bar) was added in the above reaction solution from Scheme 8b, the desired product **4a** was obtained in 33% yield (Scheme 8c).

https://doi.org/10.1021/acssuschemeng.4c03464
ACS Sustainable Chem. Eng. XXXX, XXX, XXX−XXX

Furthermore **7** and **9** were converted with **3a** and catalyst **2b** under argon to exclude that these compounds are intermediates in the reaction (Scheme 9a). Additionally, **7** and **9** were converted under the same conditions in the presence of diphenylsilane (Scheme 9b). No conversion was observed in all cases, indicating that these compounds are not intermediates of *N*-methylation or *N*-formylation.

Based on these results and previous reports, a possible pathway was proposed, which is shown in Scheme 10. In the presence of catalyst **2b**, CO_2 is initially reduced by the silane to the corresponding formate. At lower temperatures (23 °C), the formate reacts with the amine directly, forming the *N*-formylated product **5** (Scheme 10, path A). In contrast, at higher temperatures (70 °C), the formate is further reduced to the silyl acetalintermediate, which reacts with the amine to form the corresponding aminal (Scheme 10, path B). The aminal is then further reduced to *N*-methylated product **4**.

Scheme 10. Proposed Reaction Pathway of Temperature-Controlled *N*-Methylation and *N*-Formylation of Amines 3 with CO_2 in the Presence of Catalyst 2b

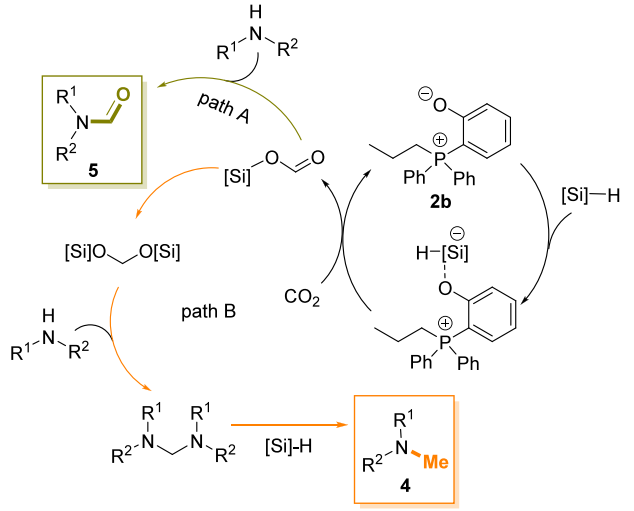

CONCLUSIONS

A series of new internal phosphonium salt catalysts were prepared by simply treating the corresponding phosphonium iodides with an aqueous sodium hydroxide solution. These salts were tested as catalysts for the *N*-methylation and *N*-formylation of amines with CO_2 as a C_1 source and silane as a reducing agent. The efficient *N*-methylation of amines was achieved at 70 °C in acetonitrile as a solvent using *n*-hexylsilane as a reducing agent. Notably, a complete switch in selectivity was achieved by simply reducing the reaction temperature to 23 °C. At this temperature, amines were converted to the *N*-formylated products under solvent-free conditions. The most efficient catalyst exhibited broad applicability. Twenty-two secondary and primary amines were converted to the corresponding *N*-methylated products in up to 99% yield. Moreover, 24 amines were *N*-formylated using the same catalyst and reducing agent. The potential of the catalyst was demonstrated by a scale-up reaction and the late-stage functionalization of the pharmaceutical sertraline. Control experiments and NMR studies indicate that the *N*-methylation proceeds at higher temperatures via silyl acetal and aminal intermediates, while the formylation proceeds at 23 °C via silyl formates. Overall, an efficient catalyst is reported that can switch between *N*-methylation and *N*-formylation of amines with CO_2 by simply changing the reaction conditions.

ASSOCIATED CONTENT

Supporting Information

The Supporting Information is available free of charge at https://pubs.acs.org/doi/10.1021/acssuschemeng.4c03464.

Synthetic procedures for the catalysts, *N*-methylation and *N*-formylation reactions, characterization data for the catalysts and products (^{1}H, ^{13}C and ^{31}P NMR spectra and X-ray crystal structure analysis) and additional experimental details for mechanism studies (PDF)

AUTHOR INFORMATION

Corresponding Author

Thomas Werner − *Leibniz Institute for Catalysis at the University of Rostock (LIKAT Rostock), D-18059 Rostock, Germany; Department of Chemistry and Center for Sustainable Systems Design (CSSD), Paderborn University, D-33098 Paderborn, Germany;* orcid.org/0000-0001-9025-3244; Email: th.werner@uni-paderborn.de

Authors

Changyue Ren − *Leibniz Institute for Catalysis at the University of Rostock (LIKAT Rostock), D-18059 Rostock, Germany*

Anke Spannenberg − *Leibniz Institute for Catalysis at the University of Rostock (LIKAT Rostock), D-18059 Rostock, Germany*

Complete contact information is available at: https://pubs.acs.org/10.1021/acssuschemeng.4c03464

Author Contributions

C.R. performed the experimental work. A.S. performed the X-ray analysis. C.R. and T.W. wrote the manuscript.

Notes

The authors declare no competing financial interest.

ACKNOWLEDGMENTS

C.R. thanks Dr. Hanna Sebode for support and the Leibniz-Program Cooperative Excellence (Project "SUPREME", K308/2020) for financial support. T.W. thanks the Leibniz Science Campus Phosphorus Research Rostock, which is cofunded by the funding line strategic networks of the Leibniz Association.

REFERENCES

(1) Grignard, B.; Gennen, S.; Jérôme, C.; Kleij, A. W.; Detrembleur, C. Advances in the use of CO_2 as a renewable feedstock for the synthesis of polymers. *Chem. Soc. Rev.* **2019**, *48*, 4466−4514.

(2) Jiang, X.; Nie, X.; Guo, X.; Song, C.; Chen, J. G. Recent Advances in Carbon Dioxide Hydrogenation to Methanol via Heterogeneous Catalysis. *Chem. Rev.* **2020**, *120*, 7984−8034.

(3) Liu, Q.; Wu, L.; Jackstell, R.; Beller, M. Using carbon dioxide as a building block in organic synthesis. *Nat. Commun.* **2015**, *6*, 5933.

(4) Sullivan, I.; Goryachev, A.; Digdaya, I. A.; Li, X.; Atwater, H. A.; Vermaas, D. A.; Xiang, C. Coupling electrochemical CO_2 conversion with CO_2 capture. *Nat. Catal.* **2021**, *4*, 952−958.

(5) Ye, J.-H.; Ju, T.; Huang, H.; Liao, L.-L.; Yu, D.-G. Radical Carboxylative Cyclizations and Carboxylations with CO_2. *Acc. Chem. Res.* **2021**, *54*, 2518−2531.

(6) Aresta, M.; Dibenedetto, A.; Angelini, A. Catalysis for the Valorization of Exhaust Carbon: from CO_2 to Chemicals, Materials, and Fuels. Technological Use of CO_2. *Chem. Rev.* **2014**, *114*, 1709−1742.

(7) Zhang, N.; Zhang, Z.; Wong, I. L. K.; Wan, S.; Chow, L. M. C.; Jiang, T. 4,5-Di-substituted benzyl-imidazol-2-substituted amines as the structure template for the design and synthesis of reversal agents against P-gp-mediated multidrug resistance breast cancer cells. *Eur. J. Med. Chem.* **2014**, *83*, 74−83.
(8) Barreiro, E. J.; Kümmerle, A. E.; Fraga, C. A. M. The Methylation Effect in Medicinal Chemistry. *Chem. Rev.* **2011**, *111*, 5215−5246.
(9) Chatterjee, J.; Rechenmacher, F.; Kessler, H. *N*-Methylation of Peptides and Proteins: An Important Element for Modulating Biological Functions. *Angew. Chem., Int. Ed.* **2013**, *52*, 254−269.
(10) Isin, E. M.; Elmore, C. S.; Nilsson, G. N.; Thompson, R. A.; Weidolf, L. Use of Radiolabeled Compounds in Drug Metabolism and Pharmacokinetic Studies. *Chem. Res. Toxicol.* **2012**, *25*, 532−542.
(11) McCarthy, D. J.; Halldin, C.; Andersson, J. D.; Pierson, M. E. Discovery of Novel Positron Emission Tomography Tracers. *Annu. Rep. Med. Chem.* **2009**, *44*, 501−513.
(12) Antoni, G.; Långström, B. Progress in ^{11}C Radiochemistry. In *Positron Emission Tomography: Basic Sciences*; Bailey, D. L., Townsend, D. W., Valk, P. E., Maisey, M. N., Eds.; Springer: London, 2005; pp 223−236.
(13) Del Vecchio, A.; Caille, F.; Chevalier, A.; Loreau, O.; Horkka, K.; Halldin, C.; Schou, M.; Camus, N.; Kessler, P.; Kuhnast, B.; et al. Late-Stage Isotopic Carbon Labeling of Pharmaceutically Relevant Cyclic Ureas Directly from CO_2. *Angew. Chem., Int. Ed.* **2018**, *57*, 9744−9748.
(14) Del Vecchio, A.; Destro, G.; Taran, F.; Audisio, D. Recent developments in heterocycle labeling with carbon isotopes. *J. Label. Compd. Radiopharm.* **2018**, *61*, 988−1007.
(15) Olah, G. A.; Ohannesian, L.; Arvanaghi, M. Formylating agents. *Chem. Rev.* **1987**, *87*, 671−686.
(16) Huffman, C. Formylation of amines. *J. Org. Chem.* **1958**, *23*, 727−729.
(17) Calverley, M. J. Selective *N*-Monomethylation of Primary Amines via *N*-Trialkylsilyl-Lithioamines. *Synth. Commun.* **1983**, *13*, 601−609.
(18) Seo, H.; Bédard, A.-C.; Chen, W. P.; Hicklin, R. W.; Alabugin, A.; Jamison, T. F. Selective *N*-monomethylation of primary anilines with dimethyl carbonate in continuous flow. *Tetrahedron* **2018**, *74*, 3124−3128.
(19) Selva, M.; Perosa, A. Green chemistry metrics: a comparative evaluation of dimethyl carbonate, methyl iodide, dimethyl sulfate and methanol as methylating agents. *Green Chem.* **2008**, *10*, 457−464.
(20) Das Neves Gomes, C.; Jacquet, O.; Villiers, C.; Thuéry, P.; Ephritikhine, M.; Cantat, T. A Diagonal Approach to Chemical Recycling of Carbon Dioxide: Organocatalytic Transformation for the Reductive Functionalization of CO_2. *Angew. Chem., Int. Ed.* **2012**, *51*, 187−190.
(21) Jacquet, O.; Das Neves Gomes, C.; Ephritikhine, M.; Cantat, T. Recycling of Carbon and Silicon Wastes: Room Temperature Formylation of N−H Bonds Using Carbon Dioxide and Polymethylhydrosiloxane. *J. Am. Chem. Soc.* **2012**, *134*, 2934−2937.
(22) Jacquet, O.; Frogneux, X.; Das Neves Gomes, C.; Cantat, T. CO_2 as a C_1-building block for the catalytic methylation of amines. *Chem. Sci.* **2013**, *4*, 2127−2131.
(23) Li, Y.; Fang, X.; Junge, K.; Beller, M. A General Catalytic Methylation of Amines Using Carbon Dioxide. *Angew. Chem., Int. Ed.* **2013**, *52*, 9568−9571.
(24) Hulla, M.; Dyson, P. J. Pivotal Role of the Basic Character of Organic and Salt Catalysts in C−N Bond Forming Reactions of Amines with CO_2. *Angew. Chem., Int. Ed.* **2020**, *59*, 1002−1017.
(25) Li, G.; Chen, J.; Zhu, D.-Y.; Chen, Y.; Xia, J.-B. DBU-Catalyzed Selective *N*-Methylation and *N*-Formylation of Amines with CO_2 and Polymethylhydrosiloxane. *Adv. Synth. Catal.* **2018**, *360*, 2364−2369.
(26) Li, W.-D.; Zhu, D.-Y.; Li, G.; Chen, J.; Xia, J.-B. Iron-Catalyzed Selective *N*-Methylation and *N*-Formylation of Amines with CO_2. *Adv. Synth. Catal.* **2019**, *361*, 5098−5104.
(27) Nicholls, R. L.; McManus, J. A.; Rayner, C. M.; Morales-Serna, J. A.; White, A. J. P.; Nguyen, B. N. Guanidine-Catalyzed Reductive Amination of Carbon Dioxide with Silanes: Switching between Pathways and Suppressing Catalyst Deactivation. *ACS Catal.* **2018**, *8*, 3678−3687.
(28) Liu, X.-F.; Li, X.-Y.; Qiao, C.; Fu, H.-C.; He, L.-N. Betaine Catalysis for Hierarchical Reduction of CO_2 with Amines and Hydrosilane To Form Formamides, Aminals, and Methylamines. *Angew. Chem., Int. Ed.* **2017**, *56*, 7425−7429.
(29) Xie, C.; Song, J.; Wu, H.; Zhou, B.; Wu, C.; Han, B. Natural Product Glycine Betaine as an Efficient Catalyst for Transformation of CO_2 with Amines to Synthesize *N*-Substituted Compounds. *ACS Sustain. Chem. Eng.* **2017**, *5*, 7086−7092.
(30) Fang, C.; Lu, C.; Liu, M.; Zhu, Y.; Fu, Y.; Lin, B.-L. Selective Formylation and Methylation of Amines using Carbon Dioxide and Hydrosilane Catalyzed by Alkali-Metal Carbonates. *ACS Catal.* **2016**, *6*, 7876−7881.
(31) Wang, M.-Y.; Wang, N.; Liu, X.-F.; Qiao, C.; He, L.-N. Tungstate catalysis: pressure-switched 2- and 6-electron reductive functionalization of CO_2 with amines and phenylsilane. *Green Chem.* **2018**, *20*, 1564−1570.
(32) Zhang, C.; Lu, Y.; Zhao, R.; Menberu, W.; Guo, J.; Wang, Z.-X. A comparative DFT study of TBD-catalyzed reactions of amines with CO_2 and hydrosilane: the effect of solvent polarity on the mechanistic preference and the origins of chemoselectivities. *Chem. Commun.* **2018**, *54*, 10870−10873.
(33) Zhang, Y.; Zhang, H.; Gao, K. Borane−Trimethylamine Complex as a Reducing Agent for Selective Methylation and Formylation of Amines with CO_2. *Org. Lett.* **2021**, *23*, 8282−8286.
(34) Zhao, W.; Chi, X.; Li, H.; He, J.; Long, J.; Xu, Y.; Yang, S. Eco-friendly acetylcholine-carboxylate bio-ionic liquids for controllable N-methylation and *N*-formylation using ambient CO_2 at low temperatures. *Green Chem.* **2019**, *21*, 567−577.
(35) Liu, X.-F.; Ma, R.; Qiao, C.; Cao, H.; He, L.-N. Fluoride-Catalyzed Methylation of Amines by Reductive Functionalization of CO_2 with Hydrosilanes. *Chem. - Eur. J.* **2016**, *22*, 16489−16493.
(36) Hu, Y.; Song, J.; Xie, C.; Wu, H.; Wang, Z.; Jiang, T.; Wu, L.; Wang, Y.; Han, B. Renewable and Biocompatible Lecithin as an Efficient Organocatalyst for Reductive Conversion of CO_2 with Amines to Formamides and Methylamines. *ACS Sustain. Chem. Eng.* **2018**, *6*, 11228−11234.
(37) Cabrero-Antonino, J. R.; Adam, R.; Beller, M. Catalytic Reductive N-Alkylations Using CO_2 and Carboxylic Acid Derivatives: Recent Progress and Developments. *Angew. Chem., Int. Ed.* **2019**, *58*, 12820−12838.
(38) Bobbink, F. D.; Das, S.; Dyson, P. J. *N*-formylation and *N*-methylation of amines using metal-free *N*-heterocyclic carbene catalysts and CO_2 as carbon source. *Nat. Protoc.* **2017**, *12*, 417−428.
(39) Ren, C.; Terazzi, C.; Werner, T. Tuneable reduction of CO_2 − organocatalyzed selective formylation and methylation of amines. *Green Chem.* **2024**, *26*, 439−447.
(40) Lasso, J. D.; Castillo-Pazos, D. J.; Li, C.-J. Green chemistry meets medicinal chemistry: a perspective on modern metal-free late-stage functionalization reactions. *Chem. Soc. Rev.* **2021**, *50*, 10955−10982.
(41) Buettner, H.; Steinbauer, J.; Wulf, C.; Dindaroglu, M.; Schmalz, H.-G.; Werner, T. Organocatalyzed Synthesis of Oleochemical Carbonates from CO_2 and Renewables. *ChemSusChem* **2017**, *10*, 1076−1079.
(42) Buettner, H.; Kohrt, C.; Wulf, C.; Schaeffner, B.; Groenke, K.; Hu, Y.; Kruse, D.; Werner, T. Life Cycle Assessment for the Organocatalytic Synthesis of Glycerol Carbonate Methacrylate. *ChemSusChem* **2019**, *12*, 2701−2707.
(43) Hu, Y.; Peglow, S.; Longwitz, L.; Frank, M.; Epping, J. D.; Brüser, V.; Werner, T. Plasma-Assisted Immobilization of a Phosphonium Salt and Its Use as a Catalyst in the Valorization of CO_2. *ChemSusChem* **2020**, *13*, 1825−1833.
(44) Hu, Y.; Wei, Z.; Frey, A.; Kubis, C.; Ren, C.-Y.; Spannenberg, A.; Jiao, H.; Werner, T. Catalytic, Kinetic, and Mechanistic Insights into the Fixation of CO_2 with Epoxides Catalyzed by Phenol-Functionalized Phosphonium Salts. *ChemSusChem* **2021**, *14*, 363−372.
(45) Ren, C.; Spannenberg, A.; Werner, T. Synthesis of Bifunctional Phosphonium Salts Bearing Perfluorinated Side Chains and Their

https://doi.org/10.1021/acssuschemeng.4c03464
ACS Sustainable Chem. Eng. XXXX, XXX, XXX−XXX

Application in the Synthesis of Cyclic Carbonates from Epoxides and CO_2. *Asian J. Org. Chem.* **2022**, *11*, No. e202200156.
(46) CCDC 2332383 contains the supplementary crystallographic data for this paper. These data are provided free of charge by the joint Cambridge Crystallographic Data Centre and Fachinformationszentrum Karlsruhe Access Structures Service (www.ccdc.cam.ac.uk/structures).
(47) Toda, Y.; Hashimoto, K.; Mori, Y.; Suga, H. A Phosphonium Ylide as a Ligand for [3 + 2] Coupling Reactions of Epoxides with Heterocumulenes under Mild Conditions. *J. Org. Chem.* **2020**, *85*, 10980−10987.
(48) Bretherick, L.; Lee, G. E.; Lunt, E.; Wragg, W. R.; Edge, N. D. Congeners of Pempidine with High Ganglion-blocking Activity. *Nature* **1959**, *184*, 1707−1709.
(49) Chen, L.; Liu, R.; Yan, Q. Polymer Meets Frustrated Lewis Pair: Second-Generation CO_2-Responsive Nanosystem for Sustainable CO_2 Conversion. *Angew. Chem., Int. Ed.* **2018**, *57*, 9336−9340.
(50) Wolf, E.; Seppi, K.; Katzenschlager, R.; Hochschorner, G.; Ransmayr, G.; Schwingenschuh, P.; Ott, E.; Kloiber, I.; Haubenberger, D.; Auff, E.; et al. Long-term antidyskinetic efficacy of amantadine in Parkinson's disease. *Mov. Disord.* **2010**, *25*, 1357−1363.
(51) Zhang, Q.; Fukaya, N.; Fujitani, T.; Choi, J.-C. Carbon Dioxide Hydrosilylation to Methane Catalyzed by Zinc and Other First-Row Transition Metal Salts. *Bull. Chem. Soc. Jpn.* **2019**, *92*, 1945−1949.
(52) Guo, Z.; Pang, T.; Yan, L.; Wei, X.; Chao, J.; Xi, C. CO_2-tuned highly selective reduction of formamides to the corresponding methylamines. *Green Chem.* **2021**, *23*, 7534−7538.

https://doi.org/10.1021/acssuschemeng.4c03464
ACS Sustainable Chem. Eng. XXXX, XXX, XXX−XXX

6.4 Tuneable reduction of CO_2 – organocatalyzed selective formylation and methylation of amines

C. Ren, C. Terazzi and T. Werner* *Green Chem.* **2024**, *26*, 439−447.

DOI: 10.1039/D3GC03993E

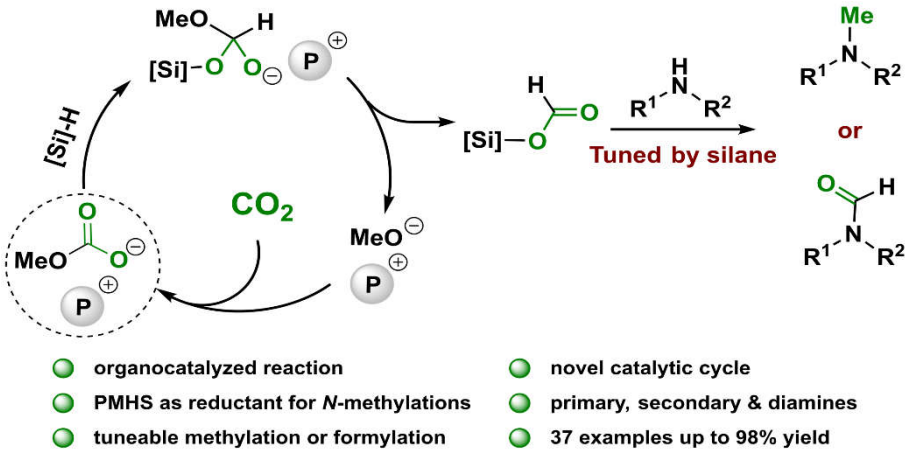

Abstract: The *N*-formylation and *N*-methylation of amines with carbon dioxide (CO_2) are important types of transformations which give access to a wide range of key intermediates and compounds. Efficient catalytic methods for both reactions are rare because of the challenge to control selectivity. Herein, we report the environmentally benign organocatalyzed *N*-formylation and *N*-methylation of primary and secondary amines using CO_2 as the C1 source in the presence of hydrosilanes as reductant. Readily available methyltriphenylphosphonium methylcarbonate proved to be an efficient catalyst for the *N*-methylation of amines and CO_2 in the presence of polymethylhydrosiloxane (PMHS) under mild conditions. In contrast the selective *N*-formylation is achieved in the presence of trimethoxysilane as reductant. In both transformations, a wide range of substrates was selectively converted. 15 primary and secondary amines were *N*-methylated and *N*-formylated and the corresponding products obtained in yields up to 98% and 94%, respectively. Moreover, benzimidazoles are accessible from diamines and CO_2 in a one-pot reaction in yields up to 83%. Mechanistic investigations revealed different reaction pathways for the *N*-methylation and *N*-formylation depending on the reductant as well as the activation of CO_2 by the catalyst.

Green Chemistry

PAPER

View Article Online
View Journal | View Issue

Cite this: *Green Chem.*, 2024, **26**, 439

Tuneable reduction of CO_2 – organocatalyzed selective formylation and methylation of amines†

Changyue Ren,[a,b] Constanza Terazzi[a] and Thomas Werner *[a,c]

The *N*-formylation and *N*-methylation of amines with carbon dioxide (CO_2) are important types of transformations which give access to a wide range of key intermediates and compounds. Efficient catalytic methods for both reactions are rare because of the challenge of controlling selectivity. Herein, we report the environmentally benign organocatalyzed *N*-formylation and *N*-methylation of primary and secondary amines using CO_2 as the C1 source in the presence of hydrosilanes as the reductant. Readily available methyltriphenylphosphonium methylcarbonate has been proven to be an efficient catalyst for the *N*-methylation of amines and CO_2 in the presence of polymethylhydrosiloxane (PMHS) under mild conditions. In contrast, the selective *N*-formylation is achieved in the presence of trimethoxysilane as the reductant. In both transformations, a wide range of substrates were selectively converted. 15 primary and secondary amines were *N*-methylated and *N*-formylated and the corresponding products were obtained in yields of up to 98% and 94%, respectively. Moreover, benzimidazoles are accessible from diamines and CO_2 in a one-pot reaction in yields of up to 83%. Mechanistic investigations revealed different reaction pathways for *N*-methylation and *N*-formylation depending on the reductant as well as the activation of CO_2 by the catalyst.

Received 19th October 2023,
Accepted 18th November 2023

DOI: 10.1039/d3gc03993e

rsc.li/greenchem

Introduction

N-Methylamines and *N*-formamides are attractive chemicals that have found extensive applications in the pharmaceutical industry, biological sciences, and agriculture.[1–8] Formamide derivatives, such as *N*-methylformamide and *N*,*N*-dimethylformamide (DMF), are among the most used solvents and important intermediates for the synthesis of other valuable materials,[9] such as isocyanides[10,11] and benzoheterocycles.[12,13] *N*-Methylamines are structural subunits that can be found in many significant bioactive compounds and drugs.[14] The common C1 sources for *N*-methylation and *N*-formylation reactions include MeI,[15] CH_2N_2,[16] dimethyl carbonate,[17] methanol,[18] formic acid[19] and CO_2.[20] In particular, the use of CO_2 in combination with reducing agents is an attractive alternative to toxic and hazardous reagents (Scheme 1a). CO_2 is a waste product of fuel combustion currently deemed as a promising surrogate of carbon feedstocks. Its utilization has been an active field of research in the past few decades. However, the kinetic inertness and thermodynamic stability of the CO_2 molecule significantly hinder its efficient valorization under mild conditions.[21–25]

Although a few catalysts have been reported to be able to perform the *N*-functionalization of amines to form both formamide and methylamine (Scheme 1a),[26–29] there are several challenges to overcome in terms of these reactions. One of them is employing cost-efficient reductants.[30] Phenylsilanes have been widely used in the fixation of CO_2 into amines,[26,28,29,31,32] but their use presents some disadvantages

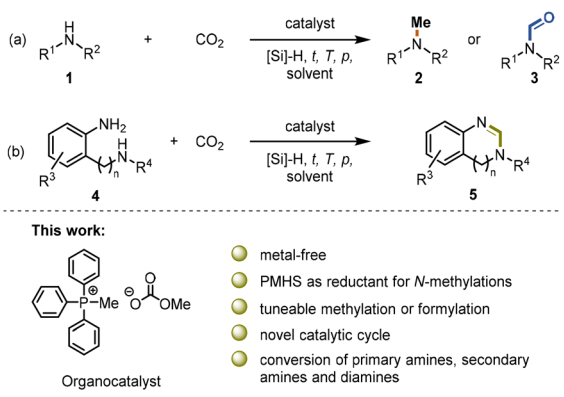

Scheme 1 (a) *N*-Methylation and *N*-formylation of amines with CO_2 and silane. (b) The formation of benzoheterocycles from diamines with CO_2 and silane.

[a]*Leibniz Institute for Catalysis e.V. at the University of Rostock, Albert-Einstein-Straße 29a, 18059 Rostock, Germany. E-mail: Thomas.Werner@catalysis.de*
[b]*College of Pharmacy, Zunyi Medical University, Zunyi 563003, China*
[c]*Department of Chemistry, Paderborn University, Warburger Str. 100, D-33098 Paderborn, Germany. E-mail: th.werner@uni-paderborn.de*

† Electronic supplementary information (ESI) available. See DOI: https://doi.org/10.1039/d3gc03993e

since they are expensive, and the byproducts formed are difficult to remove. Polymethylhydrosiloxane (PMHS) is an abundant, low-cost, non-toxic, and highly moisture-stable chemical waste product generated by the silicone industry.[33–35] Even though it would be advantageous to use PMHS as the reductant in the reduction of CO_2, very few organic catalysts are reported to be active for both PMHS and CO_2 for the methylation reaction. Dyson *et al.* reported a thiazolium carbene-based catalyst for the *N*-formylation and *N*-methylation of amines using PMHS as a reducing agent, which allows the reaction to proceed under relatively mild conditions.[36,37]

The Xia group reported diazabicycloundecene (DBU) as an organocatalyst for the selective *N*-methylation and *N*-formylation of secondary amines, converting secondary amines, CO_2 and PMHS into methylamines and formamides at 100 °C and 30 °C, respectively.[38] Furthermore, benzoheterocycles can be prepared from *o*-phenylenediamine, CO_2 and silane (Scheme 1b). The formation of the benzimidazole ring is plausible by monoformylation and subsequent imine formation with a suitable catalyst. However, due to the mismatched catalysis, the cyclization reaction normally requires two steps or harsher conditions than the *N*-formylation reaction.[13,31,32,39,40] In the previous reports, the *N*-formylation and *N*-methylation reactions are assumed to proceed by a general base-catalysed reaction mechanism, in which hydrosilanes are activated by the basic catalyst or the carbamate salt formed.[13] Most recently, the Song group reported the *N*-methylation and *N*-formylation reaction between CO_2 and secondary amines in the presence of phenylsilane catalyzed by an ammonium carboxylate ionic liquid.[41] In addition, Lin and coworkers reported Cs_2CO_3 to be an efficient inorganic catalyst for these reactions.[42] These reports and our interest in using phosphonium salts as organocatalysts for the utilization of CO_2 motivated us to explore a phosphorus-based organocatalyst in combination with PMHS as a reductant for the methylation of amines.[43–46] We focused on methylcarbonate salts which were first reported as a CO_2 surrogate in the preparation of propylene oxide in 2006,[47] and subsequently have been employed in the transesterification[48] and Henry reactions,[49] and as vinylation reagents in the Wittig reaction.[50]

Results and discussion

Methyltriphenylphosphonium methylcarbonate is commercially available and can also be prepared from phosphines and dimethylcarbonate (DMC) according to the literature.[50] PMHS was selected as the reducing agent and *N*-methylaniline (**1a**) as the model substrate for evaluating the activity of the catalyst towards methylation, utilizing CO_2 as the carbon source at 1 bar and 70 °C (Table 1). In the absence of the catalyst, no conversion was observed (entry 1). A moderate yield of 53% and good selectivity for *N*-methylated product **2a** were obtained in the presence of the catalyst (entry 2). In CH_3CN, *N*-methylaniline (**1a**) gave the *N*-methylated product **2a** and *N*-formylated product **3a** with a yield of 20% and 6%, respectively (entry 3). In EtOAc and CH_2Cl_2, **1a** failed to convert to either **2a** or **3a** (entries 4 and 5). Due to its polymeric nature, PMHS is less active than non-polymeric silanes. Thus, an excess of reductant is normally required.[36–38,51] Full conversion was achieved by increasing the amount of PMHS and **2a** was obtained in a very good yield of 87% (entry 6). Even under 1 atm of CO_2 (balloon), **2a** was accessible in 29% yield (entry 7). Replacing THF with the biomass-derived 2-methyltetrahydrofuran (Me-THF) gave **3a** in 83% yield (entry 8). At a lower catalyst loading, an increase in the formation of the *N*-formylated product **3a** was observed (entry 9). Finally, the impact of the reaction temperature was studied (entries 10–12). Neither an increase nor a decrease of the reaction temperature led to an improved yield of **2a**. Notably, at lower temperatures (50 °C), the yield of **2a** decreased to 55% but **3a** was obtained in 38% yield (entry 12).

Table 1 Optimization of the reaction conditions for the conversion of *N*-methylaniline (**1a**) with CO_2 to methylated product **2a**

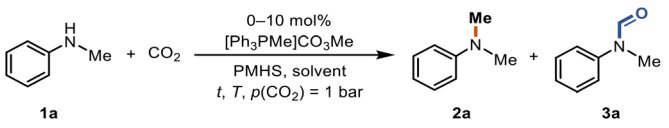

1a 2a 3a

Entry	Cat. (mol %)	Silane (equiv.)	Solvent	*T* (°C)	Yield **2a** [a] (%)	Yield **3a** [a] (%)
1	0	4	THF	70	0	0
2	10	4	THF	70	53	0
3	10	4	MeCN	70	20	6
4	10	4	EtOAc	70	0	0
5	10	4	CH_2Cl_2	70	0	0
6	**10**	**10**	**THF**	**70**	**87**	**0**
7[b]	10	10	THF	70	29	0
8	10	10	Me-THF	70	83	10
9	5	10	THF	70	62	30
10	10	10	THF	80	72	0
11	10	10	THF	60	82	17
12	10	10	THF	50	55	38

Reaction conditions: *N*-methylaniline (**1a**, 0.233 mmol, 1 equiv.), PMHS (4–10 equiv.), catalyst (0–10 mol%), $p(CO_2)$ = 1 bar, 50–80 °C, 16 h, solvent. [a] Yield was determined by ^{1}H NMR using mesitylene as the internal standard. [b] CO_2 balloon.

The scope of the reaction was next investigated by converting a variety of substituted secondary and primary amines **1** under the optimized conditions. While a reaction time of 16 h was required to achieve an appropriate yield for most substrates, full conversion was achieved within 4 h for a few substrates (Table 2). *p*-Methoxy-*N*-methylaniline (**1b**) gave the corresponding dimethylaniline **2b** in 72% yield after 16 h, while 71% yield of *o*-methoxy-*N*,*N*-dimethylaniline (**2c**) was isolated after only 4 h (entries 1 and 2). Fluoro- and bromo-substituted *N*-methylanilines gave the products **2d** and **2e** in good yields of 86% and 77%, respectively (entries 3 and 4). Substrates with strong electron-withdrawing groups were challenging for the reaction: the methylated products of *p*-nitro- (**2f**) and *p*-acetyl-*N*-methylaniline (**2g**) were isolated in 19% and 42% yields, respectively (entries 5 and 6). Further functiona-

Table 2 Substrate scope for the synthesis of *N*-methylamines from amines with CO_2 and PMHS

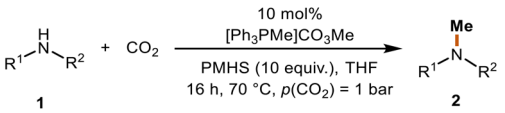

Entry	Substrate **1**	Product **2**	Yield
1	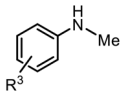	**2b**, R^3 = *p*-OCH_3	72%
2		**2c**, R^3 = *o*-OCH_3	71%[a]
3		**2d**, R^3 = *p*-F	86%
4		**2e**, R^3 = *p*-Br	77%
5		**2f**, R^3 = *p*-NO_2	19%
6		**2g**, R^3 = *p*-Ac	42%
7	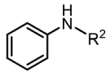	**2h**, R^2 = Bn	89%
8		**2i**, R^2 = cyclohexyl	83%
9		**2j**, R^2 = *n*-butyl	87%
10		**2k**, R^2 = allyl	82%
11		**2l**[b]	76%[a,b]
12		**2m**	90%[b]
13	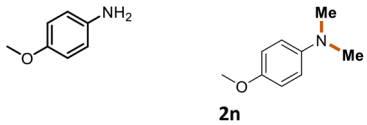	**2n**	42%
14	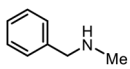	**2o**	30%[b,c]
15	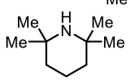	**2p**	98%[b]

Reaction conditions: amine **1** (0.600 mmol), PMHS (10 equiv.), catalyst (10 mol%), $p(CO_2)$ = 1 bar, 70 °C, 16 h, THF. Isolated yields are given. [a] 4 h. [b] Yield was determined by ^{1}H NMR using mesitylene as the internal standard. [c] The *N*-formylated product was obtained in 68% yield.

lized substrates such as *N*-benzyl-, *N*-cyclohexyl-, *N*-butyl-, and *N*-allyl-anilines were converted to the corresponding methylated products **2h–2k** in excellent yields (82–89%) (entries 7–10). Tetrahydroquinoline afforded the methylated product **2l** in a yield of 76% in 4 h (entry 11). In comparison with secondary anilines, primary anilines normally exhibit lower nucleophilicity and form multiple reduction products[42,52] However, with this catalytic system, aniline (**1m**) and *p*-methoxyaniline (**1n**) afforded dimethylanilines in yields of 90% and 42%, respectively (entries 12 and 13). Besides anilines, benzyl-*N*-methylamine (**1o**) was also tested. However, the formylated product **3o** was obtained in 68% yield as the main product while the methylated product **2o** was obtained in 30% yield (entry 14). Surprisingly, the sterically hindered substrate 2,2,6,6-tetramethylpiperidine was successfully converted to the methylated product pempidine **2p**, which is a ganglion-blocking drug (entry 15).[53]

Since the formation of the *N*-formylated product **3a** was also observed in significant amounts during the screening (Table 1, entry 12), we further explored the *N*-formylation of *N*-methylaniline (**1a**) catalyzed by $[Ph_3PMe]CO_3Me$ (Table 3). Initially, we turned our focus to other silanes. $PhSiH_3$ and Ph_2SiH_2 gave moderate yields of *N*,*N*-dimethylaniline (**2a**) and poor yields of *N*-methylformanilide (**3a**) (entries 1–5). $PhSiH_3$ and Ph_2SiH_2 mainly formed methylated product **2a**, and only 8% desired product **3a** was observed (entries 1 and 2). Ph_3SiH converted **1a** to **3a** in a yield of 39% and no **2a** or **3a** was observed with Et_3SiH (entries 3 and 4). $(MeO)_3SiH$ afforded the *N*-formylated product in an excellent yield of 98% with outstanding selectivity (entry 5). Further screening of the reaction conditions was performed in the presence of $(MeO)_3SiH$ (entries 6–10). Reducing the reaction time to 4 h led to a comparable yield and selectivity (entry 6). **1a** was quantitatively converted to the desired product **3a** even with a much lower loading of the catalyst (entry 7). An excellent yield of the formylated product **3a** (95%) was also obtained at 70 °C in 4 hours in the presence of 3 equiv. of $(MeO)_3SiH$ (entry 8). No product was obtained without the catalyst (entry 9). A lower amount of $(MeO)_3SiH$ was not sufficient to convert all the reactant (entry 10).

With the optimal conditions in hand, the scope and limitations of $[Ph_3PMe]CO_3Me$ for the catalytic conversion of amines to their formylated products were studied at 70 °C in the presence of trimethoxysilane as the reductant (Table 4). Under these conditions, *p*-methoxyaniline (**1b**) was converted to **3b** in a high yield of 86% (entry 1). In some cases, extension of the reaction time from 4 to 24 h was necessary. In contrast to the methylation reaction, *o*-methoxy-*N*-methylaniline (**1c**) needed 24 h to be converted to the corresponding formylated product in a good yield of 79% (entry 2). Electron-withdrawing groups were also evaluated: fluoro- and bromo-substituted anilines **1d** and **1e** afforded the corresponding

Table 3 Screening reaction conditions for the conversion of *N*-methylaniline (**1a**) with CO_2 into formylated product **3a**

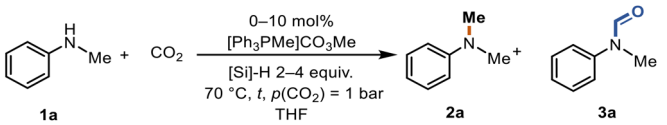

Entry	Cat. (mol%)	Si–H (equiv.)	Silane	*t* (h)	Yield **2a** (%)	Yield **3a** (%)
1	10	4	$PhSiH_3$	16	31	8
2	10	4	Ph_2SiH_2	16	55	8
3	10	4	Ph_3SiH	16	0	39
4	10	4	Et_3SiH	16	0	0
5	10	4	$(MeO)_3SiH$	16	0	98
6	10	4	$(MeO)_3SiH$	4	0	94
7	2	4	$(MeO)_3SiH$	4	0	96
8	**2**	**3**	**$(MeO)_3SiH$**	**4**	**0**	**95**
9	0	3	$(MeO)_3SiH$	4	0	0
10	2	2	$(MeO)_3SiH$	4	0	44

Reaction conditions: *N*-methylaniline (**1a**, 0.233 mmol), silane (2–4 equiv.), catalyst (0–10 mol%), $p(CO_2)$ = 1 bar, 70 °C for 4–16 h, THF. The yield was determined by ^{1}H NMR using mesitylene as the internal standard.

Table 4 Substrate scope for the conversion of amines to formamides with CO_2 and trimethoxysilane

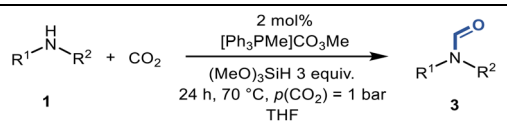

1 3

Entry	Substrate **1**	Product **3**	Yield
1	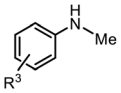	**3b**, R^3 = *p*-OCH_3	86%[a]
2		**3c**, R^3 = *o*-OCH_3	79%
3		**3d**, R^3 = *p*-F	86%[a]
4		**3e**, R^3 = *p*-Br	76%[a]
5		**3f**, R^3 = *p*-NO_2	13%
6		**3g**, R^3 = *p*-Ac	53%
7	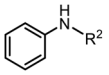	**3j**, R^2 = *n*-butyl	84%
8		**3k**, R^2 = allyl	85%
9		**3l**	94%
10	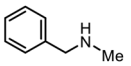	**3o**	92%
11	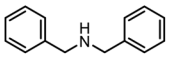	**3q**	75%
12	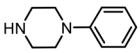	**3r**	89%
13	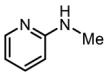	**3s**	69%
14		 **3t**	90%
15		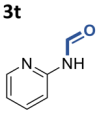 **3u**	53%

Reaction conditions: amine **1** (0.600 mmol), trimethoxysilane (220 mg, 3 equiv.), catalyst (2 mol%), $p(CO_2)$ = 1 bar, 70 °C, 24 h, THF. Isolated yields are given. [a] 4 h.

N-methylformanilide **3d** and **3e** in good yields in 4 h; while nitro- and acetyl-substituted anilines **1f** and **1g** led to lower yields of 13% and 53%, respectively (entries 3–6). *N*-Substituted anilines were also tolerated, *N*-butyl- and *N*-allyl-substituted anilines **1j** and **1k** were successfully converted to their formylated products **3j** and **3k** in 84% and 85% yield, respectively, after 24 h (entries 7 and 8). Tetrahydroquinoline **1l** gave the formylated product **3l** in 94% yield (entry 9). The conversion of the benzylamines **1o** and **1q** was also successful and 92% and 75% yield, respectively, of the formylated methylbenzeneamine **3o** and dibenzylamine **3q** were isolated (entries 10 and 11). The piperazine derivative **1r** afforded the formylated product **3r** in a yield of 89% (entry 12). A moderate yield of 69% of the formylated product **3s** was obtained from the pyridine-substituted amine **1s** (entry 13). Aniline (**1t**) and pyridine-2-amine (**1u**) were selected as representative substrates of primary amines (entries 14 and 15). An excellent yield of 90% of *N*-formanilide **3t** was obtained from aniline, while 53% of the *N*-formylated-pyridine-2-amine **3u** was isolated.

The excellent conversion and selectivity of aniline (**1t**) to *N*-phenylformamide (**3t**) encouraged us to study the possibility of the formation of benzimidazole by monoformylation of the *o*-phenylenediamine (**4a**) followed by subsequent intramolecular condensation with the amino group. Therefore, the reaction was performed under the same reaction conditions as for the formylation of aniline without other additives. To our delight, 83% of benzimidazole **5a** was isolated from 1,2-diaminobenzene and CO_2 in one step (Table 5, entry 1). This prompted us to investigate the synthesis of other imidazole derivatives **5**. *p*-Methoxy-1,2-diaminobenzene (**4b**) afforded the desired product **5b** in a yield of 47% (entry 2). *N*-Disubstituted substrates 1-*N*-methylbenzene-1,2-diamine (**4c**) and *N*-phenyl-*o*-phenylenediamine (**4d**) were evaluated in this protocol: 61% and 70% of the desired products **5c** and **5d** were obtained, respectively (entries 3 and 4). The lower yields were due to the formation of the monoformylation byproduct from the primary amino group that is less nucleophilic and reactive than secondary amino groups. There are only a few examples of the synthesis of quinazoline derivatives utilizing CO_2.[13,54,55] Under our conditions, the six-membered ring quinazoline derivative **5e** was also isolated in a yield of 64% from *o*-(aminomethyl)aniline **4e** (entry 5).

To gain insights into the reaction mechanism, control experiments were performed to identify the possible intermediates in the *N*-formylation and *N*-methylation reactions (Scheme 2). Initially, trimethoxysilane was reacted with CO_2 in the presence of the catalyst $[Ph_3PMe]CO_3Me$, affording the silyl formate in 29% yield. Characteristic signals for silylformate were observed in the ^1H and ^{13}C NMR spectra at

Table 5 Substrate scope for the conversion of diamines to benzoheterocycles with CO_2 and trimethoxysilane

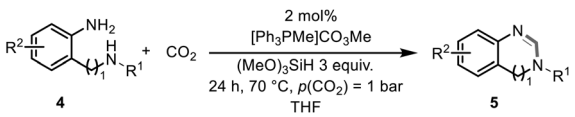

4 5

Entry	Substrate		Product		Yield
1	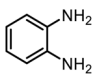	**4a**		**5a**	83%
2	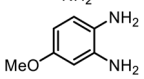	**4b**	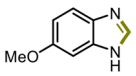	**5b**	47%
3	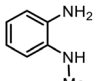	**4c**		**5c**	61%
4	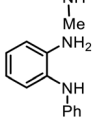	**4d**	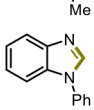	**5d**	70%
5	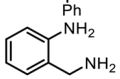	**4e**	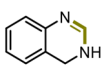	**5e**	64%

Reaction conditions: diamine **4** (0.600 mmol), trimethoxysilane (3 equiv.), catalyst (2 mol%), $p(CO_2)$ = 1 bar, 70 °C for 24 h, CH_3CN. Isolated yields are given.

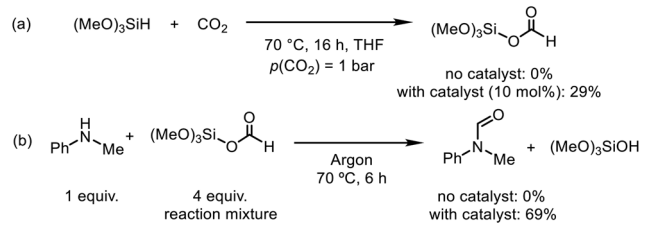

Scheme 2 Control experiments for the *N*-formylation reaction. The yields were determined by ^{1}H NMR using mesitylene as the internal standard.

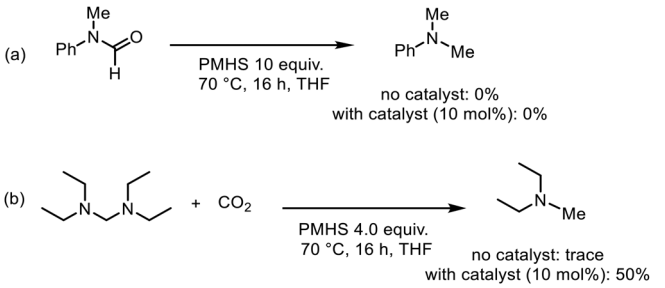

Scheme 4 Control experiments for the *N*-methylation reaction. The yield was determined by ^{1}H NMR using mesitylene as the internal standard.

δ(SiOC*H*O) = 7.96 ppm and δ(SiO*C*HO) = 158.2 ppm, respectively (Scheme 2a and Fig. S1†).[56] Notably, in the absence of the catalyst, this was not observed. Apart from silyl formate, tetramethoxysilane was also observed in the ^{1}H NMR and ^{29}Si NMR spectra at δ(SiOCH_3) = 3.40 ppm and δ(SiOCH_3) = −78.6 ppm, respectively (Fig. S1–S3†). The formation of tetramethoxysilane can be addressed by the over-reduction of silyl formate in the absence of amines.[57] The resulting reaction mixture was purged with argon to replace the remaining CO_2. *N*-Methylaniline (**1a**) was added and reacted at 70 °C for 6 h, affording *N*-methylformanilide (**2a**) in 69% yield (Scheme 2b). Without the catalyst, the silyl formate was not observed. Moreover, the silyl formate did not react with the amine **1a** in the absence of the catalyst.

Thus we conclude that *N*-formylation proceeds *via* the silyl formate intermediate which has been reported before.[58] However, for the *N*-methylation of amines by CO_2 in the presence of organocatalysts, two possible pathways are discussed in the literature. Both pathways proceed *via* the initial formation of the silyl formate (Scheme 3). Path I: the *N*-formamide is formed and further reduced to *N*-methylamine by the silane. The majority of catalytic systems were proved to follow this pathway by experimental and computational evidence.[26,29,41,59,60] Path II: the silane is reduced to silyl acetal, which reacts with the amine to afford the aminal. Subsequently, the aminal is reduced to the methylated product.[28,38]

The two routes were evaluated by performing a series of test reactions. First, the conversion of *N*-formamide to *N*-methylamine was tested using PMHS as the reductant in the presence and absence of the catalyst under the methylation reaction conditions (Scheme 4a). In both cases, the product could not be obtained. Thus, path I was ruled out. Subsequently, we considered path II. We hypothesized that the intermediate formation of the aminal in the reaction mixture should be detectable by NMR. Indeed, it was possible to detect the formation of the aminal by ^{1}H NMR spectroscopy. The spectra showed a characteristic signal for the aminal resonance at δ(N–CH_3) = 2.86 ppm which agrees with previous reports.[61] Under the optimized reaction conditions, the aminal was initially formed in 9% yield after 2 h (Table S1 and Fig. S5†). This supports the assumed formation of the aminal as an intermediate. Furthermore, the conversion of the aminal to the *N*-methylamine was studied. In this regard, *N*,*N*,*N*′,*N*′-tetramethylethanediamine (TMEDA), a commercially available aminal, was chosen to react with PMHS in the presence of CO_2 since it is reported that CO_2 contributed to the cleavage of the N–C bond.[58] Under the reaction conditions, the aminal (TMEDA) and PMHS were converted and the corresponding *N*-methylated product was obtained in 50% yield in the presence of the catalyst, which demonstrated that path II is reasonable for this catalytic system (Scheme 4b and Fig. S6†). Only traces of the product were observed in the absence of CO_2 or catalyst.

Interestingly, despite being a milder reducing agent than trimethoxysilane, PMHS was efficient for the 6-electron reduction of CO_2 in the presence of the catalyst[62] This might be explained when path II is considered. In this route, due to the polymeric nature of PMHS, the formation of a bis silyl acetal can proceed *via* an intramolecular reduction of the silyl formate (Scheme S1†).

Once the different routes to the formation of products were established, we became interested in understanding the role of

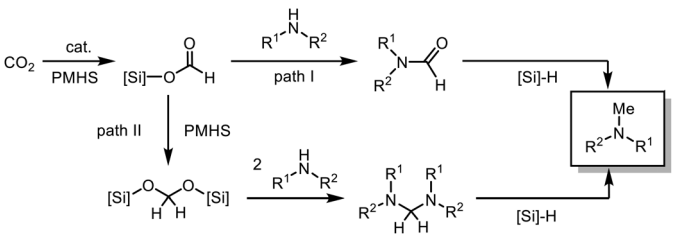

Scheme 3 Possible pathways for the *N*-methylation reaction with PMHS.

the catalyst in this reaction and the different selectivity observed for the reducing agents. Initially, a stoichiometric mixture of PMHS and catalyst $[Ph_3PMe]CO_3Me$ was heated to 70 °C and analyzed by NMR spectroscopy (Fig. 1c). The characteristic signal at δ(Si–*H*) = 4.72 ppm in PMHS (see **1a**) and the signal at $\delta(CO_3CH_3)$ = 3.37 ppm (see **1b**) for the catalyst were not observed in the mixture. Instead, a new signal at δ = 8.58 ppm was observed in the mixture which can be attributed to the formation of the formate anion.[63] A signal with the same chemical shift ($\delta(HCO_2^-)$ = 8.58 ppm) was observed in the mixture of trimethoxysilane and the catalyst (Fig. 2c). Also, in this case, the signals at δ(Si–*H*) = 4.07 ppm for the silane and for the catalyst $\delta(CO_3CH_3)$ = 3.37 ppm were not detectable in the mixture. The signals at 3.37 ppm and −78.60 ppm in the ^{29}Si NMR spectra (Fig. S7†), respectively, indicate the formation of $Si(OMe)_4$.[64] The common signal in both mixtures at around 3.30 ppm (marked as *) can be addressed to a methoxy

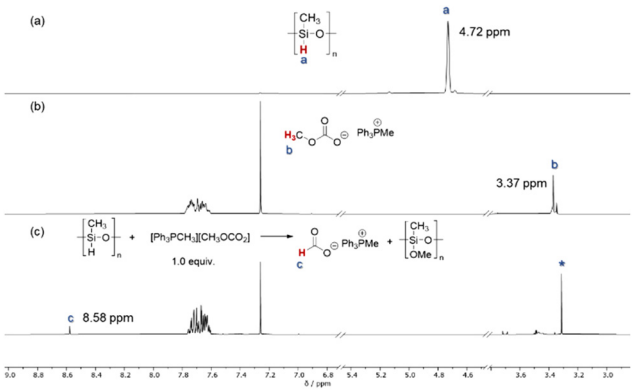

Fig. 1 (a) Section of the ^{1}H NMR spectra of PMHS. (b) Section of the ^{1}H NMR spectra of catalyst $[Ph_3PCH_3]CO_3Me$. (c) Section of the ^{1}H NMR spectra of a 1 : 1 mixture of PMHS and $[Ph_3PCH_3]CO_3Me$ after 16 h at 70 °C. * denotes the methoxy anion.

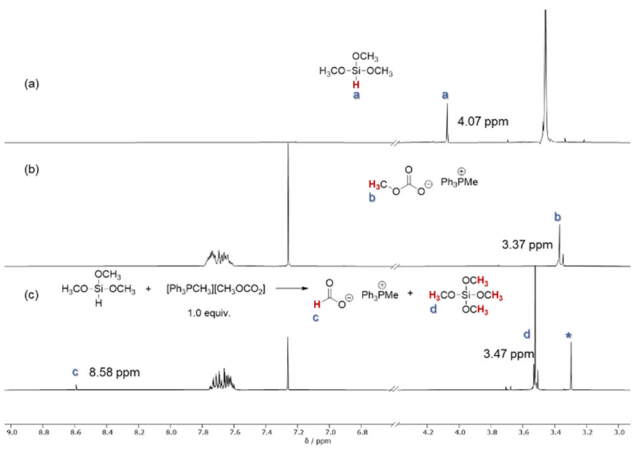

Fig. 2 (a) Section of the ^{1}H NMR spectra of PMHS. (b) Section of the ^{1}H NMR spectra of the catalyst $[Ph_3PMe]CO_3Me$. (c) Section of the ^{1}H NMR spectra of a 1 : 1 mixture of PMHS and $[Ph_3PMe]CO_3Me$ after 16 h at 70 °C. * denotes the methoxy anion.

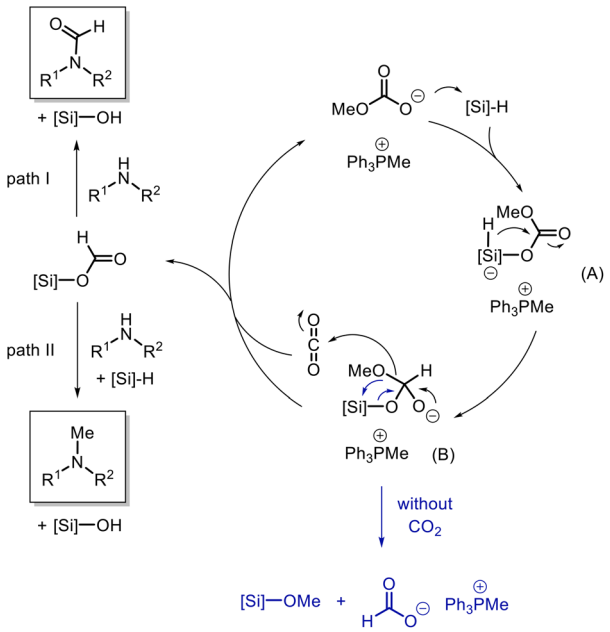

Scheme 5 Mechanistic proposal for the selective conversion of amines with CO_2 to formamides or methylamines with phosphonium methylcarbonate salts.

anion which is probably formed due to the decomposition of $[Ph_3PMe]CO_3Me$ to CO_2 and $[Ph_3PMe]OMe$.[49] These results indicate the conversion of the methylcarbonate anion and silane to formate. This led us to the assumption that the reaction is initiated in this step. Based on these results, we propose the mechanism shown in Scheme 5.

The methylcarbonate anion attacks the silane forming A which facilitates the attack of the hydride to the carbonyl center and the generation of B. The decomposition of B leads to silyl formate and a methoxy anion which reacts with CO_2 to regenerate methylcarbonate (catalyst) and it also leads to the regeneration of the catalyst in the following step, which has no negative impact on the catalytic efficiency. As indicated above, in the absence of CO_2, this B can undergo a rearrangement resulting in the formate anion, *e.g.* tetramethoxysilane. In the presence of trimethoxysilane as the reducing agent, the formate further reacts with the amine through path I to the *N*-formylated product which is not further reduced. In contrast, if PMHS is used as the reducing agent, the *N*-formylated product further reacts to form bis silyl acetal which subsequently reacts with the amine and PMHS to give the *N*-methylated product.

Conclusions

Phosphonium methylcarbonate has been proven to be an efficient organocatalyst for the conversion of CO_2 with primary and secondary amines and diamines. Notably, the selectivity of the reaction can be tuned by the choice of the reductant. In the presence of readily available PMHS, selective

N-methylation was achieved under mild conditions. In contrast, the use of trimethoxysilane as the reducing agent leads to the selective *N*-formylation of the amines. Moreover, the one-pot synthesis of imidazoles was possible when diamines were used as the starting material. Mechanistic investigations revealed different reaction pathways for *N*-methylation and *N*-formylation depending on the reductant. *N*-Methylation proceeds most probably *via* silyl formate while *N*-formylation proceeds *via* a bissilyl acetal and aminal intermediate. The mechanistic studies also suggest that the catalyst directly activates CO_2. This tuneable process was applied to a broad range of substrates. Under the optimized conditions, 15 primary and secondary amines and anilines were converted to *N*-methylated products in yields of up to 98%. The *N*-formylation of 15 amines led to the desired products in yields of up to 94%. Additionally, this procedure was evaluated for a one-pot *N*-formylation/condensation reaction of diamines leading to the corresponding heterocycles in yields of up to 83%. Thus, the presented mechanistic studies give insights into the *N*-methylation and *N*-formylation of amines with CO_2. In addition, the protocols presented provide straightforward access to valuable intermediates that use CO_2 as a C1 building block.

Experimental

Synthesis of methyltriphenylphosphonium methylcarbonate

In a 10 mL Schlenk tube, triphenylphosphine (0.235 g, 0.896 mmol), dimethylcarbonate (DMC) (0.52 mL, 6.15 mmol), and methanol (0.52 mL) as solvent were introduced in the shortest time possible to limit the exposure of phosphine to air. The Schlenk tube was heated for 24 h at 140 °C. The reaction mixture was allowed to cool to an ambient temperature and volatiles were removed in a vacuum. The off-white solid was stirred under an inert atmosphere with cyclohexane (8.3 mL) at 50 °C for 2 hours. After filtration on a Gooch crucible, the product was obtained in 64% yield as a colorless solid (0.215 mg, 0.580 mmol). ^{1}H NMR (300 MHz, $CDCl_3$): δ = 7.82–7.58 (m, 15H), 3.37 (s, 3H) ppm. The methyl protons (P-CH_3) were not detectable due to H/D exchange.[50] ^{1}H NMR (300 MHz, CD_3CN): δ = 7.98–7.81 (m, 3H), 7.79–7.62 (m, 12H), 3.29 (s, 3H), 2.89 (d, J = 15.7 Hz, 3H). ^{13}C NMR (75 MHz, $CDCl_3$): δ = 134.96 (d, J = 2.9 Hz), 133.26 (d, J = 10.7 Hz), 130.39 (d, J = 12.9 Hz), 119.41 (d, J = 88.5 Hz), 52.20. ^{13}C NMR (75 MHz, CD_3CN): δ = 162.20, 140.32 (d, J = 3.1 Hz), 138.68 (d, J = 10.8 Hz), 135.47 (d, J = 12.9 Hz), 124.98 (d, J = 88.9 Hz), 56.17, 13.50 (d, J = 57.8 Hz) ppm. ^{31}P NMR (122 MHz, $CDCl_3$): δ = 21.92 ppm. HR-MS ($MePh_3P$+): m/z calcd 277.1151, found 277.1153.

Representative procedure for *N*-methylation – the synthesis of *N*-benzyl-*N*-methylaniline (2h)

In a stainless-steel autoclave, PMHS (414 μL) was added to a solution of the catalyst (21.4 mg, 60.0 μmol) and *N*-benzylaniline (**1h**, 110 mg, 0.600 mmol) in THF (5 mL). The autoclave was purged with CO_2 and the pressure was kept constant at 1 bar. The reaction mixture was stirred at 70 °C for 16 h. Subsequently, CO_2 was released slowly. The solvent was removed in a vacuum and the residue was purified by chromatography (SiO_2, cyclohexane/ethyl acetate = 20/1) to yield *N*-benzyl-*N*-methylaniline (105 mg, 0.533 mmol, 89%) as a colorless oil. ^{1}H NMR (300 MHz, $CDCl_3$) δ = 7.37–7.28 (m, 2H), 7.28–7.19 (m, 5H), 6.81–6.69 (m, 3H), 4.55 (s, 2H), 3.03 (s, 3H).

Representative procedure for *N*-formylation – the synthesis of *N*-benzylformamide (3o)

In a stainless-steel autoclave, trimethoxysilane (220 mg, 1.80 mmol) was added to a solution of the catalyst (4.23 mg, 12.0 μmol) and *N*-methyl-1-phenylmethanamine (72.7 mg, 0.600 mmol) in THF (0.6 mL). The autoclave was purged with CO_2 and the pressure was kept constant at 1 bar. The reaction mixture was stirred at 70 °C for 24 h. Subsequently, CO_2 was released slowly. The solvent was removed in a vacuum and the residue was purified by silica gel chromatography (cyclohexane/ethyl acetate = 10/1) to afford *N*-benzylformamide (82.0 mg, 0.552 mmol, 92%) as a colourless oil. ^{1}H NMR (300 MHz, $CDCl_3$) δ = 8.21 (s, 0.57H, maj), 8.08 (s, 0.43H, min), 7.38–7.04 (m, 5H), 4.44 (s, 0.89H, min), 4.31 (s, 1.19H, maj), 2.77 (s, 1.33H, min), 2.70 (s, 1.71H, maj).

Representative procedure for the preparation of benzimidazoles – the synthesis of 1*H*-1,3-benzimidazole (4a)

In a stainless-steel autoclave, trimethoxysilane (220 mg, 1.80 mmol) was added to a solution of the catalyst (4.23 mg, 12.0 μmol) and *o*-phenylenediamine (64.9 mg, 0.600 mmol) in THF (6 mL). The autoclave was purged with CO_2 and the pressure was kept constant at 1 bar. The reaction mixture was stirred at 70 °C for 24 h. Subsequently, CO_2 was released slowly. Then the solvent was removed in a vacuum and the residue was purified by silica gel chromatography (cyclohexane/ethyl acetate = 1/1) to yield 1*H*-benzo[*d*]imidazole (58.8 mg, 0.498 mmol, 83%) as a colorless solid. ^{1}H NMR (300 MHz, $CDCl_3$) δ 8.11 (s, 1H), 7.79–7.59 (m, 2H), 7.35–7.28 (m, 2H), 6.28 (s, 1H).

Author contributions

C. Ren performed the initial reaction screening. C. Ren and C. Terazzi performed the optimization of the reaction conditions and mechanistic studies. C. Ren performed the substrate scope. C. Ren, C. Terazzi and T. Werner wrote the manuscript.

Conflicts of interest

There are no conflicts to declare.

References

1 J. Chatterjee, F. Rechenmacher and H. Kessler, *Angew. Chem., Int. Ed.*, 2013, **52**, 254–269.
2 M. Schou and C. Halldin, *J. Labelled Compd. Radiopharm.*, 2012, **55**, 460–462.
3 G. Antoni and B. Långström, in *Positron Emission Tomography: Basic Sciences*, ed. D. L. Bailey, D. W. Townsend, P. E. Valk and M. N. Maisey, Springer London, London, 2005, pp. 223–236, DOI: 10.1007/1-84628-007-9_10.
4 D. J. McCarthy, C. Halldin, J. D. Andersson and M. E. Pierson, in *Annual Reports in Medicinal Chemistry*, ed. J. E. Macor, Academic Press, 2009, vol. 44, pp. 501–513.
5 E. M. Isin, C. S. Elmore, G. N. Nilsson, R. A. Thompson and L. Weidolf, *Chem. Res. Toxicol.*, 2012, **25**, 532–542.
6 A. Del Vecchio, G. Destro, F. Taran and D. Audisio, *J. Labelled Compd. Radiopharm.*, 2018, **61**, 988–1007.
7 A. Del Vecchio, F. Caille, A. Chevalier, O. Loreau, K. Horkka, C. Halldin, M. Schou, N. Camus, P. Kessler, B. Kuhnast, F. Taran and D. Audisio, *Angew. Chem., Int. Ed.*, 2018, **57**, 9744–9748.
8 H. Bipp and H. Kieczka, in *Ullmann's Encyclopedia of Industrial Chemistry*, 2000, DOI: 10.1002/14356007.a12_001.
9 S. Kobayashi and K. Nishio, *J. Org. Chem.*, 1994, **59**, 6620–6628.
10 F. Brunelli, S. Aprile, C. Russo, M. Giustiniano and G. C. Tron, *Green Chem.*, 2022, **24**, 7022–7028.
11 S. A. Salami, X. Siwe-Noundou and R. W. Krause, *Molecules*, 2022, **27**, 6850.
12 M. L. Bennasar, T. Roca, M. Monerris and D. García-Díaz, *J. Org. Chem.*, 2006, **71**, 7028–7034.
13 M. Hulla, S. Nussbaum, A. R. Bonnin and P. J. Dyson, *Chem. Commun.*, 2019, **55**, 13089–13092.
14 A. Sharma, A. Kumar, S. A. H. Abdel Monaim, Y. E. Jad, A. El-Faham, B. G. de la Torre and F. Albericio, *Biopolymers*, 2018, **109**, e23110.
15 M. J. Calverley, *Synth. Commun.*, 1983, **13**, 601–609.
16 E. Müller, H. Huber-Emden and W. Rundel, *Justus Liebigs Ann. Chem.*, 1959, **623**, 34–46.
17 H. Seo, A.-C. Bédard, W. P. Chen, R. W. Hicklin, A. Alabugin and T. F. Jamison, *Tetrahedron*, 2018, **74**, 3124–3128.
18 V. Goyal, N. Sarki, A. Narani, G. Naik, K. Natte and R. V. Jagadeesh, *Coord. Chem. Rev.*, 2023, **474**, 214827.
19 B. N. Atkinson and J. M. J. Williams, *ChemCatChem*, 2014, **6**, 1860–1862.
20 G. Naik, N. Sarki, V. Goyal, A. Narani and K. Natte, *Asian J. Org. Chem.*, 2022, **11**, e202200270.
21 M. Aresta, A. Dibenedetto and A. Angelini, *Chem. Rev.*, 2014, **114**, 1709–1742.
22 J.-H. Ye, T. Ju, H. Huang, L.-L. Liao and D.-G. Yu, *Acc. Chem. Res.*, 2021, **54**, 2518–2531.
23 I. Sullivan, A. Goryachev, I. A. Digdaya, X. Li, H. A. Atwater, D. A. Vermaas and C. Xiang, *Nat. Catal.*, 2021, **4**, 952–958.
24 Q. Liu, L. Wu, R. Jackstell and M. Beller, *Nat. Commun.*, 2015, **6**, 5933.
25 B. Grignard, S. Gennen, C. Jérôme, A. W. Kleij and C. Detrembleur, *Chem. Soc. Rev.*, 2019, **48**, 4466–4514.
26 X.-F. Liu, R. Ma, C. Qiao, H. Cao and L.-N. He, *Chem. – Eur. J.*, 2016, **22**, 16489–16493.
27 C. Xie, J. Song, H. Wu, B. Zhou, C. Wu and B. Han, *ACS Sustainable Chem. Eng.*, 2017, **5**, 7086–7092.
28 X.-F. Liu, X.-Y. Li, C. Qiao, H.-C. Fu and L.-N. He, *Angew. Chem., Int. Ed.*, 2017, **56**, 7425–7429.
29 Y. Hu, J. Song, C. Xie, H. Wu, Z. Wang, T. Jiang, L. Wu, Y. Wang and B. Han, *ACS Sustainable Chem. Eng.*, 2018, **6**, 11228–11234.
30 X.-F. Liu, X.-Y. Li, C. Qiao and L.-N. He, *Synlett*, 2018, **29**, 548–555.
31 R. Yao, Y. Li, J. Wang, J. Chen and Y. Xu, *J. Catal.*, 2023, **418**, 78–89.
32 H. Wu, W. Dai, S. Saravanamurugan, H. Li and S. Yang, *Green Chem.*, 2020, **22**, 5822–5832.
33 N. M. Hein, Y. Seo, S. J. Lee and M. R. Gagné, *Green Chem.*, 2019, **21**, 2662–2669.
34 R. O. Sauer, W. Scheiber and S. D. Brewer, *J. Am. Chem. Soc.*, 1946, **68**, 962–963.
35 N. J. Lawrence, M. D. Drew and S. M. Bushell, *J. Chem. Soc., Perkin Trans.*, 1999, 3381–3391.
36 F. D. Bobbink, S. Das and P. J. Dyson, *Nat. Protoc.*, 2017, **12**, 417–428.
37 S. Das, F. D. Bobbink, S. Bulut, M. Soudani and P. J. Dyson, *Chem. Commun.*, 2016, **52**, 2497–2500.
38 G. Li, J. Chen, D.-Y. Zhu, Y. Chen and J.-B. Xia, *Adv. Synth. Catal.*, 2018, **360**, 2364–2369.
39 Z. Zhang, Q. Sun, C. Xia and W. Sun, *Org. Lett.*, 2016, **18**, 6316–6319.
40 X. Li, J. Zhang, Y. Yang, H. Hong, L. Han and N. Zhu, *J. Organomet. Chem.*, 2021, **954–955**, 122079.
41 W. Zhao, X. Chi, H. Li, J. He, J. Long, Y. Xu and S. Yang, *Green Chem.*, 2019, **21**, 567–577.
42 C. Fang, C. Lu, M. Liu, Y. Zhu, Y. Fu and B.-L. Lin, *ACS Catal.*, 2016, **6**, 7876–7881.
43 T. Werner and H. Büttner, *ChemSusChem*, 2014, **7**, 3268–3271.
44 H. Büttner, J. Steinbauer and T. Werner, *ChemSusChem*, 2015, **8**, 2655–2669.
45 J. Steinbauer, L. Longwitz, M. Frank, J. Epping, U. Kragl and T. Werner, *Green Chem.*, 2017, **19**, 4435–4445.
46 C. Ren, A. Spannenberg and T. Werner, *Asian J. Org. Chem.*, 2022, **11**, e202200156.
47 A. Berkessel and M. Brandenburg, *Org. Lett.*, 2006, **8**, 4401–4404.
48 M. Hatano, Y. Tabata, Y. Yoshida, K. Toh, K. Yamashita, Y. Ogura and K. Ishihara, *Green Chem.*, 2018, **20**, 1193–1198.
49 M. Fabris, M. Noè, A. Perosa, M. Selva and R. Ballini, *J. Org. Chem.*, 2012, **77**, 1805–1811.
50 L. Cattelan, M. Noè, M. Selva, N. Demitri and A. Perosa, *ChemSusChem*, 2015, **8**, 3963–3966.

51 C. Lu, Z. Qiu, Y. Zhu and B.-L. Lin, *Sci. Bull.*, 2019, **64**, 723–729.
52 H. Zhang, Y. Zhang and K. Gao, *Org. Chem. Front.*, 2023, **10**, 2491–2497.
53 A. Spinks and E. H. P. Young, *Nature*, 1958, **181**, 1397–1398.
54 O. Jacquet, C. Das Neves Gomes, M. Ephritikhine and T. Cantat, *ChemCatChem*, 2013, **5**, 117–120.
55 V. V. Phatake and B. M. Bhanage, *Catal. Lett.*, 2019, **149**, 347–359.
56 M. Tüchler, L. Gärtner, S. Fischer, A. D. Boese, F. Belaj and N. C. Mösch-Zanetti, *Angew. Chem., Int. Ed.*, 2018, **57**, 6906–6909.
57 G. Feng, C. Du, L. Xiang, I. del Rosal, G. Li, X. Leng, E. Y. X. Chen, L. Maron and Y. Chen, *ACS Catal.*, 2018, **8**, 4710–4718.
58 M. Hulla and P. J. Dyson, *Angew. Chem., Int. Ed.*, 2020, **59**, 1002–1017.
59 S. Maji, A. Das and S. K. Mandal, *Chem. Sci.*, 2021, **12**, 12174–12180.
60 Z. Huang, X. Jiang, S. Zhou, P. Yang, C.-X. Du and Y. Li, *ChemSusChem*, 2019, **12**, 3054–3059.
61 M.-Y. Wang, N. Wang, X.-F. Liu, C. Qiao and L.-N. He, *Green Chem.*, 2018, **20**, 1564–1570.
62 D. Addis, S. Das, K. Junge and M. Beller, *Angew. Chem., Int. Ed.*, 2011, **50**, 6004–6011.
63 H. Gao, J. Jia, C.-H. Tung and W. Wang, *Organometallics*, 2023, **42**, 944–951.
64 D. C. Braddock, P. D. Lickiss, B. C. Rowley, D. Pugh, T. Purnomo, G. Santhakumar and S. J. Fussell, *Org. Lett.*, 2018, **20**, 950–953.

Curriculum Vitae

Name: Changyue Ren

Date of birth: 14. 09. 1986

Place of birth: Harbin, China

Education and research experience

Since 03/2020	**PhD study at Leibniz Institute for Catalysis at University of Rostock**
	Topic: "Phosphonium salt catalysts for reductive and non-reductive CO_2 fixation"
	Supervisor: Prof. Dr. T. Werner
06/2016–12/2019	**Working at Zunyi Medical University as research assistant**
07/2012– 06/2016	**Working at Heilongjiang Vocational College of Biology Science and Technology as laboratory assistant**
09/2009–06/2012	**Master study at Heilongjiang University**
	Master thesis: "Syntheses and properties of chiral multidentate carboxylate coordination compounds "
	Supervisor: Prof. Jinsheng Gao
08/2005–06/2009	**Bachelor study at Heilongjiang University**
	Bachelor thesis: The design of gasketless Flange
08/2002–06/2005	**High school study at Harbin 14th high school**

List of Publications

11) C. Ren, A. Spannenberg and T. Werner. *ACS Sustainable Chemistry & Engineering.* **2024**, accepted.

10) C. Ren, C. Terazzi and T. Werner. Tunable reduction of CO_2 – organocatalyzed selective formylation and methylation of amines. *Green Chem*. **2024**, *26*, 439−447.

9) C. Ren, H. Zhang, Z. Chen, J. Gao, M. Yang, Z. Yuan, and X. M. Li. A Novel Utilization of Water Extract of Suaeda Salsa in the Pd/C Catalyzed Suzuki–Miyaura Coupling Reaction. *Molecules.* **2022**, *27*, 6623.

8) C. Ren, A. Spannenberg, T. Werner. Synthesis of Bifunctional Phosphonium Salts Bearing Perfluorinated Side Chains and Their Application in the Synthesis of Cyclic Carbonates from Epoxides and CO_2. *Asian J. Org. Chem*. **2022**, *11*, e202200156.

7) Y. Hu, Z. Wei, A. Frey, C. Kubis, C.-Y. Ren, A. Spannenberg, H. Jiao and T. Werner. Catalytic, Kinetic, and Mechanistic Insights into the Fixation of CO_2 with Epoxides Catalyzed by Phenol-Functionalized Phosphonium Salts. *ChemSusChem* **2021**, *14*, 363–372.

6) X. M. Li, T. T. Zhang, R. Hu, H. Zhang, C. Ren, Z. L. Yuan. A one-pot protocol for the fluorosulfonation and Suzuki coupling of phenols and bromophenols, streamlined access to biaryls and terphenyls, *Org. Biomol. Chem.* **2020**, *18*, 4748–4753.

5) X. M Li, F. F. Feng, C. Ren, Y. Teng, Q. H. Hu, Z. L. Yuan. Base-Controlled One-Pot Chemoselective Suzuki–Miyaura Reactions for the Synthesis of Unsymmetrical Terphenyls. *Synlett*, **2019**, *30*, A–E.

4) Y. Yu, H. Ye, G. Hou, C. Ren, J. Gao and P. Yan. Synthesis, Structure, and Properties of a Series of Chiral Coordination Polymers Based on (R)-4-(4-(1 Carboxyethoxy) phenoxy)-3-chlorobenzoic Acid. *Cryst. Growth Des*. **2016**, *16*, 5669–5677.

3) X. Xu, Y. Yu, G. Hou, X. Li, C. Ren, D. Ma. Syntheses, structures and catalytic properties of chiral Co(II) coordination polymers based on (R)-4-(4-(1-carboxyethoxy)phenoxy) Syntheses, structures and catalytic properties of chiral Co(II) benzoic acid. *Polyhedron* **2016**, *112*, 61–66.

2) H. Ye, C. Ren, G. Hou, Y. Yu, X. Xu, J. Gao. P. Yan, S-W. Ng. Syntheses, Structures, and Second-Order Nonlinear Optical Properties of Chiral Zinc(II) Coordination Polymers Based on (R)-4-(4-(1-Carboxyethoxy)phenoxy)-3-fluorobenzoic Acid and Effect of the Second Ligand with Imidazole Group. *Cryst. Growth Des*. **2014**, *14*, 3309–3318.

1) Y. Yu, C. Ren, G. Hou, H. Ye and J. Gao. Syntheses and properties of two chiral multidentate carboxylate copper coordination compounds. *J. Coord. Chem*. **2012**, *65*, 4137–4146.

Contribution to Conferences

2) Synthesis of Bifunctional Phosphonium Salts Bearing Perfluorinated Side Chains and Their Application in the Synthesis of Cyclic Carbonates from Epoxides and CO_2, C. Ren, A. Spannenberg, T. Werner, *18th European Workshop on Phosphorus Chemistry*, 14.–16. Sep. **2022**, Rostock, Germany.

1) Homogenous Fluorous Phosphonium Salt Catalysts for Synthesis of Cyclic Carbonates from CO_2 and its Reusable Process, C. Ren, T. Werner, *55. Jahrestreffen Deutscher Katalytiker*, 27.–29. June **2022**, Weimar, Germany.